

Real Algebraic Curves
and
Combinatorial Constructions

Inauguraldissertation zur
Erlangung der Würde eines Doktors der Philosophie
vorgelegt der
Philosophisch-Naturwissenschaftlichen Fakultät
der Universität Basel

von
Bertrand Haas
aus Guer (Morbihan, Frankreich)

Basel 1997

Genehmigt von der Philosophisch-Naturwissenschaftlichen Fakultät auf
antrag der
Professoren Dr. Norbert A'Campo von der Universität Basel, Dr. Viacheslav
Kharlamov von der Universität Louis Pasteur in Strasbourg (Frankreich),
und Dr. Ilia Itenberg von der Universität Rennes-1 in Rennes (Frankreich).

Basel. den 15. Januar 1998.

Prof. Dr. phil. Thomas A. Bickle, Dekan.

*I dedicate this work
to my mother.*

I want to thank first my two supervisors. V. Kharlamov who introduced me to the amazing world of “T-objects” and whose sharp critics helped to make this work clearer. And N. A’Campo who supported me morally and technically throughout my PhD, and who showed me so many times the right way to write this work.

I want to thank also very much the Mathematic Department of the University of Bern who employed me for two years, and particularly prof. P. Mani who beside his function of director, spent a lot of time explaining me very kindly a lot of things in combinatorial geometry.

I am very indebted to Ilia Itenberg who showed me very important results which were the starting point of this work and who accepted to be in the jury. I thank also O. Viro and E. Shustin for useful discussions.

During the period of my PhD I have been financially supported by the University of Strasbourg, the University of Bern, and the Swiss National Fond in Basel. I would like to thank these institutions for their support.

Finally I want to thank the Fields institute in Toronto for its productive atmosphere, particularly the organizers of the Singularity Theory Program who invited me there for six months, and more particularly proff. P. Milman and E. Bierstone who gave me the possibility to come back in Toronto for a post-doc.

Contents

I	Some Properties of Lattice T-curves	1
1	Introduction	2
2	Introduction to lattice T-curves	3
2.1	Lattice T-Curves on $\mathbb{R}P^2$	3
2.2	Lattice T-curves and algebraic curves	4
2.3	Some lattice definitions	6
2.4	Lattice T-curves on more general surfaces	9
2.4.1	The ambient surfaces for lattice T-curves	9
2.4.2	Lattice T-curves on their ambient surfaces	10
2.5	Congruence classes of maximal lattice T-curves	12
3	Constructions	14
3.1	A diamond model for $\mathbb{R}P^2$	14
3.2	Congruent homeomorphisms	15
4	Basic Properties of Lattice T-Curves	18
4.1	Ambient Surfaces of Lattice T-curves	18
4.1.1	The local structure around the lift of a vertex	18
4.1.2	Canonical charts for the ambient surface	19
4.1.3	Gluing two charts of the ambient surface	21
4.1.4	A basis for the 1-homology of the ambient surface	24
4.1.5	The topological characterization of an ambient surface	25
4.2	Isomorphic T-curves	26
4.2.1	Translation of the carrier polygon	26
4.2.2	Linear transformation of the carrier polygon	27
4.3	Definitions	28
5	The T-filling of a lattice T-curve K.	30
5.0.1	Incidence Graphs	30
5.1	The Construction	31
5.2	The relation with algebraic geometry	32
5.3	First Application: The Harnack Theorem	34
5.3.1	The Harnack bound	34
5.3.2	Harnack T-curves	36

5.4	Second Application: Orientation of T-curves	42
5.5	Gluing lattice T-curves	45
5.5.1	Gluing the curves	45
5.5.2	Orienting locally the T-curves to be glued	46
5.5.3	Gluing the T-fillings	48
5.5.4	Gluing maximal lattice T-curves	50
6	From Harnack T-curves to Maximal T-curves	53
6.1	No Twist Implies Harnack T-curve	53
6.2	Maximal Implies Gluing of Harnack T-curves	56
6.2.1	An algorithm to cut T-fillings	56
6.2.2	Spheres with holes glued by twists	57
6.3	Zone decompositions, and Harnack zone-wise sign distributions	63
6.3.1	Zone decompositions	63
6.3.2	Harnack zone-wise decomposition	64
7	From zone decompositions to Maximal T-Curves	66
7.1	Minimal and odd-cycle-free zone decompositions	66
7.2	From minimal zone decompositions to T-curves	68
7.3	odd-cycle-free zone decomposition and maximal T-curves . . .	69
7.3.1	Proof of the part (1) of theorem 7.3.0.10	70
7.3.2	Proof of the part (2) of theorem 7.3.0.10	73
II The Ragsdale Conjecture for Maximal Lattice T-curves		75
8	Introduction.	76
8.1	Some history.	78
8.2	The main theorems.	80
8.3	Some new definitions	80
9	The Point-Oval Correspondence.	84
9.1	Definition of the correspondence	84
9.2	Properties of the correspondence	86
10	Removing even edges	89
10.1	Which point inside which oval	89
10.1.1	Local deformation of a lattice T-curve	89

10.1.2	Points inside their corresponding ovals	90
10.2	Where $\alpha(*)$ is not	91
10.3	The sign of an oval	92
10.4	Removing one even edge	92
10.5	Removing two even edges	93
10.6	Removing all the even edges	95
11	Properties of even-node-free zone decompositions	96
11.1	Basic observations	97
11.2	Two important zone-definitions	98
11.3	Characterization of $\alpha(*)$	98
11.4	Counting points with signs	105
11.4.1	The integral points of a zone	105
11.4.2	Counting even and odd ovals via integral points	107
12	Lattice geometry	109
12.1	Integral points in polygons	109
12.2	Congruences in zones	111
12.3	Integral points in zones	116
12.4	Proof of the Main Theorem	120
12.5	Further Remarks	121

List of Figures

1	Recovering RP^2 from $\mathbf{T}(d)$	3
2	Construction of a T-curve of degree 3 on $\mathbb{R}P_2$ from the basic data (a triangulation of the triangle $\mathbf{T}(d)$, and a distribution of signs on $\mathbf{T} \cap \mathbb{Z}^2$.)	5
3	$\text{sign}(e_i) = \delta(P_j)\delta(P_k)$, so $\prod \text{sign}(e_i) = \prod \delta(P_i)^2 = 1$. Therefore either 0 or 2 edges have negative sign. Hence a T-curve is a closed curve.	6
4	The fourfold ramified covering structure of $S(\Pi)$. Here $\Pi = \mathbf{T}$, so $S(\Pi) = \mathbb{R}P^2$	9
5	An odd-cycle-free zone decomposition and a non odd-cycle-free zone decomposition. The parity of some points is written.	13
6	Diagram representing the homeomorphism between $\mathbb{R}P^2$ and $(D(d)/\sim)$	15
7	Explanation of the action of a rotation of angle $\mu/2$ around the x_1 axis.	16
8	The same action from a cutting-squeezing-and-pasting point of view. Combinatorially it correspond to a permutation $A, B, C, D \mapsto A, B, D, C$	17
9	How the segments in the lift of a broken edge are identified two by two according to their parity. Here s_1 and s_2 have same parity and have different parity than s_3	19
10	Gluing the four copies of Π to one another gives a union of two spheres when all the segments of $\partial\Pi$ have same parity.	19
11	A local orientation of all the broken edges determines the label of the quadrants by the $U_i^{a,b}$. Here the parity of the broken edges l_i is in parentheses. Notice that with the local orientations shown $U_i^{0,0}$ is always equal to Π	21
12	Gluing the four copies of Π to one another gives a sphere when Π has only two broken edges.	22
13	The tubular neighborhood of the lift $\mu^{-1}(l)$ of a broken edge l is either an annulus if l is even, either a Moebius band if l is odd.	23
14	A thick Y is glued from three ribbons, and two thick Y's are glued with or without a twist.	32

15	The T-curve (plain lines) is drawn on the incidence graph of the triangulation of $\mathbb{R}P^2$ (dotted lines). The folded T-curve on the incidence graph of the triangulation of \mathbf{T} uses every edge twice (thick plain lines).	33
16	To construct the T-filling $F(K)$, thicken the Y's in each triangle, glue any two adjacent thick Y's with or without a twist (depending on K), and close the free ends with segments. . . .	34
17	The double of a lattice T-curve of degree d on $\mathbb{R}P^2$ is a surface of genus $\frac{(d-1)(d-2)}{2}$	35
18	A Harnack T-curve of degree 5.	39
19	A Harnack T-curve of degree 6.	40
20	If an edge of Π is of odd length, then a component of K cuts the embedded circle $\mu^{-1}(l)$ an odd number of times. Therefore this component is not an oval.	41
21	When all the edges of Π are of even length, the "special" component of the Harnack T-curve can be moved onto the boundary of Π . Therefore it is an oval.	42
22	Eight types of Harnack distributions for four Harnack curves symmetric to one another.	43
23	The oriented cycles on the incidence graph on Π lift to oriented cycles on the incidence graph on $S(\Pi)$. We just sketched here small portions of two cycles meeting on an edge.	44
24	Here $K_1 \# K_2$ and $K_1 \# (\sigma_{0,1} \cdot K_2)$ are congruent curves.	47
25	Here $K_1 \# K_2$ is a Harnack curve, and $K_1 \# (\sigma_{0,1} \cdot K_2)$ is a non maximal curve.	48
26	The arcs α_1 and α_2 are cut each into two arcs. These four arcs are re-glued two by two in two different ways according to the gluing of $K_1 \# K_2$ or to gluing $K_1 \# (\sigma_{b,a} \cdot K_2)$. The orientation of α_1 being fixed, it implies two different orientations of α_2 . . .	49
27	Gluing $F(K_1)$ and $F(K_2)$ corresponding to fig. 24.	50
28	$F(K_1 \# K_2)$ and $F(K_1 \# (\sigma_{0,1} \cdot K_2))$ corresponding to fig. 25. . .	51
29	The orientation in $F(K_2)$ of a segments s' is induced from the orientation of the corresponding segment s in $F(K_1)$ and depends on whether s is identified to s' with a twist or without a twist.	52
30	A more complicated connected sum of two surfaces is equivalent to a r -connected sum (here $r = 2$).	53

31 How a T-curve intersects the four symmetric copies of a triangle of the triangulation. 54

32 If the thick Y's in t_1 and t_4 are glued with no twists, then $\delta(P_1) = \delta(P_4)$ if and only if P_1 and P_4 have same parities (here they have same parities on the right diagram, and different parities on the left diagram). 56

33 Here $F(K)$ becomes disconnected after 3 cuts along twists. . . 58

34 The holes O_1 and O_2 give rise to one or two holes in $F(K_1 \# K_2)$. Here D_1 and D_2 are the disks obtained by filling the holes of $F(K_1)$ and $F(K_2)$, except O_1 and O_2 . Unfill the holes in $D_{1,2}$ to get $F(K_1 \# K_2)$ 59

35 Double the surface, then take the half. Here it is a torus with one hole. 59

36 An end of a twisted "bridge" is slid along the boundary until it comes close to the other end. So we get a surface with one hole and an odd number of twists. Here it is a torus with two holes. 60

37 For one twist, we get a disk and for two twists we get an annulus. 61

38 The total parity $\theta(s)$ of a primitive segment s , and its action as a symmetry on the distribution of signs on s . This action doesn't change the sign of s , although it may change the signs of the integral points of s (in that case the symmetry is represented with dotted arrows). 63

39 A minimal zone decomposition of the triangle $\mathbf{T}(4)$ which is not an odd-cycle-free zone decomposition. Notice that the lattice T-curve on $\mathbb{R}P^2$ constructed from it is not maximal. . . 68

40 A zone and its completed zone. 70

41 How to undo the twists of $F(K^i)$ to get $F(K^{i+1})$ 72

42 If K is maximal, then the number of zones in a cycle of zones must be even, otherwise $F(K)$ wouldn't be orientable. Here the orientation on $F(K)$ is not reversed along a loop when the cycle has four zones, but it is reversed when the cycle has three zones. 73

43 The ambient triangle. 76

44 A curve with 3 even ovals and 5 odd ovals. 78

45 nodes and vertices of a zone. 81

46 Shape of the arc between two consecutive boundary-nodes. . . 82

47 Examples of Pie-diagrams and of completed zones. 83

48 Two different connected components of K surround the inner-
node S 85

49 The four cases arising in the definition of U 86

50 The ovals $\alpha(S)$ and $\alpha(R)$ are represented on the left pie-
diagram. On the right diagram, we see that $U(S) \cap U'(S) \cap$
 $U(R) \cap U'(R)$ contains at most two points. 87

51 The three basic deformations of an arc of the curve viewed on
a pie diagram. 90

52 Impossible shrinking of an oriented oval. 91

53 One or two connected component according to the parity of
the number of edges. 95

54 Removing two even edges. 96

55 Three observations specific to even-node-free odd-cycle-free
zone decompositions of $\mathbf{T}(2k)$ 97

56 An example of a special zone and separating zones. 99

57 The notations for subsection 11.3 (view on a pie diagram). . . 100

58 The arc surrounding all the P_i 's. 100

59 The arc surrounding all the P_i 's and Q_i 's. 101

60 The two arcs cutting e are connected. 102

61 $\alpha(*)$ surrounds all the boundary-nodes of V 103

62 A nontrivial homology cycle cutting only $\alpha(*)$ 104

63 $\alpha(*)$ is, like $\alpha'(*)$, an even oval (the arrows represent the inside
of the oval). 105

64 Examples of zones with their top node (black point). 106

65 Shrinking of $\alpha(S)$ into a circle surrounding S 107

66 The convex hull of the set of even points of a non degenerate
polygon and of two degenerate ones (a segment and a point). . 110

67 Partition of a non-convex polygon into two "more convex"
polygons. 111

68 Simple nontrivial case illustrating $p - n \equiv 0 \pmod{4}$ 112

69 Squeezing and sliding a zone to see it as a difference of two
simpler zones. 113

70 The zone Z seen as a difference of simpler zones. 113

71 The zone Z seen as a difference and union of simpler zones.
The zone Z'' is the triangular zone with vertices P, Q and A_0 . 114

72 The two cases arising in the count of $p|Z| - n|Z| \pmod{4}$ 116

73 What vertices to consider to calculate a bound for $p|Z| - n|Z|$. 117

74 These three cases seem to be not possible. 122

Part I
**Some Properties of Lattice
T-curves**

1 Introduction

This work is concerned with *lattice T-curves*. The notion of T-curves has arisen in real algebraic geometry as a special case of a method introduced by Viro [11] of patchworking algebraic varieties. T-curves can be seen also from a geometric-combinatorial point of view and can be defined in a general setting as follows:

1.0.0.1 Definition

Let S be a compact surface without boundary equipped with a smooth triangulation \mathcal{T} . A *T-curve* K on (S, \mathcal{T}) is a union of disjoint topologically embedded circles in S which lie in the 1-skeleton of some cell decomposition of S dual to the cell decomposition induced by \mathcal{T} .

A T-curve induces a sign distribution on the edges of \mathcal{T} in the following way: The edges which intersect the T-curve are of sign -1 , and the edges which don't intersect the T-curve are of sign $+1$. A sign distribution induced by a T-curve has the property that each triangle of the triangulation has either 0 or 2 edges of negative sign.

Reciprocally a sign distribution on the edges of a triangulation \mathcal{T} of a surface S , such that each triangle has either 0 or 2 edges of negative signs, gives rise to a T-curve in the following way: Consider a cell decomposition \mathcal{C} of S dual to \mathcal{T} . Assign to the edges of \mathcal{C} the sign of the corresponding edges of \mathcal{T} . The T-curve is the union of the edges of negative sign of \mathcal{C} .

Notice that any finite union of disjoint topologically embedded circles in a surface is the underlying curve of some T-curve. Therefore the underlying curve of a T-curve in this general setting has no special properties. We will define *lattice T-curves* in a setting of integral polygons (see section 2), and study some of their properties. In particular all the lattice T-curves defined from a given integral polygon have their number of connected components bounded from above. Lattice T-curves with the maximal number of connected components are called *maximal T-curves*.

2 Introduction to lattice T-curves

2.1 Lattice T-Curves on $\mathbb{R}P^2$

Viro introduced in [11] a new method to construct algebraic curves. Orevkov used a particular case of his method and started to develop the notion of *Lattice T-curves on $\mathbb{R}P^2$* (called just "T-curves" in most of the papers in the bibliography). Lattice T-curves of degree d on $\mathbb{R}P^2$ (d being a positive integer) can be constructed as follows (see an example of the construction of such a T-curve of degree 3 on fig. 2).

1. Let $\mathbf{T}(d)$ (or simply \mathbf{T}) be the triangle in \mathbb{R}^2 with vertices $(0, 0)$, $(0, d)$, $(d, 0)$. The reflections through the coordinate axis generate 4 copies of \mathbf{T} , which cover the diamond $D(d)$ with vertices $(\pm d, 0)$, $(0, \pm d)$. By identifying each point (x, y) on the boundary of the diamond with the point $(-x, -y)$, we obtain a surface which is homeomorphic to the real projective plane $\mathbb{R}P^2$ (see fig. 1). We give in section 3.1 an explicit homeomorphism which allow us to identify this surface with $\mathbb{R}P^2$.

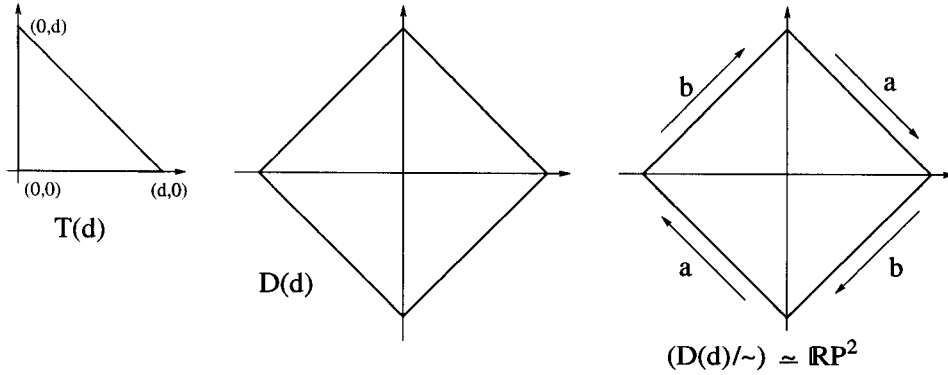


Figure 1: Recovering $\mathbb{R}P^2$ from $\mathbf{T}(d)$.

2. Let \mathcal{T} be an arbitrary rectilinear triangulation of \mathbf{T} such that its vertices are exactly the integral points of \mathbf{T} . The reflections through the coordinate axis generate from \mathcal{T} a triangulation of the diamond and then a triangulation of $\mathbb{R}P^2$.
3. Let $\delta : \mathbf{T} \cap \mathbb{Z}^2 \rightarrow \{\pm 1\}$ be an arbitrary sign distribution on the integral points (x, y) of \mathbf{T} . We extend this distribution to the diamond in the

following way:

$$\delta((-1)^a x, (-1)^b y) = (-1)^{ax+by} \delta(x, y) \quad \text{where } a, b \in \{0, 1\} \quad (1)$$

4. We assign to each edge of the triangulation of the diamond $D(d)$ the sign equal to the product of the signs of its endpoints. This distribution of signs on the edges of $D(d)$ induces a distribution of signs on the edges of the triangulation of $\mathbb{R}P^2$. Indeed, since the quotient map $D(d) \rightarrow \mathbb{R}P^2$ identifies an edge of the triangulation lying on the boundary of $D(d)$ to the opposite edge, we must check that two opposite edges have the same sign: A point $(x, y) \in \partial D(d)$ is reduced modulo two

- either to $(0, 0)$ or $(1, 1)$ if d is even. Then, in both cases $\delta(-x, -y) = \delta(x, y)$.
- either to $(0, 1)$ or $(1, 0)$ if d is odd. Then in both cases $\delta(-x, -y) = -\delta(x, y)$.

Therefore if an edge e has endpoints (x_1, y_1) and (x_2, y_2) , then the edge $-e$ will always have the same sign than e , which is $\delta(x_1, y_1)\delta(x_2, y_2)$.

5. The distribution of signs on the edges of the triangulation of the diamond has the property that each triangle has either 0 or 2 edges of negative sign. Indeed the product of the three signs of the edges of a triangle is equal to $+1$ since it is the product of the squares of the three signs of the vertices of the triangle (see fig. 3). It is clear that this property holds also on $\mathbb{R}P^2$. Therefore we get a T-curve on $(\mathbb{R}P^2, \mathcal{T})$ as explained in the introduction.

Notice that the data $(\mathbf{T}(d), \mathcal{T}, -\delta)$ gives the same T-curve than the data $(\mathbf{T}(d), \mathcal{T}, \delta)$.

2.2 Lattice T-curves and algebraic curves

2.2.0.2 Definition

Two curves on a surface are called *congruent (by homeomorphism)* if one can be transformed into the other by a homeomorphism of the surface.

A celebrated theorem of Viro [11] says that any lattice T-curve of degree d on $\mathbb{R}P^2$, under the assumption of a certain convexity property of the triangulation, is congruent to a real algebraic curve of degree d . For the moment

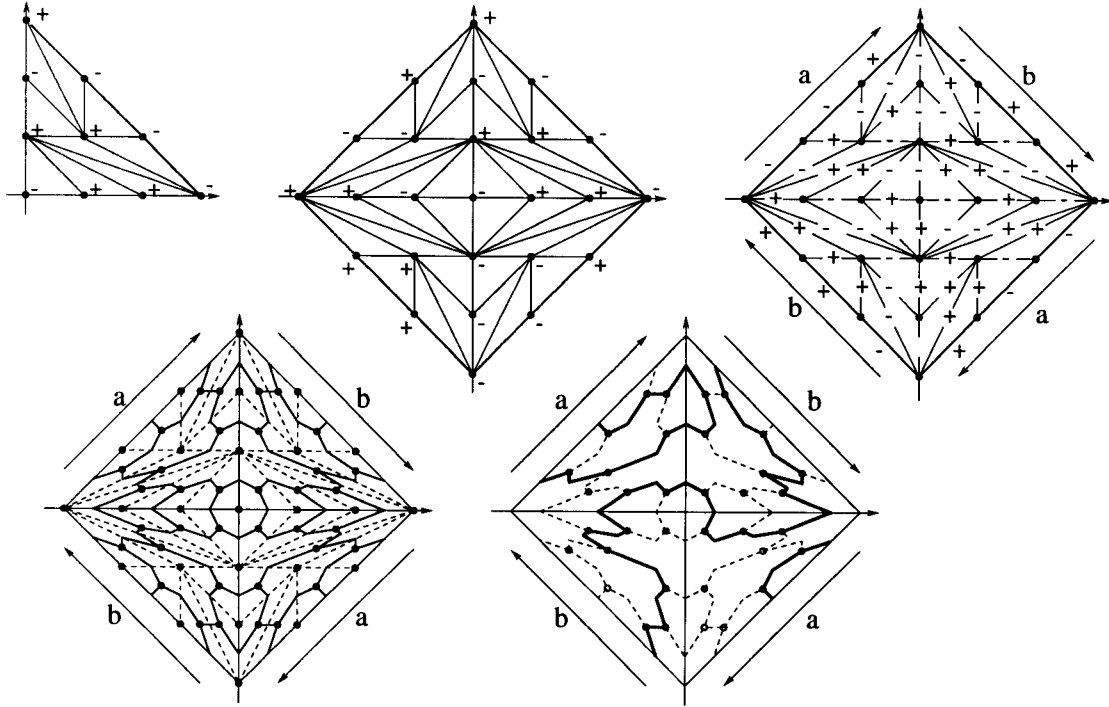


Figure 2: Construction of a T-curve of degree 3 on $\mathbb{R}P^2$ from the basic data (a triangulation of the triangle $\mathbf{T}(d)$, and a distribution of signs on $\mathbf{T} \cap \mathbb{Z}^2$.)

it is not known whether this convexity assumption is necessary for the theorem to hold. A property holding for all real plane projective nonsingular curves of degree d and not holding for a T-curve of degree d on $\mathbb{R}P^2$ would show the necessity of this assumption, but such a property is not yet known. Several important theorems of real algebraic geometry can be stated for T-curves of degree d on $\mathbb{R}P^2$ and proved combinatorially without this convexity assumption.

It is interesting to note that some properties are known to hold for all lattice T-curves on $\mathbb{R}P^2$ but not for all plane projective curves: A pair of connected components of a curve on $\mathbb{R}P^2$ is called an *injective pair* if one component bounds a subset of $\mathbb{R}P^2$ which is homeomorphic to a disk and which contains the other component. Itenberg [6] has shown that the number of injective pairs of a lattice T-curve of degree d on $\mathbb{R}P^2$ is less or equal than $3d/2$ though some families of plane projective curves have a number of injective pairs depending quadratically on their degree.

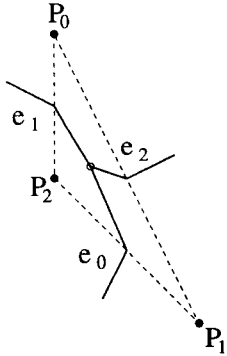


Figure 3: $\text{sign}(e_i) = \delta(P_j)\delta(P_k)$, so $\prod \text{sign}(e_i) = \prod \delta(P_i)^2 = 1$. Therefore either 0 or 2 edges have negative sign. Hence a T-curve is a closed curve.

A theorem of Harnack [3] gives a known example of a property of real algebraic curves which holds as well for all lattice T-curves on $\mathbb{R}P^2$.

2.2.0.3 Theorem (Harnack)

(1) A real plane projective nonsingular curve of degree d has the property that the number of its connected components is less or equal than $\frac{(d-1)(d-2)}{2} + 1$.

(2) For every integer $d \geq 1$, there exist curves of degree d which achieve this upper bound (they are called maximal curves).

Notice that $\frac{(d-1)(d-2)}{2}$ is also the number of integral points contained in the interior of $\mathbf{T}(d)$, so property (1) of Harnack theorem can be reformulated for lattice T-curves on $\mathbb{R}P^2$ in the following way:

2.2.0.4 Theorem (“Harnack” for lattice T-curves on $\mathbb{R}P^2$)

The number of connected components of a T-curve of degree d in $\mathbb{R}P^2$ is less or equal than one plus the number of the integral points contained in the interior of $\mathbf{T}(d)$ plus one.

See section 5.3 for a generalization and for more details.

2.3 Some lattice definitions

2.3.0.5 Definition

A segment is an *integral segment* if its two endpoints are integral points.

2.3.0.6 Definition

A *(closed) polygonal line* is a finite union of segments $s_1 \cup \dots \cup s_r \subset \mathbb{R}^2$, such that for $i = 2, \dots, r - 1$, (for i modulo r), the segment s_i shares one of its endpoints with s_{i-1} and its other endpoint with s_{i+1} . We always assume that the union of any two consecutive segments is not a segment. If all the segments are integral, the polygonal line is called *integral*.

2.3.0.7 Definition

A *(integral) polygon* is a subset of \mathbb{R}^2 bounded by a closed (integral) polygonal line and homeomorphic to a disk. An *edge of the polygon* is a segment of its boundary polygonal line. A *vertex of a polygon* is an endpoint of an edge of the polygon.

Notice that a polygon is integral if and only if all its vertices are integral points.

2.3.0.8 Definition

A *triangulation of a polygon* is a cell decomposition of the polygon into simplexes. A simplex of dimension 2 is a *triangle of the triangulation*, a simplex of dimension 1 is an *edge of the triangulation*, and a simplex of dimension 0 is a *vertex of the triangulation*.

Vertices and edges of a triangulation shouldn't be mixed up with vertices and edges of a polygon.

2.3.0.9 Definition

The *parity* of an integral point (p_1, p_2) is $(p_1 \bmod 2, p_2 \bmod 2) \in (\mathbb{Z}_2)^2 = (\mathbb{Z}/2\mathbb{Z}) \times (\mathbb{Z}/2\mathbb{Z})$. We denote the four values of the parities by $(0, 0)$, $(0, 1)$, $(1, 1)$ and $(1, 0)$.

Notice that the parity of the integral points which lie on a given integral segment takes exactly two values.

2.3.0.10 Definition

The *parity of an integral segment* is the sum of the two values that the parity takes on the integral points of the segment.

Notice that the parity of an integral segment is never $(0, 0)$.

2.3.0.11 Definition

The *parity of a vertex of an integral polygon* is the sum of the parities of the two edges of the polygon meeting in the vertex.

Notice that the parity of a vertex of an integral polygon can possibly take all four values.

2.3.0.12 Definition

The *parity of an edge of an integral polygon* is the sum of the parities of its vertices.

Parities of vertices and edges of an integral polygon shouldn't be mixed up with parities of their underlying integral points and integral segments.

2.3.0.13 Definition

A parity is called *even* if its value is $(0, 0)$. A parity is called *odd* if it is not even.

We already noticed that the parity of a segment is never even.

2.3.0.14 Lemma

If an integral polygon contains a vertex of odd parity, then it contains at least two vertices of odd parity.

proof. Let's follow the boundary of the polygon, departing from the vertex of odd parity and coming back to it. Since the vertex has odd parity, the "departing-edge" has different parity than the "coming-back-edge". So on the way we must pass through a vertex where meet two edges of different parity, i.e. through a vertex of odd parity.

2.3.0.15 Definition

The vertices of odd parity of an integral polygon divide its boundary into connected components, the closure of which we call the *broken edges of the polygon*.

Notice that the parity takes the same value on all the segments of a given broken edge.

2.3.0.16 Definition

The *parity of a broken edge of an integral polygon* is the sum of the parities of all the edges of the polygon contained in the broken edge.

Notice that if an integral polygon has vertices of odd parity, then the parity of a broken edge of the polygon is equal to the sum of the parities of the two vertices of the polygon which end the broken edge.

2.4 Lattice T-curves on more general surfaces

We slightly generalize the construction of lattice T-curves on $\mathbb{R}P^2$ in a natural way such that some analogs of real algebraic properties (in particular an analog of Harnack theorem) still hold.

2.4.1 The ambient surfaces for lattice T-curves

Let Π be an integral polygon in $\mathbb{R}_{\geq 0}^2$, and for every $a, b \in \{0, 1\}$, let $\sigma_{a,b}$ be the symmetry $(x, y) \mapsto ((-1)^a x, (-1)^b y)$. We glue the disjoint union of the four copies $(\sigma_{a,b} \cdot \Pi)$ by their boundary in the following way: For every $c, d \in \{0, 1\}$, we identify each point (x, y) on each edge e of $(\sigma_{c,d} \cdot \Pi)$ to the point $\sigma_{a,b} \cdot (x, y)$, where (b, a) is the parity of the edge e .

We obtain in this way a surface without boundary, which we will denote by $S(\Pi)$. The four maps $\sigma_{a,b}$ glue to a map $\mu : S(\Pi) \rightarrow \Pi$ which is a fourfold ramified covering. The ramifications take place along the broken edges in the following way: a point in the interior of a broken edge lifts to two points, and an endpoint of a broken edge lifts to one point.

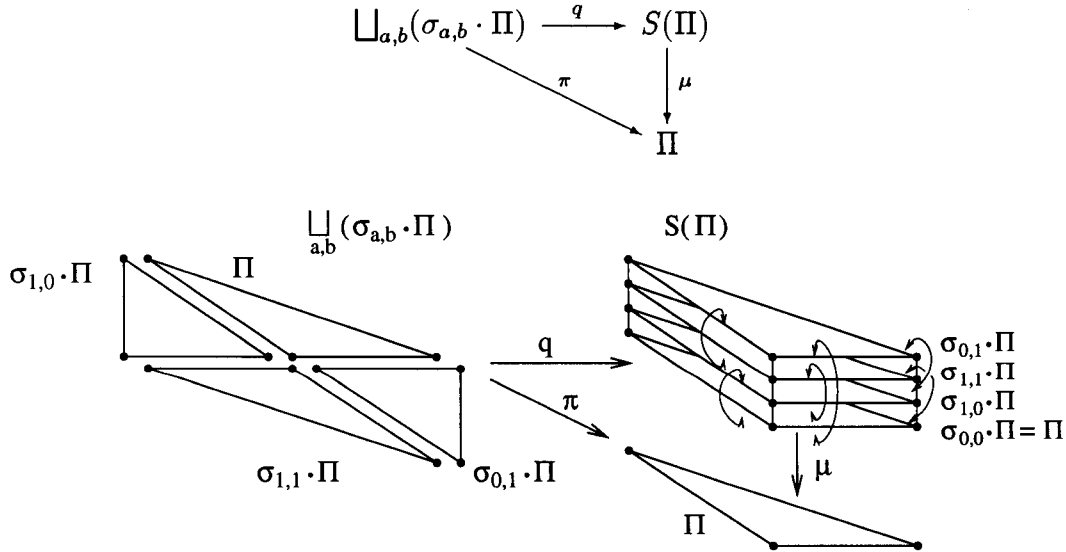


Figure 4: The fourfold ramified covering structure of $S(\Pi)$. Here $\Pi = \mathbf{T}$, so $S(\Pi) = \mathbb{R}P^2$.

If the parity of the segments of $\partial\Pi$ takes only one value, then $S(\Pi)$ has two connected components, each homeomorphic to a sphere. If the parity of

the segments of $\partial\Pi$ takes more than one value, then the next proposition, proved in 4.1.5.2 characterizes completely this surface.

Proposition: (see 4.1.5.2)

Let r be the number of broken edges of Π .

- The surface $S(\Pi)$ is orientable if and only if the parity of the segments of $\partial\Pi$ takes only two values.
- If $S(\Pi)$ is orientable, then r is even, and $S(\Pi)$ is the connected sum of $(r/2) - 1$ tori.
- If $S(\Pi)$ is not orientable, then it is the connected sum of $r - 2$ projective planes.

In particular the surface $S(\mathbf{T})$ obtained from the triangle $\mathbf{T}(d)$ is a projective plane.

2.4.1.1 Definition

The surface $S(\Pi)$ constructed above is called an *ambient surface* for lattice T-curves.

2.4.2 Lattice T-curves on their ambient surfaces

Now we can mimic the procedures 2-5 of section 2.1:

- Let \mathcal{T} be an arbitrary rectilinear triangulation of Π such that its vertices are exactly the integral points of Π . The reflections through the two coordinate axis generate a triangulation of the disjoint union $\bigsqcup_{a,b}(\sigma_{a,b} \cdot \Pi)$ which induces a triangulation of $S(\Pi)$.
- Let $(x, y) \mapsto \delta(x, y) = \pm 1$ be an arbitrary sign distributions on the integral points (x, y) of Π . We extend this distribution on $\bigsqcup_{a,b}(\sigma_{a,b} \cdot \Pi)$ with the same formula than in 2.1 which we rewrite slightly differently:

$$\delta(\sigma_{a,b} \cdot (x, y)) = (-1)^{\langle (a,b), (c,d) \rangle} \delta(x, y) \quad (2)$$

Where $a, b \in \{0, 1\}$, (c, d) is the parity of the point (x, y) , and $\langle (a, b), (c, d) \rangle = ac + bd$.

- We assign to each edge of the triangulation of $\bigsqcup_{a,b}(\sigma_{a,b} \cdot \Pi)$ the sign equal to the product of the signs of its endpoints. This edge distribution induces a distribution of signs on the edges of the triangulation of $S(\Pi)$. Indeed we check that two edges of the triangulation of $\bigsqcup_{a,b}(\sigma_{a,b} \cdot \Pi)$ which become identified in $S(\Pi)$ have same sign: For an edge e of parity (a, b) of the triangulation and for any $c, d \in \{0, 1\}$, we get from formula 2 above that,

$$\text{sign}(\sigma_{c,d} \cdot e) = (-1)^{\langle (a,b), (c,d) \rangle} \text{sign}(e) \quad (3)$$

According to 2.4.1 an edge e of the triangulation which is also an edge of some $(\sigma_{s,t} \cdot \Pi)$ is identified to $(\sigma_{c,d} \cdot e)$ if and only if $\langle (a, b), (c, d) \rangle = 0$, so e and $\sigma_{b,a} \cdot e$ have same signs.

- The same argument than in 2.1 shows that each triangle of the triangulation of $S(\Pi)$ has either 0 or 2 edges of negative sign, so we get, as explained in the introduction, a T-curve on $S(\Pi)$.

Notice like in 2.1 that the data $(\Pi, \mathcal{T}, \delta)$ and $(\Pi, \mathcal{T}, -\delta)$ define the same T-curves.

2.4.2.1 Definition

A T-curve constructed as above from the data $(\Pi, \mathcal{T}, \pm\delta)$ will be denoted by $K(\Pi, \mathcal{T}, \delta)$, (or $K(\Pi, \mathcal{T}, -\delta)$) and will be called a *lattice T-curve with carrier polygon Π* .

Notice that a lattice T-curve with carrier polygon $\mathbf{T}(d)$ is a lattice T-curve on $\mathbb{R}P^2$.

Let $\Pi \subset \mathbb{R}_{\geq 0}^2$ be a convex integral polygon. It is well known that we can define a real compact toric surface $X(\Pi)$ from Π . If for any vertex of even parity we identify its two lifts in $S(\Pi)$, we get a topological model of the toric surface defined by Π . For instance $X(\mathbf{T}(d)) = \mathbb{R}P^2$. So we can define also *lattice T-curves on a toric surface $X(\Pi)$* . In fact the theorem of Viro that we introduced in section 2.2 is stated more generally in [11]: Under the assumption of a certain convexity property of the triangulation of Π , a T-curve on a toric surface $X(\Pi)$ is congruent to an algebraic curve on $X(\Pi)$ with Newton polygon Π .

It turns out that an analog of Harnack theorem still hold for all lattice T-curve:

Theorem: (“Harnack” for all lattice T-curves, see 5.3.1.1)

Let $\Pi \in \mathbb{R}_{\geq 0}^2$ be an integral polygon.

(1) The number of connected components of a lattice T-curve with carrier polygon Π is less or equal than the number of integral points in the interior of Π plus one.

(2) For each integral polygon Π , there exist lattice T-curves with carrier polygon Π which achieve this upper-bound.

2.4.2.2 Definition

Lattice T-curves achieving the upper-bound of the above theorem are called maximal T-curves.

The analogy with algebraic curves goes further. We give in section 5 a construction of surfaces associated to lattice T-curves which are analogs to the quotients of the complexifications of real algebraic curves by the complex conjugation. These surfaces allow us for instance to give a nice proof of the Harnack-like theorem stated above and to define types and orientations for lattice T-curves. Theorems like Arnold congruence mod4 or Rokhlin formulas can then be stated for T-curves (but combinatorial proofs are still to be found). The main application of this construction that we give will be a certain determination of the congruence classes of maximal lattice T-curves (see the next subsection for a short explanation).

2.5 Congruence classes of maximal lattice T-curves

Hilbert asked in the first part of his well known 16th Problem, what are among all the real plane projective nonsingular curves of fixed degree, the possible mutual dispositions of the connected components. This is equivalent to the problem of classifying the curves up to topological congruence. Hilbert has emphasized the case of the maximal curves. The same problem arises naturally for lattice T-curves.

Though the two following theorems were motivated by the study of Ragsdale conjecture (see Part II), they can be a first step in finding a reasonable approximation of the number of congruence classes of maximal lattice T-curves with a given carrier polygon.

Definition (see 6.3.1.1)

A *zone* of an integral polygon Π is a polygon inside Π such that its boundary segments are primitive (i.e. the endpoints are the only integral points

of the edges), and such that each boundary segment meets the boundary of Π .

Definition (see 7.1.0.7)

A decomposition into zones of an integral polygon will be called an *odd-cycle-free zone decomposition* if, for any integral point in the interior of the polygon, and for any parity, the number of segments, lying on the boundary of zones of the decomposition, having the given parity, and having the given integral point as an endpoint, is even.

Let Π be an arbitrary integral polygon, and let Δ be an odd-cycle-free zone decomposition of Π . In section 7.2 we give a construction of a lattice T-curve, unique up to congruence, out of the data (Π, Δ) .

Theorem:(see 7.3.0.10)

(1) The lattice T-curves obtained by the construction of section 7.2 are maximal lattice T-curves.

(2) Every maximal T-curve is obtained up to congruence by the construction of section 7.2.

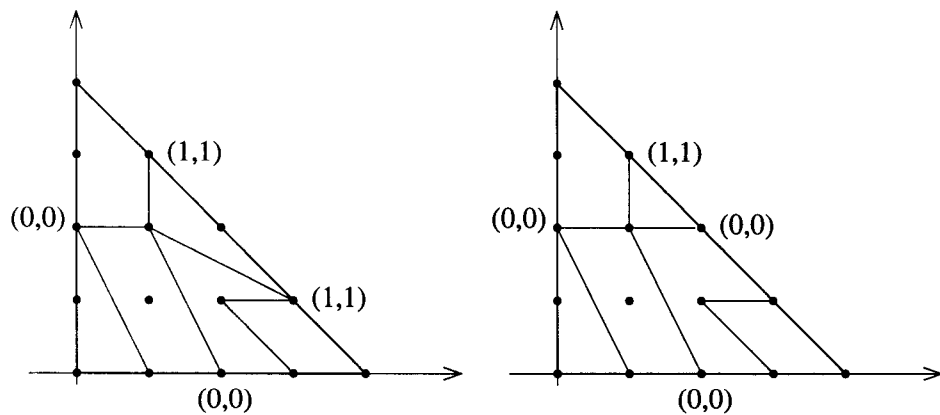


Figure 5: An odd-cycle-free zone decomposition and a non odd-cycle-free zone decomposition. The parity of some points is written.

3 Constructions

For every $a, b \in \{0, 1\}$, let $\sigma_{a,b}$ be the symmetry $(x, y) \mapsto ((-1)^a x, (-1)^b y)$. Let d be a positive integer, and recall that $\mathbf{T}(d)$ is the triangle of \mathbb{R}^2 with vertices $(0, 0), (0, d), (d, 0)$, and that the union $\bigcup_{a,b}(\sigma_{a,b} \cdot \mathbf{T})$ covers the diamond $D(d)$ with vertices $\pm(0, d), \pm(d, 0)$ (see fig. 1).

3.1 A diamond model for $\mathbb{R}P^2$

We have introduced in 2.1 a diamond model of the real projective plane. We give now an explicit homeomorphism which allow us to identify the model with the real projective plane.

Let Ω be the octahedron $\{x \in \mathbb{R}^3 : \sum |x_i| = d\}$. A line through the origin in \mathbb{R}^3 cuts Ω in two opposite points, so the real projective plane $\mathbb{R}P^2$ is identified to Ω / \sim , where $(x_0, x_1, x_2) \sim (-x_0, -x_1, -x_2)$ is the antipodal relation. The interior of the diamond $D(d)$ is the image of (one-to-one) projection μ_0 of the upper-half $\Omega(x_0 > 0)$ of Ω onto the coordinate plane $\{x_0 = 0\}$. This projection gives the chart $U_0 = \{(x_0 : x_1 : x_2), x_0 \neq 0\} \simeq \mathbb{R}^2$:

$$\begin{aligned} \mu_0 : U_0 &\rightarrow \text{int}(D) \\ (x_0 : x_1 : x_2) &\mapsto \left(\frac{dx_1}{\sum x_i}, \frac{dx_2}{\sum x_i} \right) \end{aligned}$$

If we complete this mapping by allowing $x_0 = 0$, then we complete U_0 by the line at infinity $\{x_0 = 0\}$ (which gives $\mathbb{R}P^2$), and the image becomes the whole diamond with the antipodal relation on its boundary: $(X_1, X_2) \sim (-X_1, -X_2)$ where $X_i = \frac{dx_i}{x_1 + x_2}$. Therefore this completed mapping is the required homeomorphism (see fig. 6).

$$\mathbb{R}P^2 \xrightarrow{\text{hom.}} (\Omega / \sim) \xrightarrow{\text{hom.}} (D(d) / \sim)$$

$$(x_0 : x_1 : x_2) \longmapsto \left(\frac{dx_0}{\sum |x_i|}, \frac{dx_1}{\sum |x_i|}, \frac{dx_2}{\sum |x_i|} \right) \longmapsto \left(0, \frac{dx_1}{\sum |x_i|}, \frac{dx_2}{\sum |x_i|} \right)$$

Notice that for any $a, b \in \{0, 1\}$, the copy $(\sigma_{a,b} \cdot \mathbf{T}) = \{(x, y), ((-1)^a x, (-1)^b y) \in \mathbf{T}\}$ of \mathbf{T} is in one-to-one correspondence with the subset $\{(x : y : z), (-1)^b y z \geq 0, z(-1)^a x \geq 0, (-1)^a x (-1)^b y \geq 0\}$.

3.1.0.3 Definition

We will call the subset $\{(x : y : z), (-1)^b y z \geq 0, z (-1)^a x \geq 0, (-1)^a x (-1)^b y \geq 0\}$ a *quadrant* of $\mathbb{R}P^2$. The above remark allows us to identify (abusively) the quadrants to the corresponding copies $(\sigma_{a,b} \cdot \mathbf{T})$.

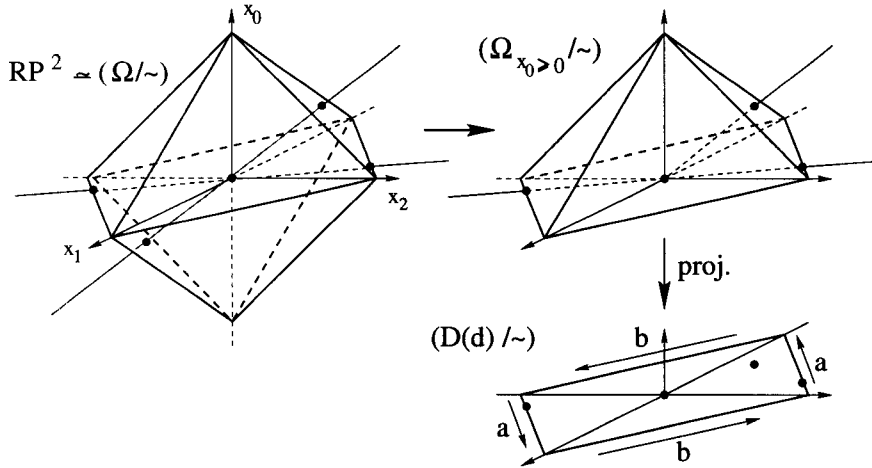


Figure 6: Diagram representing the homeomorphism between $\mathbb{R}P^2$ and $(D(d)/\sim)$

3.2 Congruent homeomorphisms

The group of the octahedron Ω is a group of 48 elements. It is decomposed into a group of order two (the group of symmetries through the origin) which we identify with $\mathbb{Z}_2 = (\mathbb{Z}/2\mathbb{Z})$, and a group Oct of orientation preserving motions composed by:

- The identity (one element),
- The rotations of angles $\pi/2, \pi, 3\pi/2$ around each of the three coordinate axis (nine elements),
- The rotations of angles $\pi/3, 2\pi/3$ around each of the four lines $\{\pm x_i = \pm x_j = \pm x_k\}$ (eight elements),
- The rotations of angle π around the six lines $\{x_i = \pm x_j, x_k = 0\}$ (six elements).

Since $\mathbb{R}P^2$ can be identified with the octahedron quotiented by the antipodal relation Ω/\sim , the group of the octahedron acts on the charts of $\mathbb{R}P^2$. It is clear that \mathbb{Z}_2 acts trivially, and Oct acts nontrivially. This gives 24 congruent mappings of $\mathbb{R}P^2$ to the diamond D .

For instance let ρ be the rotation of angle $\pi/2$ around the x_1 -axis, let U_i , $i = 1, 2, 3$ be the usual charts $\{(x_0 : x_1 : x_2) \in \mathbb{R}P^2, x_i \neq 0\}$, and let μ_0 be the homeomorphism introduced in section (3.1) $\mathbb{R}P^2 = U_0 \cup \{x_0 = 0\} \rightarrow D/\sim$. Then $\rho \cdot \mu_0 = \mu_2$ as shown in the following commutative diagram:

$$\begin{array}{ccc}
 U_0 \cup \{x_0 = 0\} & \xrightarrow{\rho} & U_2 \cup \{x_2 = 0\} \\
 \mu_0 \downarrow & & \downarrow \mu_2 \\
 (D(d)/\sim) & \longrightarrow & \rho \cdot (D(d)/\sim)
 \end{array}$$

Where $\mu_2(x_0 : x_1 : x_2) = (\frac{dx_0}{\sum x_i}, \frac{dx_1}{\sum x_i})$.

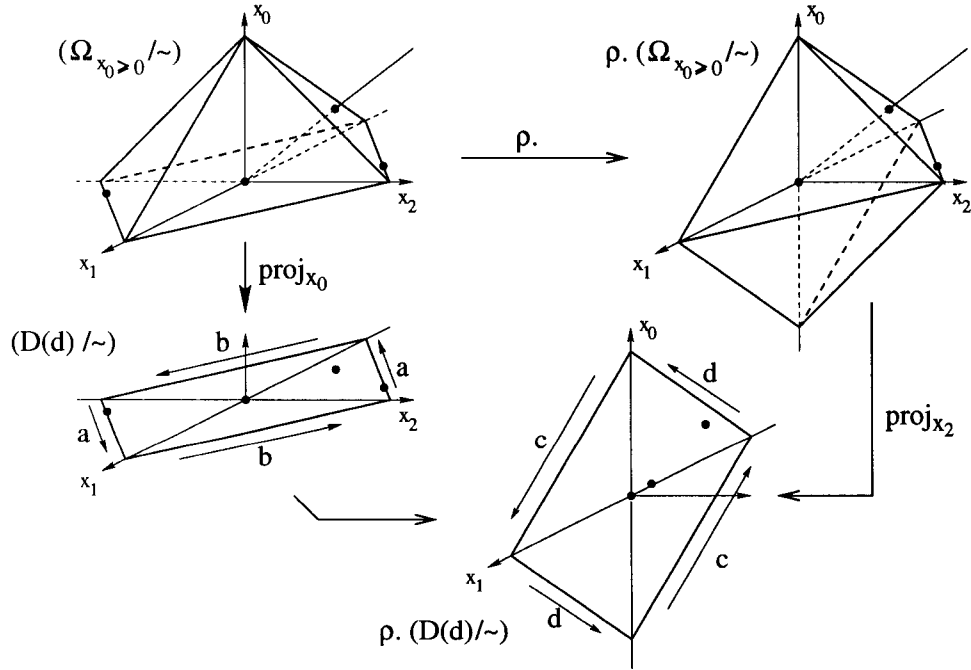


Figure 7: Explanation of the action of a rotation of angle $\mu/2$ around the x_1 axis.

The transformation $D(d) \rightarrow \rho \cdot D(d)$ is detailed from a geometric and combinatorial viewpoint on figures 7 and 8. Notice that the action on $D(d)$

of Oct corresponds to the action on the four symbols “ $(\sigma_{a,b} \cdot \mathbf{T})$ ”, $a, b \in \{0, 1\}$ of the group of permutation of four elements.

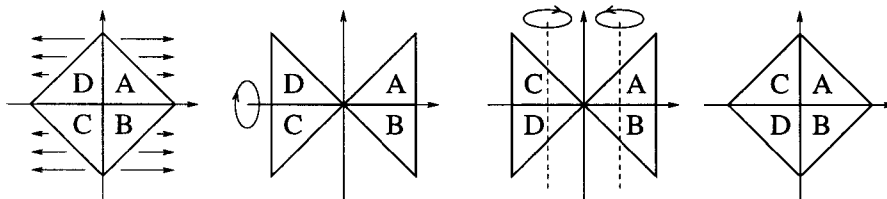


Figure 8: The same action from a cutting-squeezing-and-pasting point of view. Combinatorially it correspond to a permutation $A, B, C, D \mapsto A, B, D, C$.

4 Basic Properties of Lattice T-Curves

4.1 Ambient Surfaces of Lattice T-curves

Recall that in 2.4 we constructed from an arbitrary integral polygon $\Pi \in \mathbb{R}_{\geq 0}^2$ the surface $S(\Pi)$, which we called the ambient surface of lattice T-curves. We give now some properties of this surface. We note $\sigma_{a,b}$, like in 2.4, the symmetry $(x, y) \mapsto ((-1)^a x, (-1)^b y)$, where $a, b \in \{0, 1\}$.

4.1.0.4 Definition

The image of a copy $(\sigma_{a,b} \cdot \Pi)$ by the quotient map $q : \bigsqcup_{a,b} (\sigma_{a,b} \cdot \Pi) \rightarrow S(\Pi)$ is a *quadrant* of $S(\Pi)$. Since q is one-to-one from a given copy $(\sigma_{a,b} \cdot \Pi)$ to its image, we will identify (abusively) a quadrant with its pre-image $(\sigma_{a,b} \cdot \Pi)$.

4.1.1 The local structure around the lift of a vertex

Let u be a vertex of Π . Assume first that u is of even parity, so the two segments l and l' of $\partial\Pi$ meeting at u are of same parity. The construction in section 2.4.1 implies then that two copies of Π will be glued to one another by identifying the two corresponding copies of $l \cup l'$, and the two other copies of Π will be glued to one another by identifying the two other copies of $l \cup l'$ (see fig. 9).

Assume now that u is of odd parity. The construction in section 2.4.1 implies that the four copies of Π are glued to one another in the following way: The union of l with a reflection of l through a coordinate axis is identified to the union of the two other copies of l and the union of l' with a reflection of l' through the other coordinate axis is identified to the union of the two other copies of l' (see fig. 9).

If all the segments of $\partial\Pi$ are of the same parity, then two copies of Π will be glued to one another by all their edges, and the two other copies of Π will be also glued to one another by all their edges. We get this way two connected components, each homeomorphic to a sphere (see an example on fig. 10).

Assume now that the parity of the segments of $\partial\Pi$ takes at least two values. Notice that since the two endpoints u and u' of a broken edge l are vertices of odd parity, they lift each to only one point in $S(\Pi)$. All the other points of l lift to two points. Therefore the lift $\mu^{-1}(l)$ of l in $S(\Pi)$ is a circle which is a ramified twofold covering of l , where the ramifications take place in the lifts $\mu^{-1}(u)$ and $\mu^{-1}(u')$.

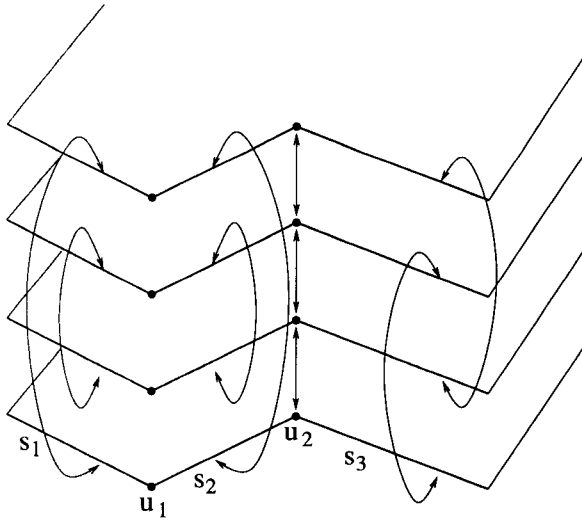


Figure 9: How the segments in the lift of a broken edge are identified two by two according to their parity. Here s_1 and s_2 have same parity and have different parity than s_3 .

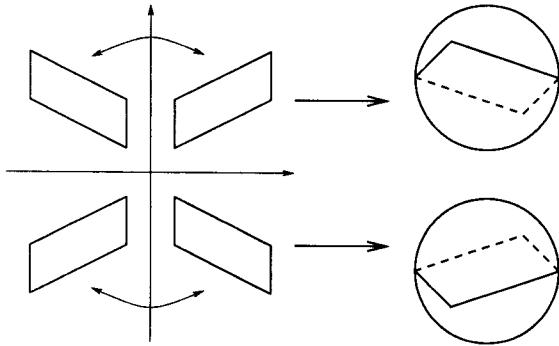


Figure 10: Gluing the four copies of Π to one another gives a union of two spheres when all the segments of $\partial\Pi$ have same parity.

4.1.2 Canonical charts for the ambient surface

Let l_1, \dots, l_r be the broken edges of Π , indexed such that l_i meets l_{i+1} , $i \bmod r$, and let u_i be the vertex of Π where they meet. Let

$$U_i = S(\Pi) \setminus \left(\bigcup_{j \neq i, j \neq i+1} \mu^{-1}(l_j) \right)$$

So U_i is an open neighborhood of $\mu^{-1}(u_i)$ in $S(\Pi)$ and is homeomorphic to \mathbb{R}^2 . We will assume that the broken edges are oriented locally near their endpoints, away from their endpoints. So $\mu^{-1}(l_i)$ and $\mu^{-1}(l_{i+1})$ are oriented in U_i .

4.1.2.1 Definition

The open neighborhood U_i equipped with a homeomorphism $U_i \rightarrow \mathbb{R}^2$ mapping $\mu^{-1}(l_i)$ and $\mu^{-1}(l_{i+1})$, with their orientations, onto the coordinate axis Ox and Oy is a (*oriented*) *chart* of $S(\Pi)$. The system of charts U_1, \dots, U_r will be called a *canonical system of charts* for $S(\Pi)$.

Notice that the chart U_i tell how to glue the four quadrants of $S(\Pi)$ onto $\mu^{-1}(l_i)$ and $\mu^{-1}(l_{i+1})$.

4.1.2.2 Definition

We call (*open*) *quadrants of the chart* U_i and denote $U_i^{0,0}$, $U_i^{0,1}$, $U_i^{1,1}$, and $U_i^{1,0}$ the connected components of $U_i \setminus (\mu^{-1}(l_i) \cup \mu^{-1}(l_{i+1}))$ such that $U_i^{a,b}$ is mapped to the set $\{(x, y) \in \mathbb{R}^2, (-1)^a x > 0, (-1)^b y > 0\}$.

Notice that the closure in $S(\Pi)$ of an open quadrant $U_i^{a,b}$ is a quadrant $(\sigma_{c,d} \cdot \Pi)$ of $S(\Pi)$. So the chart is determined by the correspondence $(c, d) \mapsto (a, b)$.

4.1.2.3 Definition

We call *the parity matrix of the chart* U_i , the matrix $M_i = \begin{pmatrix} \alpha_i & \alpha_{i+1} \\ \beta_i & \beta_{i+1} \end{pmatrix}$ where (α_j, β_j) is the parity of the segments of the broken edge l_j .

4.1.2.4 Lemma

If the closed quadrant $\bar{U}_i^{a,b}$ of the chart U_i is equal to the quadrant $(\sigma_{c,d} \cdot \Pi)$ of $S(\Pi)$, then $(a, b) = ((c, d) \cdot M_i)$.

proof. With our choice of local orientations for the broken edges, $\bar{U}_i^{0,0}$ is always equal to $\Pi = (\sigma_{0,0} \cdot \Pi)$, so the permutation $(c, d) \mapsto (a, b)$ can be considered as an element of $GL(2, \mathbb{Z}_2)$. Since $\bar{U}_i^{0,1}$ and $\bar{U}_i^{1,0}$ correspond to the quadrants $(\sigma_{c,d} \cdot \Pi)$ glued to quadrant Π along $\mu^{-1}(l)_i$ and $\mu^{-1}(l)_{i+1}$ respectively, we get from the construction in section 2.4.1 that

$$(c, d) = \begin{cases} (\beta_i, \alpha_i) & \text{if } (a, b) = (0, 1) \\ (\beta_{i+1}, \alpha_{i+1}) & \text{if } (a, b) = (1, 0) \end{cases}$$

Notice that this is equivalent to $(c, d) = M_i^{-1}(a, b)$. □

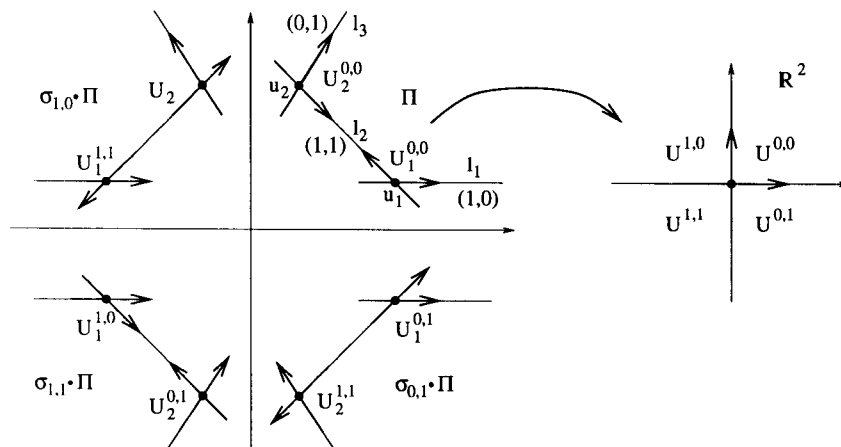


Figure 11: A local orientation of all the broken edges determines the label of the quadrants by the $U_i^{a,b}$. Here the parity of the broken edges l_i is in parentheses. Notice that with the local orientations shown $U_i^{0,0}$ is always equal to Π .

Notice that the transformations $M_i \mapsto M_j$ correspond to the gluing of the chart U_i with the chart U_j .

4.1.2.5 Definition

We will call $M_{i,j} : M_i \mapsto M_j$ the *gluing transformation* of the parity matrices M_i and M_j .

4.1.3 Gluing two charts of the ambient surface

Assume now that Π has more than two broken edges. Let U_1, \dots, U_r be a canonical system of charts of $S(\Pi)$.

Let $\eta_i = 0$ if the broken edge l_i has even parity, and $\eta_i = 1$ if l_i has odd parity. Then the gluing of two consecutive charts U_1 and U_{i+1} is easily stated:

4.1.3.1 Lemma

The gluing transformation $M_{i,i+1}$ is given by the matrix $\begin{pmatrix} 0 & 1 \\ 1 & \eta_i \end{pmatrix}$ and the right-product: $M_{i+1} = M_i \cdot M_{i+1,i}$

proof. We assume without loss of generality that $i = 2$, so we will compute

with:

$$M_1 = \begin{pmatrix} \alpha_1 & \alpha_2 \\ \beta_1 & \beta_2 \end{pmatrix} \quad \text{and} \quad M_2 = \begin{pmatrix} \alpha_2 & \alpha_3 \\ \beta_2 & \beta_3 \end{pmatrix}$$

Notice that the parities (α_1, β_1) and (α_3, β_3) of the segments of the broken edges l_1 and l_3 are equal if and only if l_2 has even parity, so the lemma holds when $\eta_2 = 0$. Assume that $(\alpha_3, \beta_3) \neq (\alpha_1, \beta_1)$, so $\eta_2 = 1$. Since the parities belong to $(\mathbb{Z}_2)^2$ and are never even, and since $(\alpha_1, \beta_1) \neq (\alpha_2, \beta_2)$, then $(\alpha_3, \beta_3) = (\alpha_1, \beta_1) + (\alpha_2, \beta_2)$. \square

Notice that if an integral polygon Π has only two broken edges, then the canonical system of charts for $S(\Pi)$ has only two charts. Since the parity of the segments of $\partial\Pi$ take only two values the gluing of the two charts make up a surface $S(\Pi)$ which is a sphere (see fig. 12).

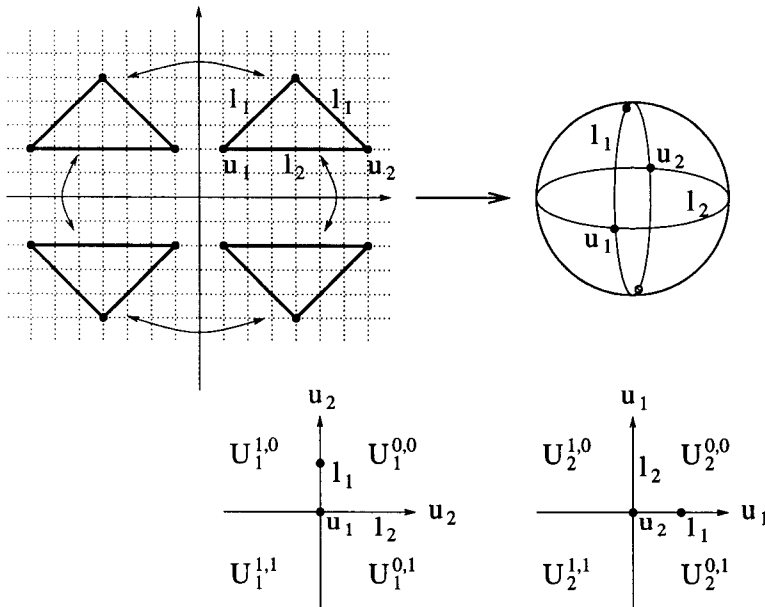


Figure 12: Gluing the four copies of Π to one another gives a sphere when Π has only two broken edges.

Notice that the gluing transformation of any parity matrices is equal to the product of the transformations of consecutive parity matrices:

$$M_{i,j} = \prod_{k=0}^{j-i-1} M_{i+k,i+k+1}$$

4.1.3.2 Definition

The canonical system of charts U_i equipped with the gluing transformations $M_{i,j}$ is the *canonical atlas structure* of $S(\Pi)$.

4.1.3.3 Corollary

If l_i has even parity, then a tubular neighborhood of $\mu^{-1}(l_i)$ is an annulus.

If l_i has odd parity, then a tubular neighborhood of $\mu^{-1}(l_i)$ is a Moebius band.

proof. With our choice of local orientations for the broken edges of Π we have always

$$U_{i+1}^{0,0} = U_i^{0,0} \quad \text{and} \quad U_{i+1}^{0,1} = U_i^{1,0}$$

and either

$$U_{i+1}^{1,0} = U_i^{0,1} \quad \text{and} \quad U_{i+1}^{1,1} = U_i^{1,1}$$

In which case the tubular neighborhood of l_i is an annulus (see fig. 13), or

$$U_{i+1}^{1,0} = U_i^{1,1} \quad \text{and} \quad U_{i+1}^{1,1} = U_i^{0,1}$$

In which case the tubular neighborhood of l_i is a Moebius band (see fig. 13).

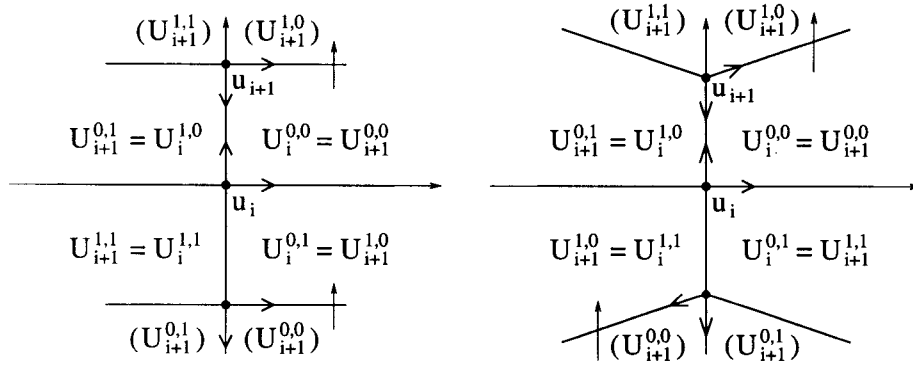


Figure 13: The tubular neighborhood of the lift $\mu^{-1}(l)$ of a broken edge l is either an annulus if l is even, either a Moebius band if l is odd.

So let's compute $U_{i+1}^{1,0}$. The closed quadrants $U_{i+1}^{\bar{0},0}$ are always represented by Π . Let $(\sigma_{c,d} \cdot \Pi)$ be the quadrant representing $U_{i+1}^{\bar{0},1}$, so

$$(0, 1) = (c, d) \cdot M_i$$

$(\sigma_{c,d} \cdot \Pi)$ represents also a closed quadrant $U_{i+1}^{-a,b}$, so

$$(a, b) = (c, d) \cdot M_{i+1}$$

Since $M_{i+1} = M_i \cdot M_{i,i+1}$ we get that

$$(a, b) = (0, 1) \cdot M_{i,i+1}$$

From lemma 4.1.3.1 we get directly that $(a, b) = (1, 0)$ if l_i is even (hence we get an annulus), and $(a, b) = (1, 1)$ if l_i is odd (hence we get a Moebius band). \square

Notice from lemma 4.1.3.1 that, given a canonical system of charts, the gluing transformations of consecutive charts are determined by the sequence of the η_i 's equal to 0 when the broken edge l_i is even, and to 1 when l_i is odd. So two integral polygons with the same sequence of η_i 's up to circular permutation give rise to homeomorphic ambient surfaces.

4.1.4 A basis for the 1-homology of the ambient surface

Let $S(\Pi)$ be the ambient surface of a lattice T-curve, and assume that Π has more than two broken edges. Let U_1, \dots, U_r be a canonical system of charts on $S(\Pi)$. Recall that with the notations of the charts, the l_i 's are the broken edges of Π with endpoints u_{i-1} and u_i .

4.1.4.1 Lemma

The lifts $\mu^{-1}(l_3), \dots, \mu^{-1}(l_r)$ of the broken edges l_3, \dots, l_r form a basis for the 1-homology space $H_1(S(\Pi))$ (with coefficients in \mathbb{Z} if $S(\Pi)$ is orientable, and with coefficients in \mathbb{Z}_2 if $S(\Pi)$ is not orientable).

proof. To prove this lemma it suffices to check three points:

- The set $\{\mu^{-1}(l_3), \dots, \mu^{-1}(l_r)\}$ is free in H_1 since $S(\Pi) \setminus (\cup_3^r \mu^{-1}(l_i))$ is connected.
- The set $\{\mu^{-1}(l_3), \dots, \mu^{-1}(l_r)\}$ is complete since $S(\Pi) \setminus (\cup_3^r \mu^{-1}(l_i))$ is simply connected.
- The set $\{\mu^{-1}(l_3), \dots, \mu^{-1}(l_r)\}$ has no trivial elements since for any $\mu^{-1}(l_j)$, the surface $(S(\Pi) \setminus (\cup_3^r \mu^{-1}(l_i))) \cup \mu^{-1}(l_j)$ is either an open annulus, either an open Moebius band.

\square

4.1.5 The topological characterization of an ambient surface

We have seen in 4.1.1 that if the parity of the segments of the boundary of an integral polygon Π takes only one value, then the surface $S(\Pi)$ has two connected components, each homeomorphic to a sphere. Assume now that the parity of the segments of $\partial\Pi$ takes more than one value. This implies with lemma 2.3.0.14 that Π has at least two broken edges.

4.1.5.1 Lemma

- *If Π has a broken edge of odd parity, then it has two broken edges of odd parity.*
- *If Π has two consecutive broken edges of odd parity, then it has three broken edges of odd parity.*

proof. Let U_1, \dots, U_r be a canonical system of charts on the surface $S(\Pi)$. From lemma 4.1.3.1, we get that, to each broken edge of odd parity, correspond a gluing matrix $A_1 = \begin{pmatrix} 0 & 1 \\ 1 & 1 \end{pmatrix}$ and to each broken edge of even parity correspond a gluing matrix $A_0 = \begin{pmatrix} 0 & 1 \\ 1 & 0 \end{pmatrix}$. The product \prod of all gluing matrices of consecutive charts must be the identity. Since the product with A_0 just permutes the columns, if \prod contains a matrix A_1 then it must contains at least two matrices A_1 . Since $A_1^2 = \begin{pmatrix} 1 & 1 \\ 1 & 0 \end{pmatrix}$, if \prod contains two consecutive matrices A_1 , then it must contains at least three matrices A_1 . \square

4.1.5.2 Proposition

Let $r > 1$ be the number of broken edges of Π .

- *The surface $S(\Pi)$ is orientable if and only if the parity of the segments of $\partial\Pi$ takes only two values.*
- *If $S(\Pi)$ is orientable, then r is even, and $S(\Pi)$ is the connected sum of $r/2 - 1$ tori.*
- *If $S(\Pi)$ is not orientable, then it is the connected sum of $r - 2$ projective planes.*

proof. From corollary 4.1.3.3 we know that the tubular neighborhoods of the lifts of the broken edges of Π are all annuli if and only if all the broken

edges are of even parity. From lemma 4.1.4.1, we know that the lifts of all the broken edges but two consecutive ones is a basis of the 1-dimensional homology space of $S(\Pi)$. From lemma 4.1.5.1 we know that if all but two consecutive broken edges are known to be of even parity, then all the broken edges are of even parity.

Therefore $S(\Pi)$ is orientable if and only if all its broken edges are of even parity. From definition 2.3.0.16 it is clear that the broken edges are all of even parity if and only if the parity of the segments of $\partial\Pi$ takes only two values.

From lemma 4.1.4.1 we know that the dimension of the 1-dimensional homology space of $S(\Pi)$ is $r - 2$. Since $r > 1$, the parity of the segments of $\partial\Pi$ takes more than one value, and then $S(\Pi)$ is connected. So if $S(\Pi)$ is orientable, it is the connected sum of $(r - 2)/2$ tori, and if it is non-orientable, it is the connected sum of $r - 2$ projective planes. \square

4.2 Isomorphic T-curves

4.2.1 Translation of the carrier polygon

Let Π be an integral polygon in $\mathbb{R}_{\geq 0}^2$, and (s, t) be an integral vector such that the translated polygon $\Pi' = \Pi + (s, t)$ lies in $\mathbb{R}_{\geq 0}^2$, and let $K(\Pi, \mathcal{T}, \delta)$ be a T-curve. Let \mathcal{T}' be the triangulation of Π' translated from \mathcal{T} , and let δ' be the sign distribution on $\Pi' \cap \mathbb{Z}^2$ defined by $\delta'(x, y) = \delta(x - s, y - t)$.

4.2.1.1 Proposition

The T-curves $K = K(\Pi, \mathcal{T}, \delta)$ and $K' = K(\Pi', \mathcal{T}', \delta')$ are equal.

proof. It is clear that the construction of the ambient surface $S(\Pi)$ depends on Π up to translation by an integral vector, so $S(\Pi') = S(\Pi)$. Let (c, d) be the parity of the point (s, t) , and let $a, b \in \{0, 1\}$. If $(x, y) \in \Pi$, then $\delta'((-1)^a(x + s), (-1)^b(y + t)) = (-1)^{(a,b),(c,d)}\delta((-1)^ax, (-1)^by)$. Recall that the sign of an edge of a triangulation is the product of the signs of its two endpoints. Therefore the edges of the triangulation of $S(\Pi')$ have the same sign than the corresponding edges of the triangulation of $S(\Pi)$, so $K = K'$. \square

4.2.2 Linear transformation of the carrier polygon

If K is a lattice T-curve with carrier polygon Π , and $c, d \in \{0, 1\}$, let $K^{c,d}$ be the restriction of K to the quadrant $(\sigma_{c,d} \cdot \Pi)$.

Let $K(\Pi, \mathcal{T}, \delta)$ be a lattice T-curve and let $A \in GL(2, \mathbb{Z})$. We will note A_2 the reduction of A in $GL(2, \mathbb{Z}_2)$. Let \mathcal{T}' be the triangulation of $(A \cdot \Pi)$ transformed by A from \mathcal{T} , let $\delta'(x, y) = \delta(A^{-1} \cdot (x, y))$, and let $A \cdot K$ be the T-curve defined by $(A \cdot \Pi, \mathcal{T}', \delta')$.

4.2.2.1 Proposition

- $A \cdot K$ and K are congruent.
- The homeomorphism $S(\Pi) \rightarrow S(A \cdot \Pi)$ which transforms K to $A \cdot K$, transforms each restriction $K^{c,d}$ into a restriction $(A \cdot K)^{s,t}$.
- $(c, d) = (s, t) \cdot A_2$.

proof. Since all the parities are transformed by A_2 , an edge e of the triangulation \mathcal{T} is of even parity if and only if the edge $A \cdot e$ of \mathcal{T}' is of even parity. So it is clear from prop. 4.1.5.2 that $S(A \cdot \Pi)$ and $S(\Pi)$ are homeomorphic.

Let U and U' be canonical charts of $S(\Pi)$ and of $S(A \cdot \Pi)$ around an arbitrary vertex (of odd parity) u and around $A \cdot u$ respectively. For any $a, b \in \{0, 1\}$, let $(\sigma_{c,d} \cdot \Pi)$ be the quadrant of $S(\Pi)$ representing $U^{a,b}$, and $(\sigma_{s,t} \cdot (A \cdot \Pi))$ be the quadrant of $S(A \cdot \Pi)$ representing $(U')^{a,b}$. Let M be the parity matrix of U . Then $(A_2 \cdot M)$ is the parity matrix of U' . From lemma 4.1.2.4 we get that

$$(a, b) = (c, d) \cdot M \quad \text{and} \quad (a, b) = (s, t) \cdot (A_2 \cdot M)$$

Therefore $(c, d) = (s, t) \cdot A_2$.

To prove the proposition, we must show that the T-curve K is congruent to $A \cdot K$ by a homeomorphism $U \rightarrow U'$ such that for any $a, b \in \{0, 1\}$, $U^{a,b} \mapsto U'^{a,b}$. It suffices then to show that the sign of an edge of the triangulation of $(\sigma_{c,d} \cdot \Pi)$ is equal to the sign of the corresponding edge of the triangulation of $(\sigma_{s,t} \cdot (A \cdot \Pi))$:

Let e be a segment of $\partial\Pi$ and (a, b) its parity. So $((a, b) \cdot {}^t A_2)$ is the parity of $(A \cdot e)$. From the definition of the sign distribution δ' of $(A \cdot K)$, we get that the sign of $(A \cdot e)$ is equal to the sign of e . Then from the construction in section 2.4.1 we get that

$$\begin{aligned}
\text{sign}(\sigma_{s,t} \cdot (A \cdot e)) &= (-1)^{\langle (s,t), (a,b) \cdot {}^t A_2 \rangle} \text{sign}(A \cdot e) \\
&= (-1)^{\langle (s,t) \cdot A_2, (a,b) \rangle} \text{sign}(e) \\
&= (-1)^{\langle (c,d), (a,b) \rangle} \text{sign}(e) \\
&= \text{sign}(\sigma_{c,d} \cdot e)
\end{aligned}$$

□

4.3 Definitions

4.3.0.2 Definition

A *primitive segment* is an integral segment such that the only integral points it contains are its two ends. The *integral length* (or simply *length*) of an integral polygonal line is the number of primitive segments contained in it. Two integral points are *neighbors* if they can be connected by a primitive segment.

4.3.0.3 Definition

A *primitive triangulation* of an integral polygon is a triangulation of the polygon such that the vertices of the triangulation are integral points, and the only integral points a triangle contains are its three vertices.

Notice that a triangulation of an integral polygon is primitive if and only if its set of vertices is exactly the set of integral points of the polygon. So the triangulation \mathcal{T} of a lattice T-curve $K(\Pi, \mathcal{T}, \delta)$ is a primitive triangulation of Π .

4.3.0.4 Definition

A piece of a curve homeomorphic to the segment $[0, 1] \subset \mathbb{R}$ is called an *arc* of the curve.

4.3.0.5 Definition

Let K be a collection of disjoint embedded circles in a surface. A connected component of K is called an *oval* if it bounds a subset of the surface homeomorphic to a disk. The interior of this subset is called the *inside* of the oval. The interior of the complementary of the inside is the *outside* of the oval. An oval with no other ovals inside will be called an *empty oval*, and an oval inside no other ovals will be called an *outermost oval*. A connected component of K which is not an oval is called a *nontrivial component* of K .

4.3.0.6 Proposition

Let $K(\mathbf{T}(d), \mathcal{T}, \delta)$ be a lattice T-curve on $\mathbb{R}P^2$. Then

- K has only ovals as connected components if its degree d is even.
- K has one and only one nontrivial component if its degree d is odd.

proof. It is clear that on $\mathbb{R}P^2$ two nontrivial embedded circles which intersect transversally, intersect an odd number of times, and an oval which is intersected by any embedded circle transversally is intersected an even number of times. Therefore, since K is a disjoint union of embedded circles, it has at most one nontrivial connected component.

Consider now a path on the diamond $D(d)$ through the edges of the triangulation \mathcal{T} , going from one point of the boundary of the diamond to its opposite point. This path lifts to a loop on $\mathbb{R}P^2$ which is a nontrivial embedded circle and which cuts transversally K . So the loop intersects K an odd number of times if and only if K has a nontrivial connected component.

Let's follow the path from one endpoint to the other. If the loop intersects the T-curve r times, then the integral points on the path change signs r times. So r is odd if and only if the two endpoints of the path have opposite signs. The formula 1 for the extension of the sign distribution from the triangle $\mathbf{T}(d)$ to the diamond $D(d)$ shows that two opposite points on the boundary of $D(d)$ have opposite signs if and only if the degree d of the T-curve is odd. \square

Notice that this lemma holds for a real projective nonsingular curve and can be proved in a similar way which is in that case a direct consequence of Bezout theorem applied to the curve and a generic line.

Notice that if an oval O of a T-curve lies inside a quadrant of the ambient surface then all the integral points lying inside O and outside any oval which lies inside O have same sign.

4.3.0.7 Definition

Let O be an oval of a T-curve, which lies inside a quadrant of the ambient surface. The *sign of the oval* O is the sign of the integral points lying inside O and outside any oval which lies inside O . The remark above shows that this definition is coherent.

5 The T-filling of a lattice T-curve K .

Recall from definition 1.0.0.1 that a T-curve on a surface S lies on the 1-skeleton of a dual cell decomposition of the triangulation of S . For lattice T-curves $K(\Pi, \mathcal{T}, \delta)$, we always work with the dual barycentric cell decomposition of the triangulation of the ambient surface $S(\Pi)$. An edge of the 1-skeleton of the dual decomposition connects the barycentres of two adjacent triangles.

5.0.1 Incidence Graphs

5.0.1.1 Definition

The *incidence graph of the triangulation of $S(\Pi)$* is the graph obtained from the 1-skeleton of the dual decomposition by subdividing each edge by a new vertex at the intersection of the edge with its dual. The image G by the projection $\mu : S(\Pi) \rightarrow \Pi$ of this graph will be called the *incidence graph of the triangulation of Π* .

In accordance with section 2.4.2, every edge of the incidence graphs inherit of the sign of the edge of the triangulation it intersects.

Notice that each edge of the incidence graph G of the triangulation of Π lifts to four edges of the incidence graph $\mu^{-1}G$ of the triangulation of $S(\Pi)$.

5.0.1.2 Lemma

For each edge of G , there is exactly two edges, among its four lifts in $\mu^{-1}G$, which have negative sign.

proof. Let e be an edge of the triangulation \mathcal{T} of Π , and let (a, b) be its parity. Recall the formula 3 which gives the sign of a copy $(\sigma_{c,d} \cdot e)$ of an edge e :

$$\text{sign}(\sigma_{c,d} \cdot e) = (-1)^{\langle (a,b), (c,d) \rangle} \text{sign}(e)$$

Notice that $\langle (a, b), (c, d) \rangle = 0$ if and only if $(c, d) = (0, 0)$ or $(c, d) = (b, a)$. Since the parity of a segment is never even, (b, a) is not $(0, 0)$. Therefore there is exactly two edges, among the four which lift from e , which have same sign than e (so there is also two edges which have opposite sign than e). This proves the assertion, since every edge of $\mu^{-1}G$ inherits of the sign of the edge of the triangulation of $S(\Pi)$ that it intersects. \square

5.1 The Construction

Let $K(\Pi, \mathcal{T}, \delta)$ be a lattice T-curve, and let G be the incidence graph of \mathcal{T} . Each component \tilde{C} of K is a cycle (in the language of graph theory) in the incidence graph $\mu^{-1}G$ of the triangulation of $S(\Pi)$, i.e. \tilde{C} is a cyclic sequence of edges of G , each edge sharing one end with the previous edge and the other end with the next edge. These cycles don't intersect. The projection $C = \mu(\tilde{C})$ on Π will be considered as the cycle made up by the projections of the edges of \tilde{C} . These cycles may intersect.

5.1.0.3 Definition

a *thick Y* is a tubular neighborhood of the three edges of G lying in a triangle of the triangulation \mathcal{T} .

Let e_1, e_2 and e_3 be the three edges of G lying in a triangle t of \mathcal{T} , and indexed counterclockwise, and let A and B_i be the endpoints of e_i . The thick Y is obtained by gluing three ribbons $e_i \times [-1, +1]$ by identifying $A \times [-1, 0]$ in e_i with $A \times [0, +1]$ in e_{i+1} by $(A, x) \mapsto (A, -x)$ (see fig. 14).

From lemma 5.0.1.2 we get that every union $e_i \cup e_{i+1}$ is an arc of some cycle C of G , image by the projection $\mu : S(\Pi) \rightarrow \Pi$ of a connected component of the T-curve.

Let t' be a triangle of \mathcal{T} adjacent to t , and let e'_1, e'_2 and e'_3 be the three edges of G lying in t' , indexed counterclockwise, with endpoints A' and B'_i , and such that $B'_1 = B_1$. Let $s_1 = B_1 \times [-1, +1]$ be an end-segment of the thick Y in t , and let $s'_1 = B'_1 \times [-1, +1]$ be the corresponding end-segment of the thick Y in t' .

In the disjoint union of the two thick Y 's in $t \cup t'$, we identify s_1 with s'_1 :

1. either by $(B_1, x) \mapsto (B'_1, -x)$ if $(e_2 \cup e_1) \cup (e'_1 \cup e'_3)$ is an arc of some cycle C . So $(e_3 \cup e_1) \cup (e'_1 \cup e'_2)$ is an arc of some cycle C' .
2. either by $(B_1, x) \mapsto (B'_1, x)$ if $(e_2 \cup e_1) \cup (e'_1 \cup e'_2)$ is an arc of some cycle C . So $(e_3 \cup e_1) \cup (e'_1 \cup e'_3)$ is an arc of some cycle C' .

Notice that in each case C' may be equal to C .

5.1.0.4 Definition

We will say that two thick Y 's are *glued with a twist* in the case (2) above, and *glued without a twist* in the case (1) above (see fig. 14).

Since the adjacency graph is connected, we obtain, by gluing in this way the thick Y 's of all the triangles of \mathcal{T} , a surface with boundary.

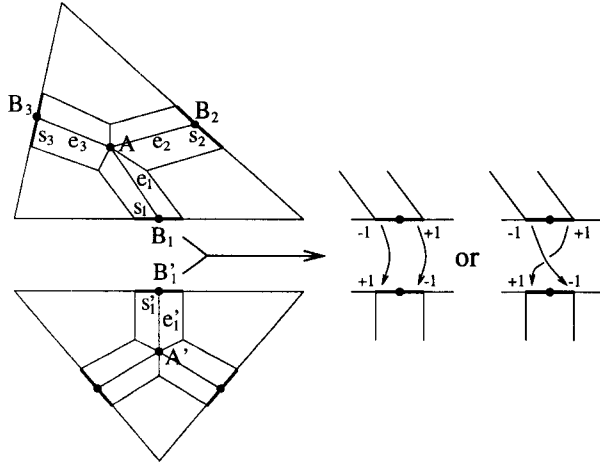


Figure 14: A thick Y is glued from three ribbons, and two thick Y's are glued with or without a twist.

5.1.0.5 Definition

The surface with boundary constructed above from a lattice T-curve K will be called a *T-filling*, and will be denoted $F(K)$.

Notice from the construction of the T-filling $F(K)$, that the connected components of $F(K)$ are in one-to-one correspondence with the connected components of K .

5.2 The relation with algebraic geometry

A real plane projective curve $C(f)$ of degree d is a subset $\{(x_0 : x_1 : x_2) \in \mathbb{R}P^2, f(x_0, x_1, x_2) = 0\}$ for some homogeneous polynomial f of degree d with real coefficients. The complexification $\mathbb{C}C$ of C is the surface $\{(x_0 : x_1 : x_2) \in \mathbb{C}P^2, f(x_0, x_1, x_2) = 0\}$ in $\mathbb{C}P^2$. The curve is non-(complex)-singular if the derivative is a nonzero function in all points of the curve (of its complexification). Notice that $\mathbb{C}C$ is invariant under the complex conjugation.

Let K be a lattice T-curve of degree d on $\mathbb{R}P^2$. We have seen in section 2.2 that the algebraic analog of K is a real plane projective nonsingular curve of degree d , and with a convexity assumption on the triangulation defining K , this is more than an analogy, this is a theorem (Viro [11]). Now the algebraic analog of the T-filling $F(K)$ is the quotient of the complexification of a real

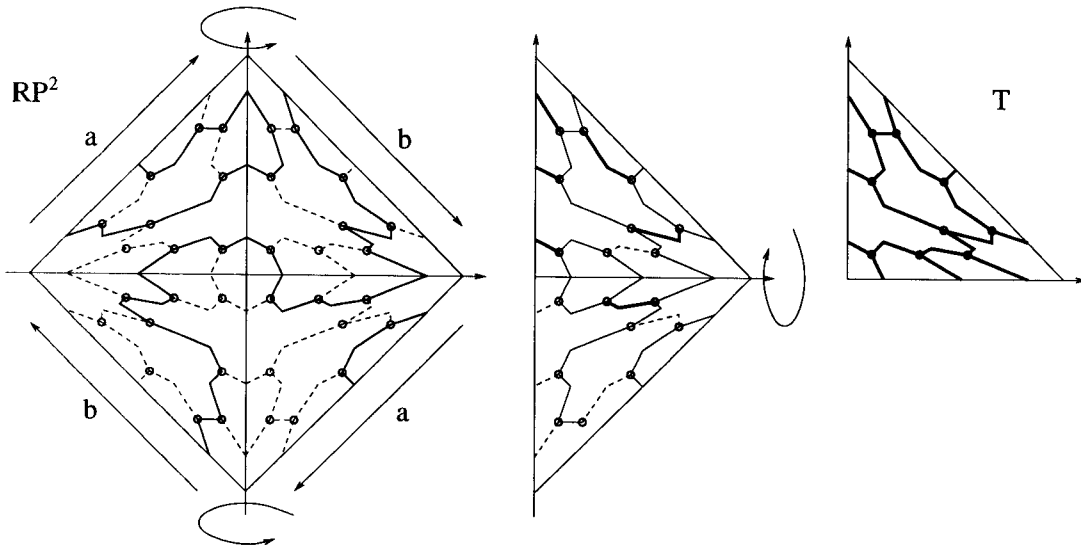


Figure 15: The T-curve (plain lines) is drawn on the incidence graph of the triangulation of $\mathbb{R}P^2$ (dotted lines). The folded T-curve on the incidence graph of the triangulation of \mathbf{T} uses every edge twice (thick plain lines).

plane projective non-complex-singular curve C of degree d by the complex conjugation.

It is well known that $\mathbb{C}C$ is an orientable surface of genus $\frac{(d-1)(d-2)}{2}$. Similarly the double of $F(K)$ is also a surface of genus $\frac{(d-1)(d-2)}{2}$. Indeed to double it we just have to let the (flat) thick Y's become "hollow Y's", to glue them without worrying about the the twists, and to close the open ends upon $\partial\mathbf{T}$ by disks (see fig. 17). The number of handles of this surface is equal to the number of interior integral points of \mathbf{T} , and this is precisely $\frac{(d-1)(d-2)}{2}$. Moreover the number of connected components of the boundary is the number of connected components of K . Therefore the T-filling of a lattice T-curve is characterized topologically the same way than the quotient of $\mathbb{C}C$ by the complex conjugation.

The analogy goes further. The quotient of the complexification of a real projective nonsingular curve C defines the type (I or II) of C . If C is of type I, then it gets two opposite (complex)-orientations. Similarly the T-filling of a lattice T-curve K gives rise naturally to a type (I or II) of K , and two opposite orientations if K is of type I (see definitions in section 5.4). If K is a lattice T-curve on $\mathbb{R}P^2$, these definitions correspond to the types and

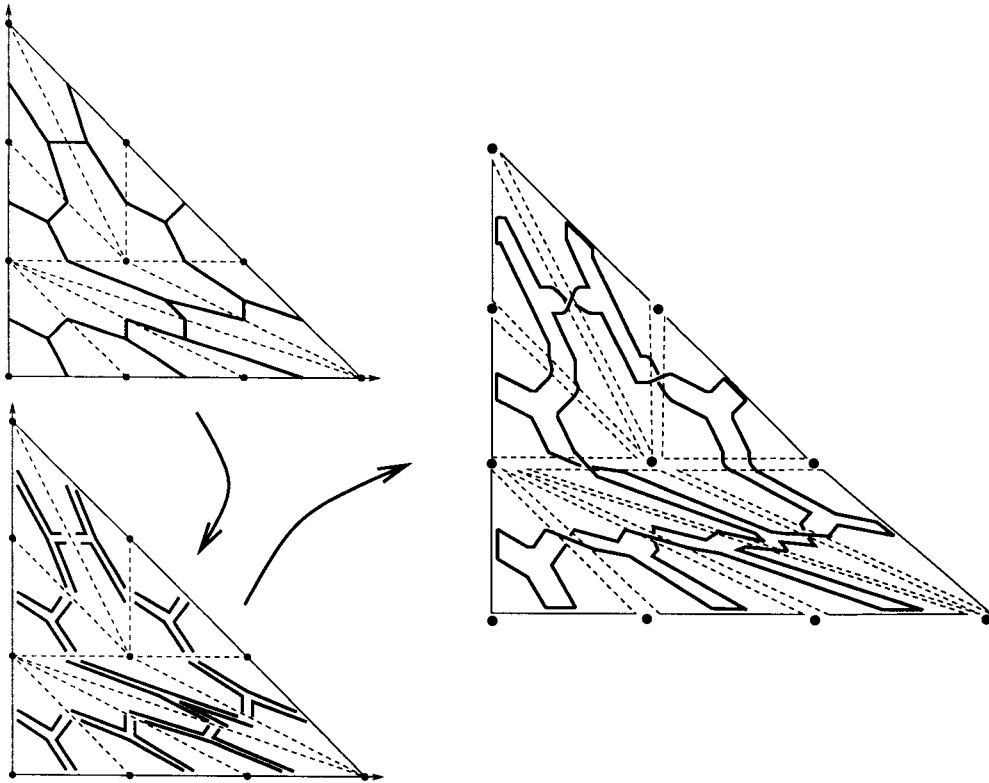


Figure 16: To construct the T-filling $F(K)$, thicken the Y's in each triangle, glue any two adjacent thick Y's with or without a twist (depending on K), and close the free ends with segments.

orientations of a real plane projective nonsingular curve of same degree.

5.3 First Application: The Harnack Theorem

5.3.1 The Harnack bound

5.3.1.1 Theorem (“Harnack” for lattice T-curves)

(1) *The number of connected components of a lattice T-curve is no more than the number of integral points in the interior of its carrier polygon, plus one.*

(2) *There are lattice T-curves with arbitrary carrier polygons which achieve the upper bound above.*

proof. Let's prove just (1) for the moment. (2) will be proved in prop. 5.3.2.5

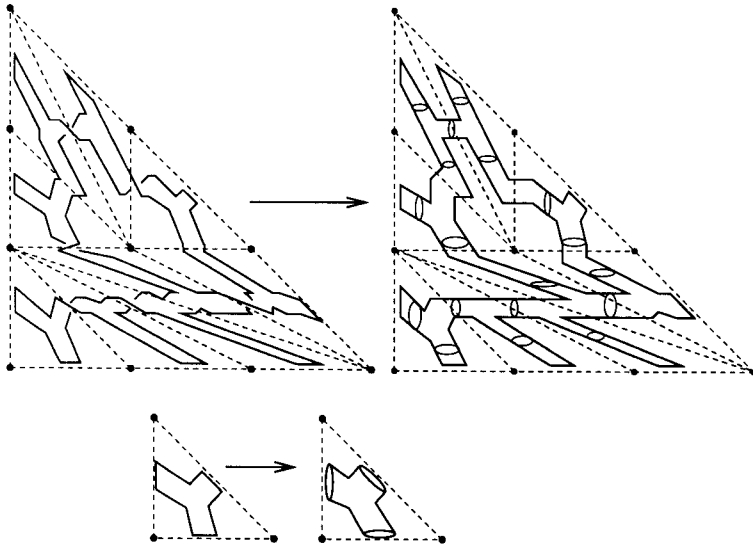


Figure 17: The double of a lattice T-curve of degree d on $\mathbb{R}P^2$ is a surface of genus $\frac{(d-1)(d-2)}{2}$.

where we will construct lattice T-curves with arbitrary carrier polygon which achieve the upper bound.

Let $K(\Pi, \mathcal{T}, \delta)$ be a lattice T-curve, and let i be the number of integral points in the interior of Π . Let's glue disks along $\partial F(K)$ to obtain from $F(K)$ a closed surface $S(K)$. It is clear from the construction of $F(K)$ that the incidence graph G of the triangulation \mathcal{T} is a retraction of $F(K)$, so let's consider $S(K)$ as the cell complex obtained by gluing disks on G along the cycles $\mu(C)$.

Let D be the number of disks glued to G , and let E' and V' be respectively the number of edges and vertices of G . Let T , E and V be respectively the numbers of triangles, edges and vertices of the triangulation \mathcal{T} of Π , and let l be the length of $\partial\Pi$. Each triangle of \mathcal{T} contains three edges of G so $E' = 3T$. The vertices of G lie in each triangle and each edge of \mathcal{T} , so $V' = T + E$.

On one hand the Euler characteristic of $S(K)$ is

$$\begin{aligned}
\chi(S') &= D - E' + V' \\
&= D - 3T + (T + E) \\
&= D + T - E + l && \text{Indeed since } \mathcal{T} \text{ is a triangulation} \\
&&& \text{we have } 3T = 2E - l \\
&= D + 1 - V + l && \text{Indeed from the Euler relation on } \mathcal{T} \\
&&& \text{we have } T - E + V = 1
\end{aligned}$$

On the other hand $\chi(S')$ is equal to $2 - 2g$ where g is the genus of S' . Therefore we get

$$\begin{aligned}
D &= (V - l) + 1 - 2g \\
&\leq i + 1 && \text{Since } V - l = i \text{ and } g \geq 0
\end{aligned}$$

This proves (1) since D is also the number of connected components of K .
□

5.3.1.2 Definition

A T-curve $K(\Pi, \mathcal{T}, \delta)$ with $i + 1$ connected component is called a *maximal* T-curve.

5.3.1.3 Corollary

A T-curve is maximal if and only if its T-filling is homeomorphic to a sphere with a positive number of holes.

proof. This statement follows from the proof of 5.3.1.1. Indeed the curve is maximal if the surface $S(K)$ has genus 0. Since a T-curve has at least one connected component, $F(K)$ is obtained from $S(K)$ by removing a positive number of disks. □

5.3.2 Harnack T-curves

Let K be a lattice T-curve with carrier polygon Π . Recall that the quadrants of the ambient surface $S(\Pi)$ are represented by the copies $(\sigma_{a,b} \cdot \Pi) = \{(x, y), ((-1)^a x, (-1)^b y) \in \Pi\}$, where $a, b \in \{0, 1\}$.

5.3.2.1 Definition

Let $c, a, b \in \{0, 1\}$, and let δ be the distribution of signs defined on the points $(x, y) \in (\sigma_{a,b} \cdot \Pi)$ by:

$$\delta(x, y) = \begin{cases} (-1)^c & \text{if } (x, y) \text{ is of even parity} \\ (-1)^{c+1} & \text{if } (x, y) \text{ is of odd parity} \end{cases}$$

The distribution of sign of a lattice T-curve deduced from δ by the formula 2 of section 2.4.2 will be called a *Harnack sign distribution*, and (c, a, b) will be called the *type* of δ . A lattice T-curve with a Harnack sign distribution will be called a *Harnack T-curve*.

In order to write a unique formula to describe a Harnack distribution of sign, let introduce the Iverson symbol $[P]$ equal to 1 if the proposition P is true, and equal to 0 if the proposition P is false. Now let $g, h = 0$ or 1 , let (x, y) be an integral point of $(\sigma_{g,h} \cdot \Pi)$, let (e, f) be the parity of (x, y) , and let (c, a, b) be the type of a Harnack distribution of signs δ on Π . Then we deduce immediately from the definition 5.3.2.1 above that

$$\delta(x, y) = (-1)^{c[(e,f) \neq (a,b)] + \langle (e,f), (g+a, h+b) \rangle} \quad (4)$$

5.3.2.2 Definition

Let Π be an integral polygon, and let a be an arc which splits Π into two connected components. We will say that a *surrounds an integral point P in Π* if P is the only integral point in the closure of one of the connected component of $\Pi \setminus a$.

5.3.2.3 Lemma

Let $K(\Pi, \mathcal{T}, \delta)$ be a Harnack curve, and let (c, a, b) be the type of δ . Then for every $g, h = 0$ or 1 , the integral points of parity $(b+h, a+g)$ will be surrounded in the quadrant $(\sigma_{g,h} \cdot \Pi)$ by an oval of K if they belong to the interior of the quadrant, or by an arc of K if they are on the boundary of the quadrant.

proof. According to formula 4 above, the sign of an integral point of parity (e, f) in quadrant (g, h) depend only on the value of the expression

$$[(e, f) \neq (0, 0)] + \langle (e, f), (g+a, h+b) \rangle \quad (5)$$

The following array displays the value of this expression for each parity (e, f) (one parity per line) in each quadrant $(g+a, h+b)$ (one quadrant per column):

	(0,0)	(1,0)	(1,1)	(0,1)
(0,0)	$0 + 0 = 0$	$0 + 0 = 0$	$0 + 0 = 0$	$0 + 0 = 0$
(1,0)	$1 + 0 = 1$	$1 + 1 = 0$	$1 + 1 = 0$	$1 + 0 = 1$
(1,1)	$1 + 0 = 1$	$1 + 1 = 0$	$1 + 0 = 1$	$1 + 1 = 0$
(0,1)	$1 + 0 = 1$	$1 + 0 = 1$	$1 + 1 = 0$	$1 + 1 = 0$

By looking at each row of the array we see that in a given quadrant, points of parity $(e, f) = (b+h, a+g)$ have opposite signs than their neighbors. This implies that they are separated from their neighbors by K (by an arc if the point is on the boundary of the quadrant, and by an oval otherwise). \square

Harnack T-curves are called so because in the case of lattice T-curve on $\mathbb{R}P^2$, they are congruent to the well known curves constructed by Harnack [3] which have

- One one-sided component and $\frac{(d-1)(d-2)}{2}$ outermost empty ovals if they have odd degree d (see example fig. 18).
- One outermost oval containing $\frac{(k-1)(k-2)}{2}$ empty ovals and $\frac{3k(k-1)}{2}$ outermost empty ovals if they have even degree $d = 2k$ (see example fig. 19).

The additive group $(\mathbb{Z}_2)^3 = \{0, 1\} \times \{0, 1\} \times \{0, 1\}$ acts on the distributions of signs as follows: Let $\theta = (c, a, b) \in (\mathbb{Z}_2)^3$, and let δ be a distribution of signs on some integral points. Then

$$(\theta \cdot \delta)(x, y) = (-1)^{c+\langle(a,b),(x,y)\rangle} \delta(x, y) \quad (6)$$

Therefore $(\mathbb{Z}_2)^3$ acts also on the set of lattice T-curves with a given carrier polygon:

$$\theta \cdot K(\Pi, \mathcal{T}, \delta) = K(\Pi, \mathcal{T}, \theta \cdot \delta)$$

Notice that $\theta \cdot \delta(x, y) = (-1)^c \delta(\sigma_{a,b}(x, y))$, and since $K(\Pi, \mathcal{T}, \delta) = K(\Pi, \mathcal{T}, -\delta)$, the group $(\mathbb{Z}_2)^3$ must be considered as $(\mathbb{Z}_2) \times ((\mathbb{Z}_2)^2)$, where the first factor (\mathbb{Z}_2) acts trivially and the second factor $(\mathbb{Z}_2)^2 = \{(a, b), a, b = 0 \text{ or } 1\}$ acts as the group of symmetries $\{\sigma_{a,b} : (x, y) \mapsto ((-1)^a x, (-1)^b y)\}$ on the four quadrants of $S(\Pi)$.

5.3.2.4 Lemma

A Harnack T-curve $K'(\Pi, \mathcal{T}, \delta')$, with δ' of type $\theta' = (c, a, b)$, is the image by the symmetry $\sigma_{a,b}$ of the Harnack T-curve $K(\Pi, \mathcal{T}, \delta)$ with δ of type $(1, 0, 0)$.

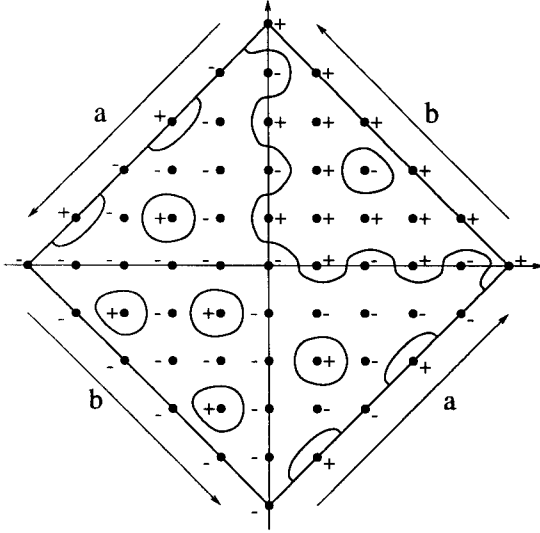


Figure 18: A Harnack T-curve of degree 5.

proof. Indeed from the definition 5.3.2.1 of the Harnack distributions and from formula 6 above we get that, for any $\theta \in (\mathbb{Z}_2)^3$, the distribution $\theta \cdot \delta'$ is a Harnack distribution of type the sum $\theta + \theta'$. So for $\theta = (c + 1, a, b)$ we get that $\theta \cdot K' = K$. This is equivalent to $K' = \theta \cdot K$. Since $\theta \cdot K = K(\Pi, \mathcal{T}, \theta \cdot \delta)$ we get from the remark above that $K' = \sigma_{a,b}(K)$. \square

5.3.2.5 Proposition

Let $K = K(\Pi, \mathcal{T}, \delta)$ be a Harnack T-curve with Harnack distribution of type (c, a, b) . Let $g(s, t)$ be the number of points of parity (s, t) in the interior of Π . Then

1. K is a maximal T-curve.
2. The connected components of K are distributed on its ambient surface as follows:
 - (a) $g(0, 0)$ empty ovals of sign $(-1)^c$ in the quadrant $(\sigma_{a,b} \cdot \Pi)$.
 - (b) $g(s, t)$ empty ovals of sign $(-1)^{c+1}$ in the quadrant $\sigma_{ta, sb} \cdot \Pi$, for each odd parity (s, t) .
 - (c) either a nontrivial connected component if Π has one broken edge of odd length.

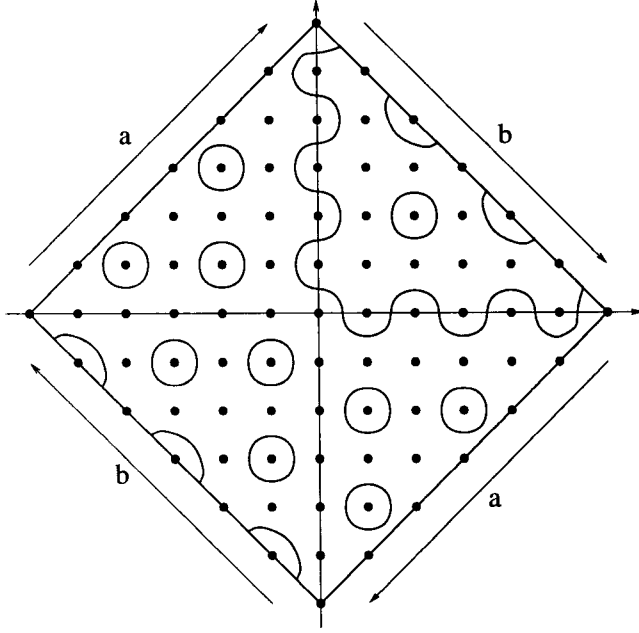


Figure 19: A Harnack T-curve of degree 6.

(d) either an oval surrounding all the empty ovals of sign $(-1)^c$, if all the broken edges of Π are of even length.

proof. Thanks to lemma 5.3.2.4 we assume without loss of generality that $(c, a, b) = (1, 0, 0)$.

From lemma 5.3.2.3 we get that every point of even parity which lies in the interior of Π is surrounded by an oval of K . From the definition 5.3.2.1 of Harnack distribution of sign, we know that this oval is of sign -1 . This proves assertion 2a.

From lemma 5.3.2.3 we get as well that for every point P of odd parity (s, t) which lies in the interior of Π , its copy $(\sigma_{t,s} \cdot P)$ is surrounded by an oval of K . From the definition 5.3.2.1 of Harnack distribution, and from formula 4 we get that this oval is of sign $+1$. This proves assertion 2b.

Let $g = \sum_{s,t} g(s, t)$. We just proved that K has g empty ovals. Moreover from lemma 5.3.2.3 we get that for every integral point $\partial\Pi$ one of its symmetric copy is surrounded by an arc of K , so there is at least one more connected component of K . So from the part (1) of theorem 5.3.1.1 we deduce that K has exactly $g + 1$ connected component. This proves assertion 1.

Let's call O the connected component of K which intersects (transversally) all the lifts in $S(\Pi)$ of the broken edges of Π .

Assume first that Π has a broken edge l of odd length. From lemma 5.0.1.2 we know that among the two lift of an edge e of the triangulation \mathcal{T} one is of negative sign and the other one is of positive sign. Therefore the lift $\mu^{-1}(l)$ in $S(\Pi)$ is intersected transversally an odd number of times by O , which implies, since $\mu^{-1}(l)$ is an embedded circle, that O is not an oval of K (see fig. 20). This proves assertion 2c.

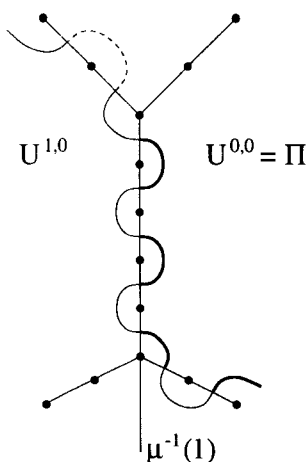


Figure 20: If an edge of Π is of odd length, then a component of K cuts the embedded circle $\mu^{-1}(l)$ an odd number of times. Therefore this component is not an oval.

Assume now that all the broken edges of Π are of even length. This implies that all the endpoints $\mu^{-1}(u_i)$ of the broken edges are of same parity. Thanks to prop. 4.2.1.1, we assume without loss of generality that they are of even parity. Therefore one integral point over two on $\partial\Pi$ is of even parity. Since δ is assumed to be of type $(1, 0, 0)$, all the points of even parity lying on $\partial\Pi$ are surrounded by arcs of Π in the quadrant Π , and all the other points lying on $\partial\Pi$ are surrounded in another quadrant.

By retracting each arc, which surrounds an integral point lying on $\partial\Pi$, toward this point, we shrink O onto the boundary of the quadrant Π . Since Π is homeomorphic to a disk, this boundary, and hence O , is an oval. It is clear that during the shrinking no crossing with another connected component of K happened, so O , like the boundary of Π , surrounds exactly the empty ovals within Π (see fig.21). This proves assertion 2d. \square

Notice that the assertion 1 of proposition 5.3.2.5 proves (2) of theorem 5.3.1.1, and therefore finishes the proof of 5.3.1.1. \square

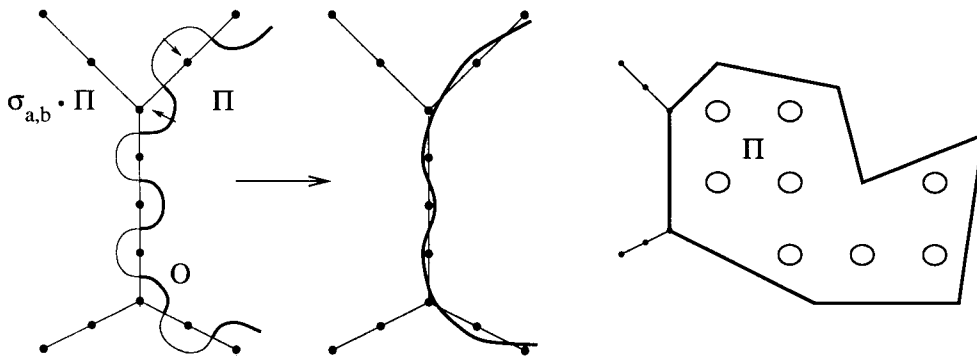


Figure 21: When all the edges of Π are of even length, the “special” component of the Harnack T-curve can be moved onto the boundary of Π . Therefore it is an oval.

5.3.2.6 Corollary

Any two Harnack T-curves with same carrier polygon, with same Harnack distribution, and with two arbitrary triangulations, are congruent by an homeomorphism of $S(\Pi)$ which is the identity on the boundary of the quadrants of $S(\Pi)$.

proof. Indeed since the sign distributions on the integral points are the same, the sign of the segments on the boundary of the quadrants of $S(\Pi)$ are also the same. This fixes the T-curves on this boundary. Prop. 5.3.2.5 shows that the connected components of any two such Harnack T-curves, restricted to a given quadrant, are congruent. \square

5.4 Second Application: Orientation of T-curves

5.4.0.7 Definition

A real algebraic curve is called a *dividing curve* (or a curve of *type I*) if it divides its complexification into two connected components, and is called a *non-dividing curve* (or a curve of *type II*) if it does not divide its complexification.

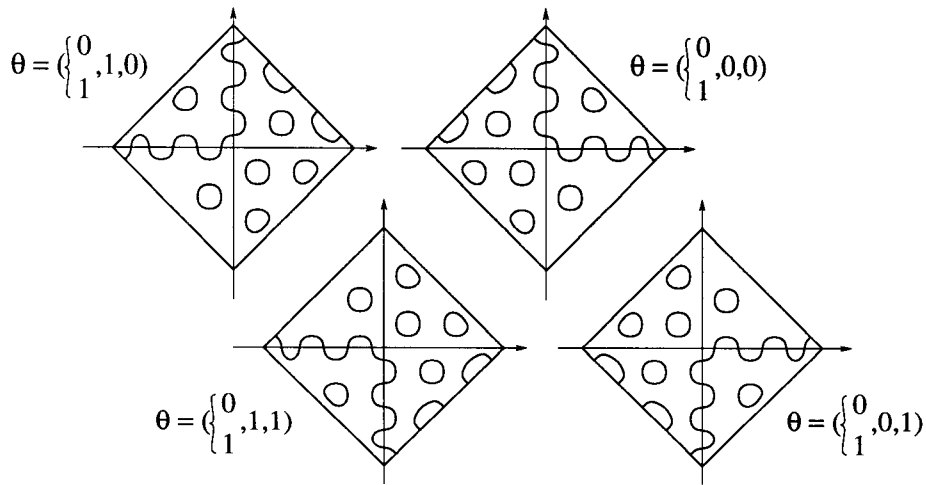


Figure 22: Eight types of Harnack distributions for four Harnack curves symmetric to one another.

5.4.0.8 Lemma

A real plane projective nonsingular curve is of type I if and only if the quotient of its complexification by the complex conjugation is orientable.

proof. Let K be a real plane projective nonsingular curve of degree d , let $\mathbb{C}K$ be its complexification, and let τ be the complex conjugation. Recall that $\mathbb{C}K$ is an orientable surface of genus $\frac{(d-1)(d-2)}{2}$. If the curve K is of type I, then the quotient $\mathbb{C}K/\tau$ is homeomorphic to a component of $\mathbb{C}K \setminus K$, and therefore orientable.

Recall that K is the set of fixed points of τ . Assume now K is of type II. Let $P \in \mathbb{C}K$ a point not in K , and let γ be a path connecting P to its conjugate $\tau(P)$ which doesn't intersect K . Since τ reverses the orientation of $\mathbb{C}K$, the image of the path γ in $\mathbb{C}K/\tau$ is a closed path which reverses the orientation. \square

5.4.0.9 Definition

A lattice T-curve is of type I if its T-filling is orientable, and of type II if its T-filling is non-orientable.

Let K be a real plane projective nonsingular curve of type I. The curve K divides its complexification $\mathbb{C}K$ into two orientable halves. An orientation on $\mathbb{C}K$ induces an orientation on each of the halves. These orientations induce

in turn two opposite orientations on K (since it is the boundary of each of the halves).

Let $K = K(\Pi, \mathcal{T}, \delta)$ be a lattice T-curve of type I. Since $F(K)$ is orientable, an orientation on it induces an orientation on its boundary. Let's retract $F(K)$ to the incidence graph G of the triangulation \mathcal{T} , so we get an orientation of the cycles $C = \mu(\tilde{C})$ which are the images of the connected components of K . An segment e of C lifts to a segment $\sigma_{a,b} \cdot e$ of \tilde{C} . If e is oriented from endpoint (x, y) to endpoint (x', y') , then segment $\sigma_{a,b} \cdot e$ will be oriented from $\sigma_{a,b} \cdot (x, y)$ to $\sigma_{a,b} \cdot (x', y')$. We get this way an orientation of all the connected components \tilde{C} of K (see fig. 23). The two opposite orientations on $F(K)$ induce then two opposite orientations on K .

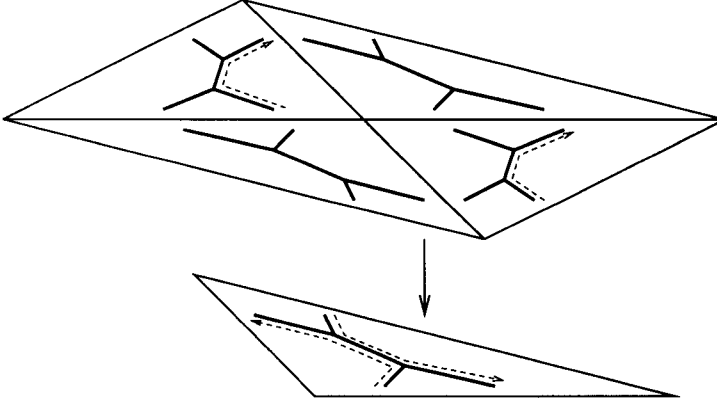


Figure 23: The oriented cycles on the incidence graph on Π lift to oriented cycles on the incidence graph on $S(\Pi)$. We just sketched here small portions of two cycles meeting on an edge.

5.4.0.10 Definition

The orientation described above on a lattice T-curve of type I will be called a *(type I)-orientation* of the T-curve.

Now we have defined type I and type II, and type-I-orientation for a lattice T-curve, it would be interesting to prove for lattice T-curves of given degree on $\mathbb{R}P^2$ theorems known for real plane projective nonsingular curves which take into account type and orientation. That would be useful in order to find extensions of these theorems to all lattice T-curves. For instance:

Arnold congruence. An oval is even (odd) if it is contained inside an even (odd) number of other ovals. Let P and N be the number of even and

odd ovals. For a dividing curve of even degree $d = 2k$, this congruence, of Arnold [1], holds:

$$P - N \equiv k^2 \pmod{4}$$

Rokhlin formulas. Let K be a dividing curve. So we can compare the orientation of any two connected components of K . A pair of nested ovals is called an injective pair. An injective pair is positive if the orientation of the two ovals can be recovered by an orientation of the annulus they bound, and the pair is negative if the orientation of the two ovals is not coherent with any orientation of the annulus they bound.

If K has odd degree, an oval O can be of two kind: The one sided component can be doubled and then deformed and moved to the boundary of O , and if its orientation coincide with the orientation of O , then O is positive, otherwise O is negative. Let Π^+ and Π^- be the number of positive and negative pairs, let Λ^+ and Λ^- be the number of positive and negative ovals, let l be the total number of connected component of the curve, and let d be the degree of the curve. These two formulas, of Rokhlin [10], hold:

$$2(\Pi^+ - \Pi^-) = l - \frac{d^2}{4} \quad \text{if } d \text{ is even}$$

$$(\Lambda^+ - \Lambda^-) + 2(\Pi^+ - \Pi^-) = l - \frac{(d-1)(d+1)}{4} \quad \text{if } d \text{ is odd}$$

5.5 Gluing lattice T-curves

5.5.1 Gluing the curves

5.5.1.1 Definition

If two lattice T-curves $K_1 = K(\Pi_1, \mathcal{T}_1, \delta_1)$ and $K_2 = K(\Pi_2, \mathcal{T}_2, \delta_2)$ satisfy the following *gluing conditions*:

1. $\Pi_1 \cup \Pi_2$ is a polygon Π , and $\Pi_1 \cap \Pi_2$ is a polygonal line.
2. δ_1 is equal to $\pm\delta_2$ on $\Pi_1 \cap \Pi_2$.

then their *gluing* $K_1 \# K_2$ is the curve $K(\Pi, \mathcal{T}, \delta)$ where (\mathcal{T}, δ) is equal, on Π_1 , to $(\mathcal{T}_1, \delta_1)$, and on Π_2 , either to $(\mathcal{T}_2, \delta_2)$ if $\delta_2 = \delta_1$ on $\Pi_1 \cap \Pi_2$, or to $(\mathcal{T}_2, -\delta_2)$ if $\delta_2 = -\delta_1$ on $\Pi_1 \cap \Pi_2$.

Recall that for a lattice T-curve $K(\Pi, \mathcal{T}, \delta)$ and a symmetry $\sigma_{a,b} : (x, y) \mapsto ((-1)^a x, (-1)^b y)$, $a, b \in \{0, 1\}$, the symmetric lattice T-curve $(\sigma_{a,b} \cdot K)$ is defined by $K(\Pi, \mathcal{T}, \sigma_{a,b} \cdot \delta)$, where $\sigma_{a,b} \cdot \delta(x, y) = (-1)^{\langle (a,b), (x,y) \rangle} \delta(x, y)$.

5.5.1.2 Lemma

Let $a, b \in \{0, 1\}$. If two lattice T-curves $K_1 = K(\Pi_1, \mathcal{T}_1, \delta_1)$ and $K_2 = K(\Pi_2, \mathcal{T}_2, \delta_2)$ satisfy the gluing conditions and if the primitive segments of $\Pi_1 \cap \Pi_2$ have all parity (a, b) , then K_1 and $(\sigma_{b,a} \cdot K_2)$ satisfy also the gluing conditions.

proof. Since the primitive segments of $\Pi_1 \cap \Pi_2$ have all same parity, the parity of the integral points of $\Pi_1 \cap \Pi_2$ takes only two values, say (a', b') and (a'', b'') . If e is an edge of the triangulation \mathcal{T} lying on $\Pi_1 \cap \Pi_2$ with endpoints (x', y') and (x'', y'') , then

$$\begin{aligned} (\sigma_{b,a} \cdot \delta_2(x', y'))(\sigma_{b,a} \cdot \delta_2(x'', y'')) &= \text{sign}(\sigma_{b,a} \cdot e) \\ &= (-1)^{\langle (a'+a'', b'+b''), (b,a) \rangle} \text{sign } e \\ &= \text{sign}(e) \quad \text{since } a' + a'' = a \\ &\quad \text{and } b' + b'' = b \\ &= \delta_1(x', y')\delta_1(x'', y'') \end{aligned}$$

Therefore $\sigma_{b,a} \cdot \delta_2$ equals to $\pm\delta_1$ on $\Pi_1 \cap \Pi_2$. \square

Notice that $K_1 \# (\sigma \cdot K_2)$ can be, up to congruence, the same curve than $K_1 \# K_2$ (see fig. 24), or another curve (see fig. 25).

5.5.2 Orienting locally the T-curves to be glued

A symmetric copy $(\sigma_{a,b} \cdot \gamma)$ of an oriented arc γ gets an orientation induced by symmetry from (the orientation of) γ : If γ is oriented locally away from (toward) one of its endpoint P , then $(\sigma_{a,b} \cdot \gamma)$ is oriented locally away from (toward) $(\sigma_{a,b} \cdot P)$. So we can always compare the orientation of two symmetric arcs.

Let $K_1 = K(\Pi_1, \mathcal{T}_1, \delta_1)$ and $K_2 = K(\Pi_2, \mathcal{T}_2, \delta_2)$ be two lattice T-curves satisfying the gluing conditions, and such that the parity of the segments of $\Pi_1 \cap \Pi_2$ takes only one value (b, a) . We denote like in section 2.4.1 the quotient maps

$$\begin{aligned} q_i &: \bigsqcup (\sigma_{c,d} \cdot \Pi_i) \rightarrow S(\Pi_i) \quad \text{and} \\ q &: \bigsqcup (\sigma_{c,d} \cdot (\Pi_1 \cup \Pi_2)) \rightarrow S(\Pi_1 \cup \Pi_2) \end{aligned}$$

and the projections

$$\begin{aligned} \mu_i &: S(\Pi_i) \rightarrow \Pi_i \quad \text{and} \\ \mu &: S(\Pi_1 \cup \Pi_2) \rightarrow (\Pi_1 \cup \Pi_2) \end{aligned}$$

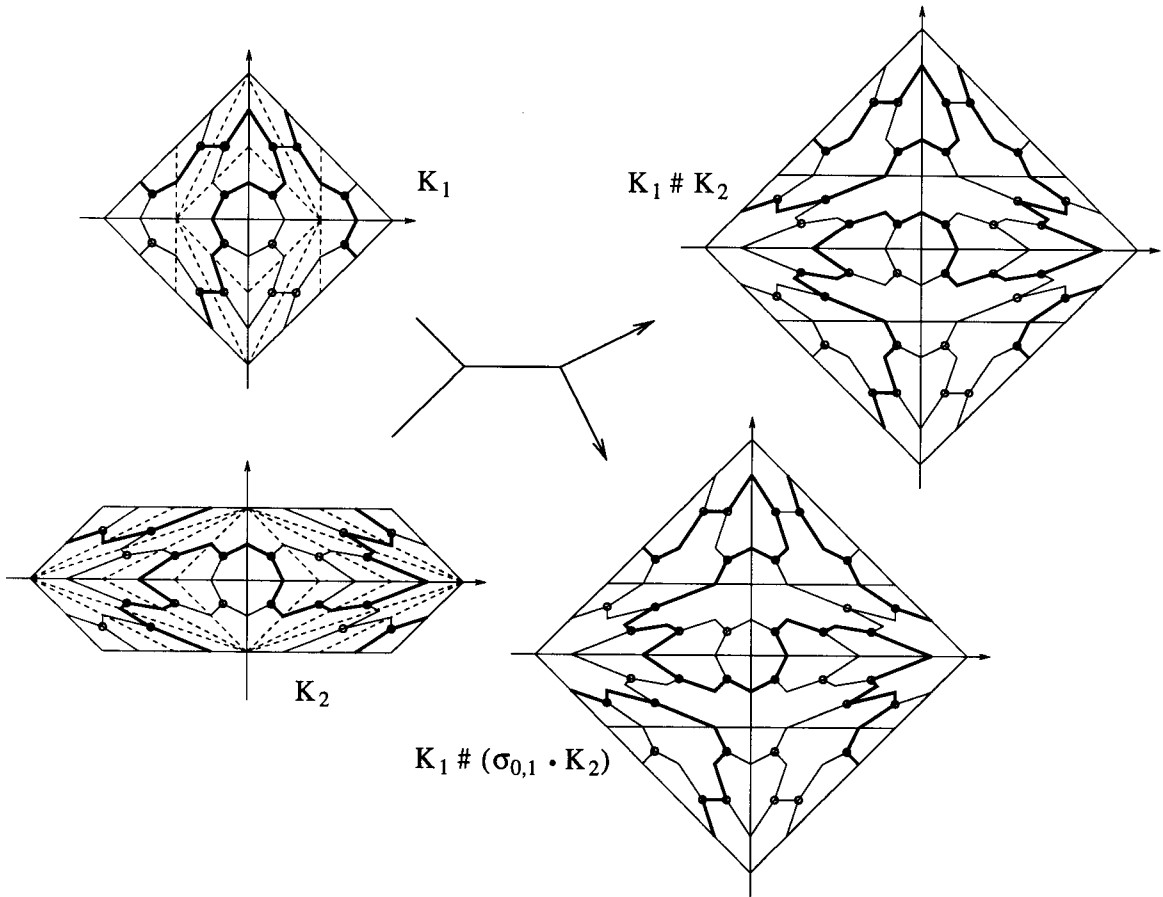


Figure 24: Here $K_1 \# K_2$ and $K_1 \# (\sigma_{0,1} \cdot K_2)$ are congruent curves.

Let \tilde{P}_1 be a point of intersection of K_1 with the lift $\mu_1^{-1}(\Pi_1 \cap \Pi_2)$. Let $P = \mu_1(\tilde{P}_1)$ and let \tilde{P}_2 be the point of intersection of K_2 with $\mu_2^{-1}(\Pi_1 \cap \Pi_2)$ such that $\mu(\tilde{P}_2) = P$. We have $q_1^{-1}(\tilde{P}_1) = q_2^{-1}(\tilde{P}_2) = (\sigma_{c,d} \cdot P) \cup (\sigma_{a+c,b+d} \cdot P)$ for some $c, d \in \{0, 1\}$.

For $i = 1, 2$, let α_i be a small arc of K_i through \tilde{P}_i . The point \tilde{P}_i disconnects α_i into two connected components, one in quadrant $\sigma_{c,d} \cdot \Pi_i$; the closure of which we denote α'_i and one in quadrant $\sigma_{c+a,d+b} \cdot \Pi_i$; the closure of which we denote α''_i . An orientation on α_1 induces an orientation on α'_1 and on α''_1 which in turn induces

- an orientation on α'_2 and on α''_2 by the gluing $K_1 \# K_2$.

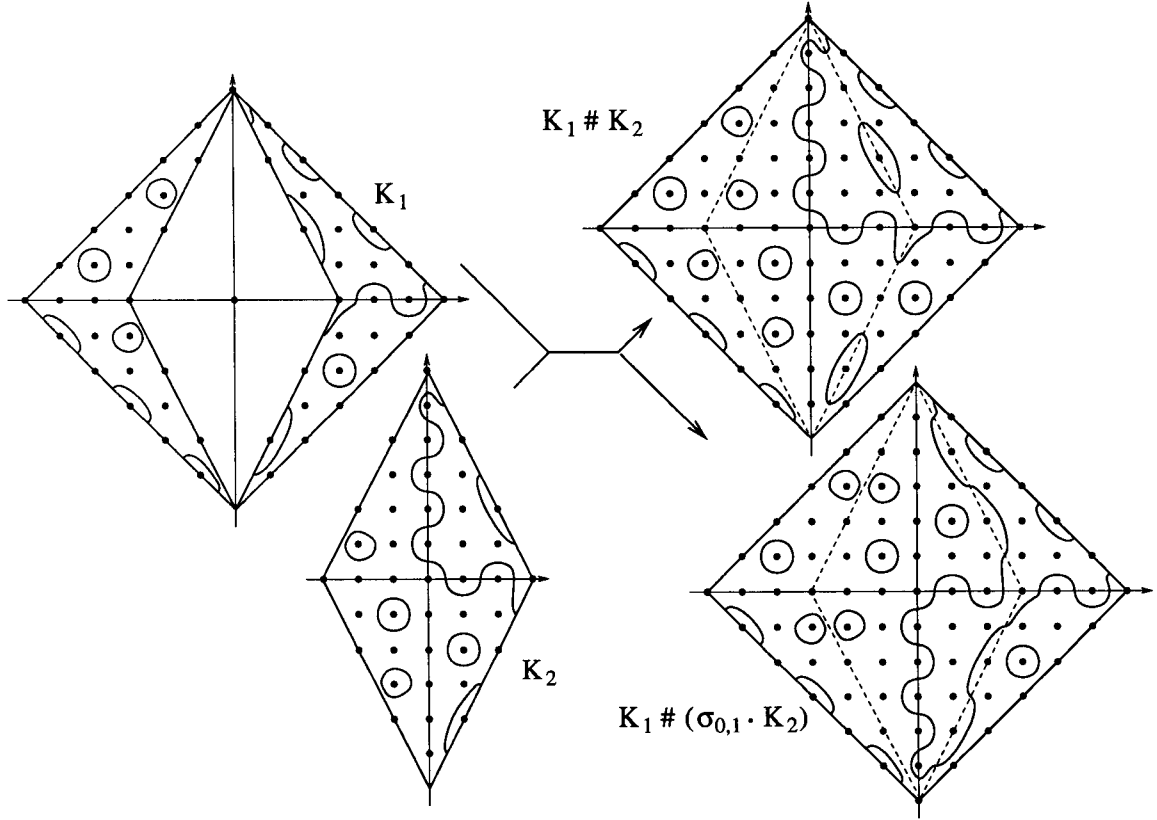


Figure 25: Here $K_1 \# K_2$ is a Harnack curve, and $K_1 \# (\sigma_{0,1} \cdot K_2)$ is a non maximal curve.

- an orientation on $(\sigma_{a,b} \cdot \alpha'_2)$ and on $(\sigma_{a,b} \cdot \alpha''_2)$ by the gluing $K_1 \# (\sigma_{a,b} \cdot K_2)$.

5.5.2.1 Lemma

The orientation on α'_2 and α''_2 , and on $(\sigma_{a,b} \cdot \alpha'_2)$ and $(\sigma_{a,b} \cdot \alpha''_2)$ defined above induce an orientation on α_2 and on $(\sigma_{a,b} \cdot \alpha_2)$ which are opposite to each other.

The proof is illustrated on fig. 26. □

5.5.3 Gluing the T-fillings

Let $K_1 = K(\Pi_1, \mathcal{T}_1, \delta_1)$ and $K_2 = K(\Pi_2, \mathcal{T}_2, \delta_2)$ be two lattice T-curves satisfying the gluing conditions. For $i = 1, 2$, we denote like in section 2.4.1, the

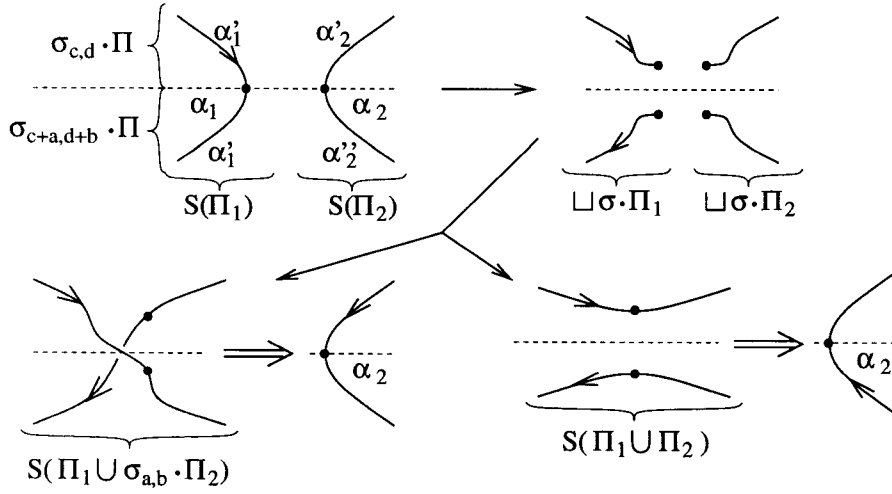


Figure 26: The arcs α_1 and α_2 are cut each into two arcs. These four arcs are re-glued two by two in two different ways according to the gluing of $K_1 \# K_2$ or to gluing $K_1 \# (\sigma_{b,a} \cdot K_2)$. The orientation of α_1 being fixed, it implies two different orientations of α_2 .

projections $\mu_i : S(\Pi_i) \rightarrow \Pi_i$ and $\mu : S(\Pi_1 \cup \Pi_2) \rightarrow (\Pi_1 \cup \Pi_2)$.

$F(K_1 \# K_2)$ is obtained from $F(K_1)$ and $F(K_2)$ by identifying segments s of $\partial F(K_1)$ with segments s' of $\partial F(K_2)$, with or without a twist, as explained in section 5.1. An orientation on a segment s correspond to an orientation on an arc of K_1 going through the lift $\mu_1^{-1}(\Pi_1 \cap \Pi_2)$. As explained in section 5.5.2 this orientation induces an orientation on the corresponding arc of K_2 by $K_1 \# K_2$.

Notice from fig. 5.5.3.1 that s and s' are identified with a twist if they have same orientation and without a twist if they have opposite orientation.

5.5.3.1 Lemma

Assume that the parity of the segments of $\Pi_1 \cap \Pi_2$ takes only one value (b, a) . Then the segments s and s' are identified in $F(K_1 \# (\sigma_{a,b} \cdot K_2))$ with (without) a twist when they are identified without (with) a twist in $F(K_1 \# K_2)$.

proof. An arc γ of K_2 with an orientation and a symmetric arc $(\sigma_{a,b} \cdot \gamma)$ with the orientation induced from γ by symmetry, project by μ_2 to the same arc on the incidence graph of \mathcal{T}_2 and with the same orientation. Since $F(K_2)$ is constructed from the images of the connected components of K_2 by μ_2 , the T-fillings $F(K_2)$ and $F(\sigma_{a,b} \cdot K_2)$ are equals but we get from lemma 5.5.2.1 that

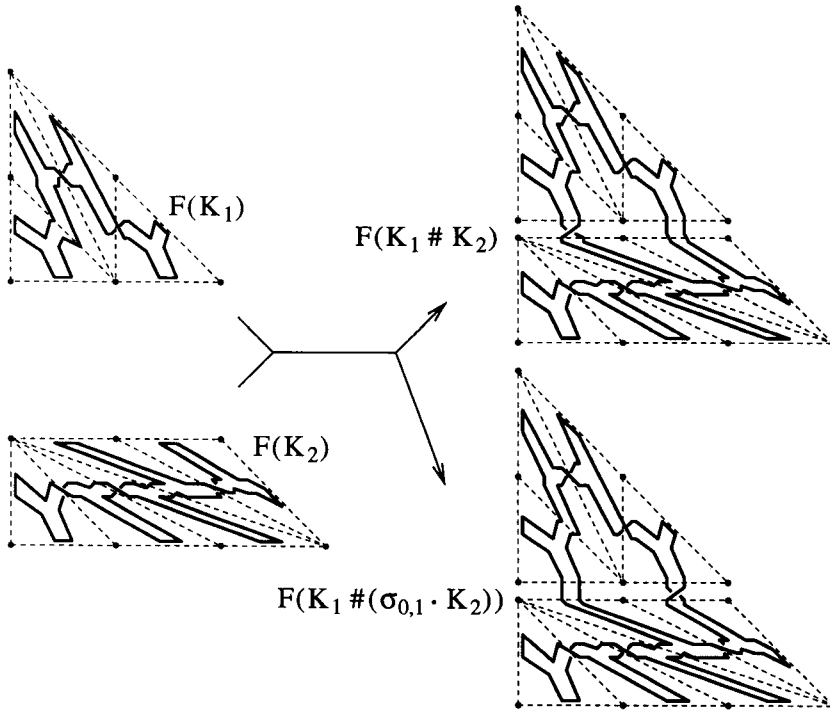


Figure 27: Gluing $F(K_1)$ and $F(K_2)$ corresponding to fig. 24.

the orientation of s' induced from s by $K_1 \# K_2$ is opposite to the orientation of s' induced from s by $K_1 \# (\sigma_{a,b} \cdot K_2)$. The remark above finishes the proof. \square

5.5.4 Gluing maximal lattice T-curves

Let $K_1 = K(\Pi_1, \mathcal{T}_1, \delta_1)$ and $K_2 = K(\Pi_2, \mathcal{T}_2, \delta_2)$ be two lattice T-curves satisfying the gluing conditions. Like previously the segments on $\partial F(K_1)$ which are identified in the gluing $F(K_1 \# K_2)$ with segments on $\partial F(K_2)$ will be denoted s when considered as part of $\partial F(K_1)$ and s' when considered as part of $\partial F(K_2)$.

5.5.4.1 Lemma

If $K_1 \# K_2$ is a maximal T-curve, then K_1 and K_2 are also maximal T-curves.

proof. Recall from lemma 5.3.1.3 that a T-curve is maximal if and only if its T-filling is a sphere with holes. If $F(K_1)$ or $F(K_2)$ has the property of being

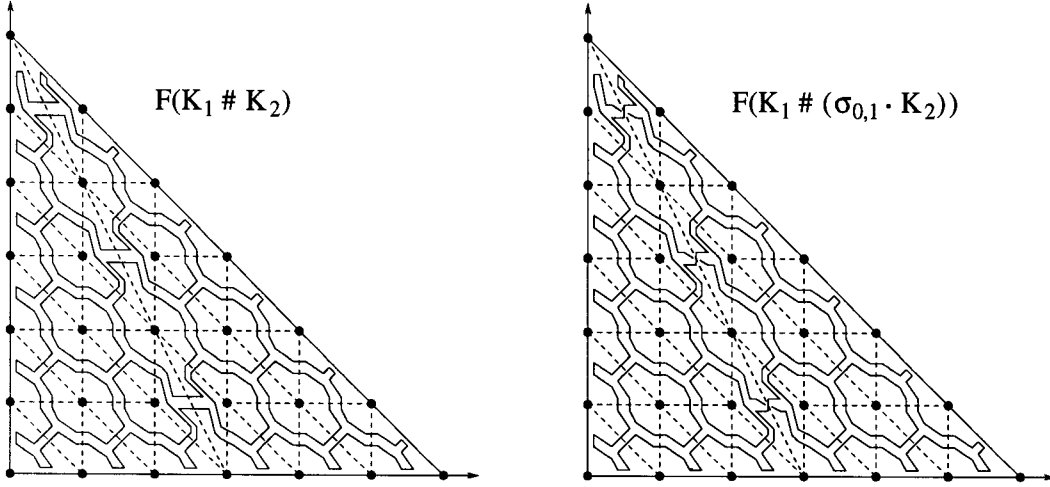


Figure 28: $F(K_1 \# K_2)$ and $F(K_1 \# (\sigma_{0,1} \cdot K_2))$ corresponding to fig. 25.

not orientable or having some handle, this property remains in $F(K_1 \# K_2)$. Since $K_1 \# K_2$ is maximal, $F(K_1 \# K_2)$ is a sphere with holes, $F(K_1)$ and $F(K_2)$ should be as well spheres with holes. Therefore K_1 and K_2 are maximal. \square

5.5.4.2 Definition

Let S_1 and S_2 be two surfaces. The r -connected sum of S_1 and S_2 is the surface obtained by removing r disks from S_1 , and r disks from S_2 , and by gluing on the holes made up this way r cylinders connecting S_1 to S_2 .

Notice on fig. 30 that more complicated connected sums are equivalent to r -connected sums.

5.5.4.3 Lemma

If $K_1 \# K_2$ is a maximal T-curve, then the segments s belong all to only one connected component of $\partial F(K_1)$, and the segments s' belong all to only one connected component of $\partial F(K_2)$.

proof. Let's glue disks along the boundary of $F(K_1)$, $F(K_2)$, and $F(K_1 \# K_2)$, so we get three surfaces $S(K_1)$, $S(K_2)$ and $S(K_1 \# K_2)$ without boundary. Now the assertion of the lemma can be restated as follows: "The surface $S(K_1 \# K_2)$ is a 1-connected sum of the surfaces $S(K_1)$ and $S(K_2)$ ". Since $K_1 \# K_2$ is maximal, we get from lemma 5.3.1.3 that $S(K_1 \# K_2)$ is homeomorphic to a sphere, and from lemma 5.5.4.1 that $S(K_1)$ and $S(K_2)$ are also

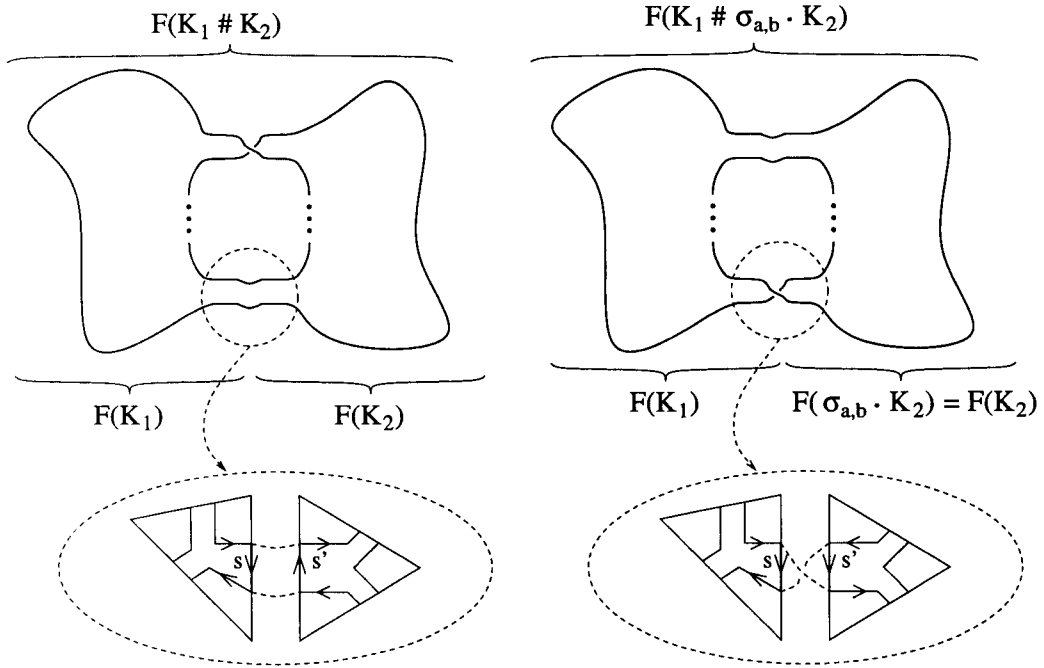


Figure 29: The orientation in $F(K_2)$ of a segments s' is induced from the orientation of the corresponding segment s in $F(K_1)$ and depends on whether s is identified to s' with a twist or without a twist.

homeomorphic to spheres. And it is clear that the r -connected sum of two spheres is a sphere if and only if $r = 1$. □

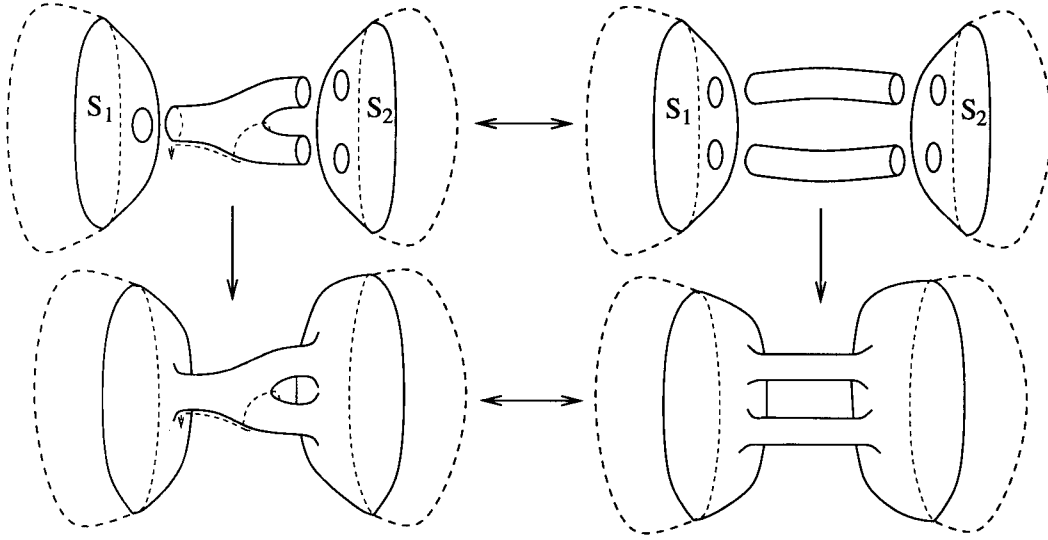


Figure 30: A more complicated connected sum of two surfaces is equivalent to a r -connected sum (here $r = 2$).

6 From Harnack T-curves to Maximal T-curves

6.1 No Twist Implies Harnack T-curve

Let $K(\Pi, \mathcal{T}, \delta)$ be a T-curve. Recall that the T-filling $F(K)$ is constructed by gluing the thick Y's with or without a twist.

6.1.0.4 Lemma

For every triangle t of \mathcal{T} , the T-curve K doesn't intersect some copy $(\sigma_{a,b} \cdot t)$, and in each other copy of t the T-curve K surrounds a copy of a different vertex of t (see fig. 31).

proof. Let P_1, P_2, P_3 be the vertices of t and let (c_i, d_i) be the parity of P_i . Then the lemma can be restated arithmetically as follows:

For some indexation $\{(a_1, b_1), \dots, (a_4, b_4)\}$ of the four element set $\{0, 1\} \times \{0, 1\}$, and for every circular permutation $\{i, j, k\}$ of $\{1, 2, 3\}$, we have:

1. $\delta(\sigma_{a_i, b_i} \cdot P_j) = \delta(\sigma_{a_i, b_i} \cdot P_k) \neq \delta(\sigma_{a_i, b_i} \cdot P_i)$
2. $\delta(\sigma_{a_4, b_4} \cdot P_1) = \delta(\sigma_{a_4, b_4} \cdot P_2) = \delta(\sigma_{a_4, b_4} \cdot P_3)$

Let $(-1)^n = \delta(P_i)$. Then from formula 2 of section 2.4.2, we get that assertion (1) is equivalent to

$$\begin{aligned} \langle (a_i, b_i), (c_j, d_j) \rangle + \eta_j &= \langle (a_i, b_i), (c_k, d_k) \rangle + \eta_k && \text{or more simply:} \\ \langle (a_i, b_i), (c_j + c_k, d_j + d_k) \rangle &= \eta_j + \eta_k && (7) \end{aligned}$$

$$\begin{aligned} \langle (a_i, b_i), (c_j, d_j) \rangle + \eta_j &= \langle (a_i, b_i), (c_i, d_i) \rangle + \eta_i + 1 && \text{or more simply:} \\ \langle (a_i, b_i), (c_j + c_i, d_j + d_i) \rangle &= \eta_j + \eta_i + 1 && (8) \end{aligned}$$

Since $(c_i, d_i) \neq (c_k, d_k)$, equations 7 and 8 are linearly independent. So this system has a unique solution (a_i, b_i) .

Similarly assertion (2) is equivalent to

$$\begin{aligned} \langle (a_4, b_4), (c_1, d_1) \rangle + \eta_1 &= \langle (a_4, b_4), (c_2, d_2) \rangle + \eta_2 && \text{or more simply:} \\ \langle (a_4, b_4), (c_1 + c_2, d_1 + d_2) \rangle &= \eta_1 + \eta_2 && (9) \end{aligned}$$

$$\begin{aligned} \langle (a_4, b_4), (c_1, d_1) \rangle + \eta_1 &= \langle (a_4, b_4), (c_3, d_3) \rangle + \eta_3 + 1 && \text{or more simply:} \\ \langle (a_4, b_4), (c_1 + c_3, d_1 + d_3) \rangle &= \eta_1 + \eta_3 && (10) \end{aligned}$$

For the same reason this system has a unique solution (a_4, b_4) . \square

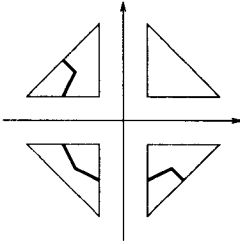


Figure 31: How a T-curve intersects the four symmetric copies of a triangle of the triangulation.

6.1.0.5 Lemma

Let t_1 and t_4 be two adjacent triangles of \mathcal{T} such that the corresponding thick Y 's are glued without a twist. Let P_1, P_2, P_3 and P_2, P_3, P_4 be the vertices of t_1 and t_4 respectively.

1. P_1 and P_4 have same parity if and only if $\delta(P_1) = \delta(P_4)$.
2. If P_1 has a different parity than P_4 , then K will surround copies of P_1 and P_4 in different quadrants.

proof. Without loss of generality we assume that in Π the point P_1 is surrounded by an arc of K . Let (a_i, b_i) be the parity of P_i .

For some $c, d \in \{0, 1\}$, $(c, d) \neq (0, 0)$, an arc of K surrounds a copy of P_2 in $(\sigma_{c,d} \cdot t_1)$. Since the thick Y 's in t_1 and t_4 are glued together without a twist, the same arc must surround the same copy of P_2 in $\sigma_{c,d} \cdot t_4$. The same is true with P_3 instead of P_2 with some $e, f \neq c, d$ (and $e, f \neq (0, 0)$) (see fig. 32). We have then

$$(a) \begin{cases} \delta(\sigma_{c,d} \cdot P_1) = \delta(\sigma_{c,d} \cdot P_4) \\ \delta(\sigma_{e,f} \cdot P_1) = \delta(\sigma_{e,f} \cdot P_4) \end{cases}$$

From formula 2 of section 2.4.2 we get that $\delta(P_1) = \delta(P_4)$ if and only if the following system has a solution:

$$(b) \begin{cases} \langle (c, d), (a_1 + a_4, b_1 + b_4) \rangle = 0 \\ \langle (e, f), (a_1 + a_4, b_1 + b_4) \rangle = 0 \end{cases}$$

Since $(c, d) \neq (e, f)$ this is equivalent to $(a_1 + a_4, b_1 + b_4) = (0, 0)$, which means that P_1 and P_4 have same parity.

Assume now that $\delta(P_1) \neq \delta(P_4)$, so K doesn't intersect t_4 . The T-curve K surrounds P_1 in t_1 . We get from lemma 6.1.0.4 that K surrounds a copy of P_4 in some $(\sigma \cdot t_4)$, where $\sigma \neq \sigma_{0,0}$ (in fact it is easy to compute that $\sigma = \sigma_{c+e, d+f}$). \square

6.1.0.6 Proposition

If all the thick Y 's are glued in $F(K)$ without twists, then K is a Harnack T-curve.

proof. Thanks to prop. 4.2.1.1, we assume without loss of generality that Π contains an even point.

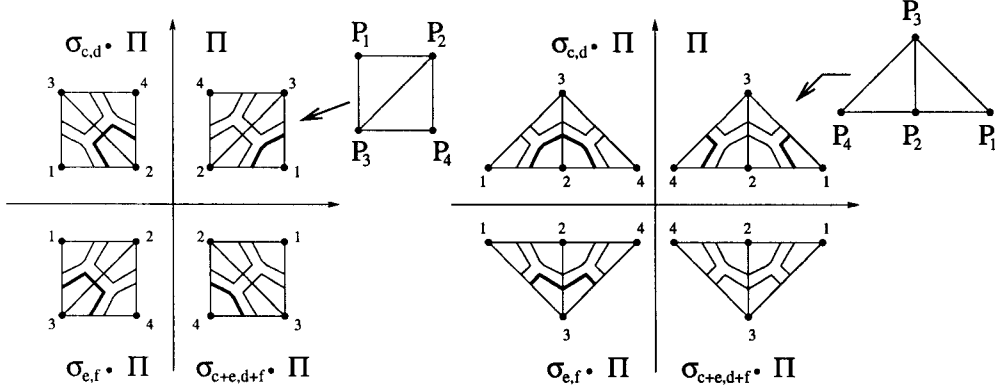


Figure 32: If the thick Y's in t_1 and t_4 are glued with no twists, then $\delta(P_1) = \delta(P_4)$ if and only if P_1 and P_4 have same parities (here they have same parities on the right diagram, and different parities on the left diagram).

Since the incidence graph in every quadrant of $S(\Pi)$ is connected, we get from lemma 6.1.0.5 that all the even points in some quadrant $(\sigma_{a,b} \cdot \Pi)$ have a certain sign and all the odd points in $(\sigma_{a,b} \cdot \Pi)$ have opposite sign. This is the definition of a Harnack distribution, so K is a Harnack T-curve. \square

6.2 Maximal Implies Gluing of Harnack T-curves

Let $K(\Pi, \mathcal{T}, \delta)$ be a T-curve. Recall that the T-filling $F(K)$ is constructed by gluing thick Y's: Let t_i and t_j be two adjacent triangles of \mathcal{T} . Denote $s_{i,j}$ the segment of the thick Y of t_i , which lie on $t_{i,j} = t_i \cap t_j$ and denote $s_{j,i}$ the same segment when considered as a segment of the thick Y of t_j . Then $s_{i,j}$ is identified to $s_{j,i}$ with or without a twist. When $s_{i,j}$ is identified with a twist, we will denote it $s_{i,j} \tilde{tw} s_{j,i}$.

6.2.1 An algorithm to cut T-fillings

If K is not a Harnack T-curve, we describe now an algorithm which splits $F(K)$ into two connected components F_1 and F_2 . The algorithm finds a sequence of oriented surfaces S_0, \dots, S_r , together with a sequence of twists $s_{i_1, j_1} \tilde{tw} s_{j_1, i_1}, \dots, s_{i_r, j_r} \tilde{tw} s_{j_r, i_r}$. The initial data is:

- $S_0 = F(K)$. Notice that S_0 is orientable.

- The first twist $s_{i_1, j_1} \overset{\sim}{tw} s_{j_1, i_1}$ is chosen arbitrarily.

The algorithm itself is given as follows:

- S_k is the surface obtained by cutting S_{k-1} along the k^{th} twist, $(s_{i_k, j_k} \overset{\sim}{tw} s_{j_k, i_k}) \mapsto (s_{i_k, j_k} \sqcup s_{j_k, i_k})$. The surface S_k is orientable since S_{k-1} is orientable.
- If S_k has two connected components, the algorithm stops, i.e. $k = r$.
- There exist a loop around a vertex of \mathcal{T} in S_{k-1} , which passes through $s_{i_k, j_k} \overset{\sim}{tw} s_{j_k, i_k}$, otherwise it is clear that cutting $s_{i_k, j_k} \overset{\sim}{tw} s_{j_k, i_k}$ to form S_k would disconnect S_k , and the algorithm would have already stopped.
- Let's orient such a loop. This loop must pass through an odd number of other twist, otherwise S_{k-1} wouldn't be orientable. Let $s_{i_{k+1}, j_{k+1}} \overset{\sim}{tw} s_{j_{k+1}, i_{k+1}}$ be the next twist encountered when following the loop from $s_{i_k, j_k} \overset{\sim}{tw} s_{j_k, i_k}$.

The algorithm stops since there is a finite number of twists. By this algorithm, $F(K)$ may be cut along too many twists. So for each twist cut $(s_{i_k, j_k} \overset{\sim}{tw} s_{j_k, i_k}) \mapsto (s_{i_k, j_k} \sqcup s_{j_k, i_k})$, if its re-gluing $(s_{i_k, j_k} \sqcup s_{j_k, i_k}) \mapsto (s_{i_k, j_k} \overset{\sim}{tw} s_{j_k, i_k})$ doesn't reconnect the two connected components of S_r , then let's re-glu it. After this operation let F_1 and F_2 be the two connected components into which $F(K)$ is split.

Notice that the algorithm gives also a decomposition of Π into two connected components. Since the twists are located on the edges of the triangulation \mathcal{T} , at each cut of a twist $s_{i_k, j_k} \overset{\sim}{tw} s_{j_k, i_k}$, let's cut also Π along the edge t_{i_k, j_k} of \mathcal{T} . Let's re-glu also the cuts which are not necessary, so at last we get from Π two connected components, one is a polygon, but the other one may not be a polygon (but may be a polygon with a hole).

6.2.2 Spheres with holes glued by twists

6.2.2.1 Proposition

If K is maximal, then either K is a Harnack T-curve, either it is a gluing of two maximal T-curves K_1 and K_2 such that $F(K_1)$ is glued to $F(K_2)$ by one or two twists and nothing else.

proof. If $F(K)$ has no twist, then we know from 6.1.0.6 that K is a Harnack T-curve. So assume now that $F(K)$ has a twist.

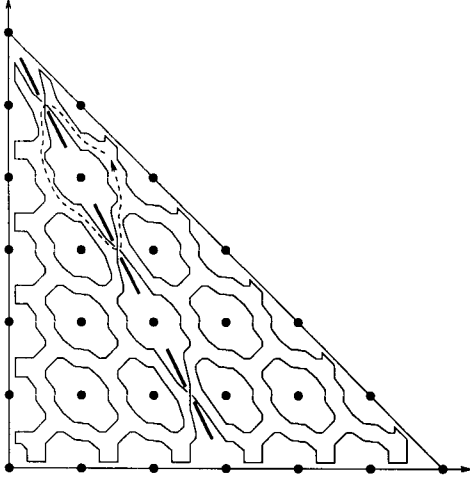


Figure 33: Here $F(K)$ becomes disconnected after 3 cuts along twists.

Let F_1 and F_2 be the two connected components into which $F(K)$ is decomposed by the above algorithm. Since K is maximal, $F(K)$ is homeomorphic to a sphere with holes (see cor. 5.3.1.3) and each of F_1 and F_2 is also homeomorphic to a sphere with holes (for the same arguments than in lemma 5.5.4.1). So for the same arguments than in lemma 5.5.4.3, we get that F_1 and F_2 are glued to one another along one connected component O_1 of ∂F_1 and one connected component O_2 of ∂F_2 .

Let D_1 and D_2 be the two disks obtained from F_1 and F_2 by gluing disks along the connected components of their boundary other than O_1 and O_2 . Let S' be the surface obtained from $F(K)$ by gluing disks along the connected components of $\partial F(K)$. The surface S' is also obtained by

- gluing D_1 to D_2 into a surface $D_{1,2}$ by the r twists used in the algorithm:
 $(s_{i_k, j_k} \sqcup s_{j_k, i_k}) \mapsto (s_{i_k, j_k} \overset{\sim}{tw} s_{j_k, i_k})$, $k = 1, \dots, r$.
- gluing disks along the connected components of $\partial D_{1,2}$.

Since D_1 is glued to D_2 only by twists, it is easy to compute that $\partial D_{1,2}$ has two connected components if the number r of twists is even, and only one connected component if r is odd (see fig. 34). If r is odd, by doubling

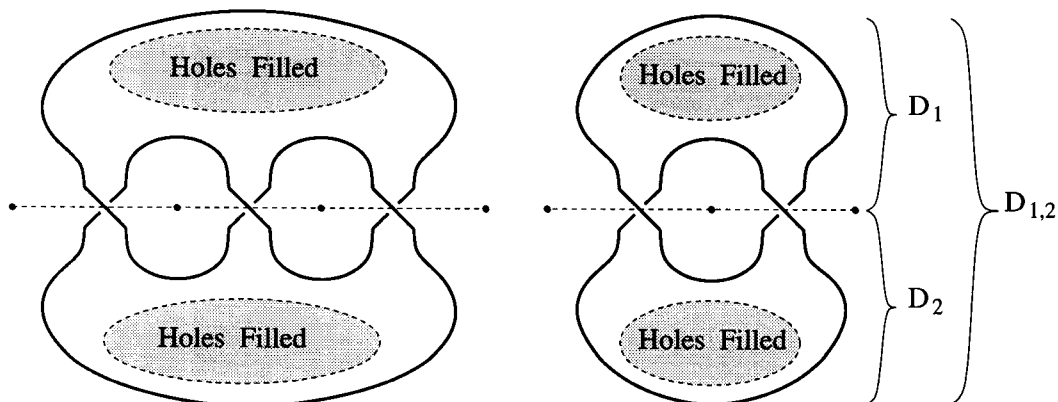


Figure 34: The holes O_1 and O_2 give rise to one or two holes in $F(K_1 \# K_2)$. Here D_1 and D_2 are the disks obtained by filling the holes of $F(K_1)$ and $F(K_2)$, except O_1 and O_2 . Unfill the holes in $D_{1,2}$ to get $F(K_1 \# K_2)$.

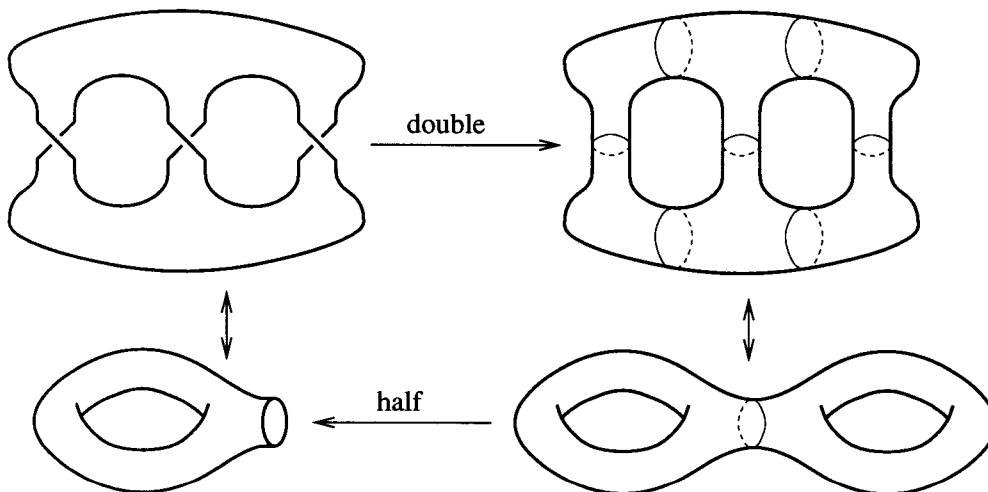


Figure 35: Double the surface, then take the half. Here it is a torus with one hole.

$D_{1,2}$ along its boundary and by taking the half of it (see fig. 35), it is easy to see that $D_{1,2}$ is a sphere with $\frac{r-1}{2}$ handles and one hole.

If r is even, it is easy to make a hole from one twist (see fig. 36): Let's slide along ∂D_2 an end of a "twisted bridge" (between D_1 and D_2) until it comes close to the other end of the twisted bridge. Since the slid end passes through an odd number of twists, it become untwisted. Now by the same

trick than above, it is easy to compute that $D_{1,2}$ is a sphere with $\frac{r-2}{2}$ handles and two holes.

Since K is maximal, S' is a sphere, so $D_{1,2}$ is a sphere with holes. Therefore $r = 1$ or 2 (see fig. 37).

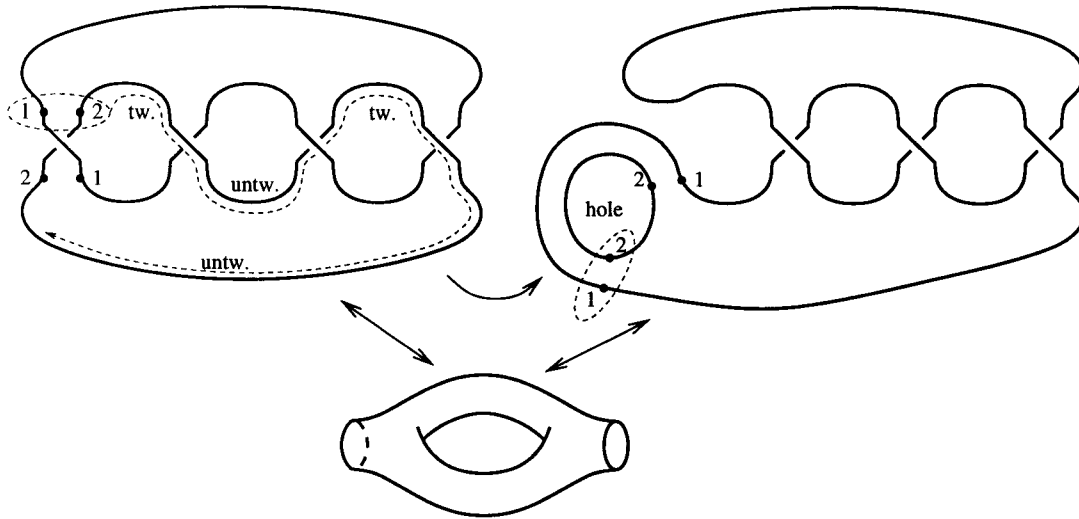


Figure 36: An end of a twisted "bridge" is slid along the boundary until it comes close to the other end. So we get a surface with one hole and an odd number of twists. Here it is a torus with two holes.

Let's cut the polygon Π along the edges of \mathcal{T} on which lie the one or two twist. Then Π becomes decomposed into two polygons Π_1 and Π_2 . Indeed to decompose Π into a polygon and a polygon with a hole, one would need to cut Π at least along three edges of \mathcal{T} . Therefore K is the gluing of two lattice T-curves $K_1 = K(\Pi_1, \mathcal{T}_1, \delta_1)$ and $K_2 = K(\Pi_2, \mathcal{T}_2, \delta_2)$, where $(\mathcal{T}_i, \delta_i)$ is the restriction to Π_i of (\mathcal{T}, δ) . Moreover $F_1 = F(K_1)$ and $F_2 = F(K_2)$, and since these two surfaces are spheres, K_1 and K_2 are maximal. \square

6.2.2.2 Definition

The *total parity of an integral segment* is the element $\theta = (e, f, g) \in (\mathbb{Z}_2)^3$ defined as follows:

$$\begin{aligned} e &= ab' + a'b \\ f &= b + b' \\ g &= a + a' \end{aligned}$$

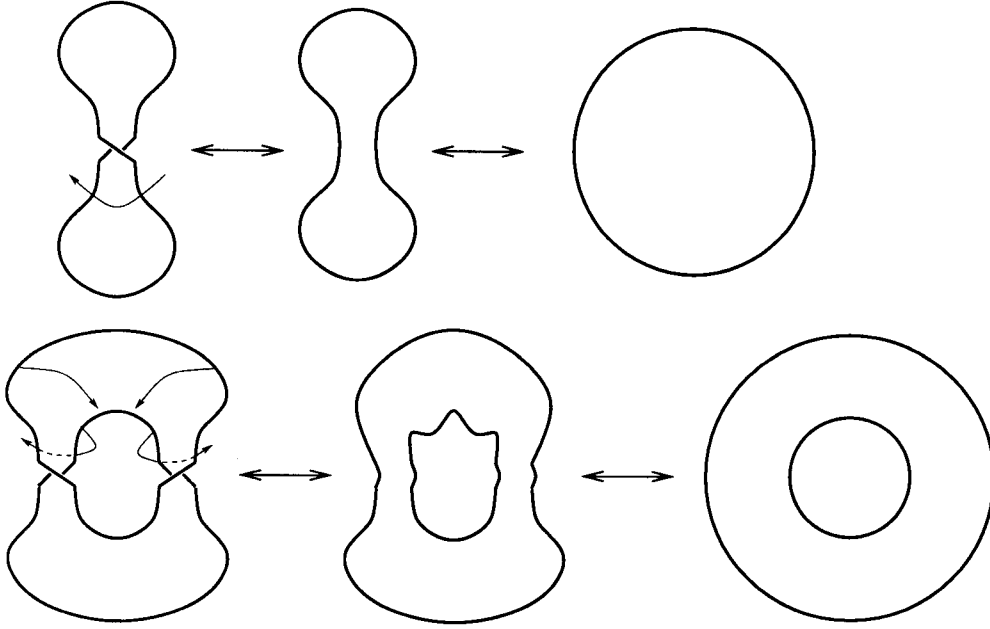


Figure 37: For one twist, we get a disk and for two twists we get an annulus.

where (a, b) and (a', b') are the two values that the parity takes on the integral points of the segment.

Notice that the total parity (e, f, g) of a segment contains its parity (f, g) . Notice that there is exactly six total parities of integral segments though $(\mathbb{Z}_2)^3$ contains eight elements. Parities $(0, 0, 0)$ and $(1, 0, 0)$ cannot exist since they correspond to a segment having even parity. This definition which embed some edge parities in $(\mathbb{Z}_2)^3$ may seem strange at first glance, but it allows us to present in a nice way the following property.

6.2.2.3 Lemma

Let $K_1 = K(\Pi_1, \mathcal{T}_1, \delta_1)$ and $K_2 = K(\Pi_2, \mathcal{T}_2, \delta_2)$ two Harnack T-curves which satisfy the gluing conditions and such that the parity of the segments of $\Pi_1 \cap \Pi_2$ takes only one value. Let $\theta(s)$ be the total parity of the segments of $\Pi_1 \cap \Pi_2$. Let θ_1 and θ_2 be the types of δ_1 and δ_2 . Then either $\theta_2 = \theta_1$ either $\theta_2 = \theta(s) + \theta_1$.

proof. Let (a, b) and (a', b') be the two values that the parity takes on the integral points of $\Pi_1 \cap \Pi_2$. Since the additive group $(\mathbb{Z}_2)^3$ is transitive, we have $\theta_2 = \theta + \theta_1$ for some $\theta = (e, f, g) \in (\mathbb{Z}_2)^3$, so $\delta_2(x, y) = \theta \cdot \delta_1(x, y)$ for any

$(x, y) \in (\Pi_1 \cap \Pi_2)$. Recall from formula 6 of section 5.3.2 that $\theta \cdot \delta(x, y) = (-1)^{e+\langle(f,g),(c,d)\rangle} \delta(x, y)$, where (c, d) is the parity of (x, y) . Since K_1 and K_2 satisfy the gluing condition, $\delta_1 = \delta_2$ on $\Pi_1 \cap \Pi_2$ so $\delta_1(x, y) = \theta \cdot \delta_1(x, y)$ for any (x, y) of parity (a, b) or (a', b') . Therefore to find θ we must solve:

$$\begin{aligned} e + \langle(f, g), (a, b)\rangle &= 0 \\ e + \langle(f, g), (a', b')\rangle &= 0 \end{aligned}$$

Which is equivalent to the following Kramer system:

$$\begin{cases} fa + gb = e \\ fa' + gb' = e \end{cases} \quad (11)$$

It is clear that $(e, f, g) = (0, 0, 0)$ is a (degenerate) solution. In that case $\theta_1 = \theta_2$, so let's assume that $(e, f, g) \neq (0, 0, 0)$, so $\theta_1 \neq \theta_2$.

- Either the system 11 above is degenerate:

$$\begin{aligned} ab' + a'b &= 0 \\ \Leftrightarrow \langle(a, b), (b', a')\rangle &= 0 \\ \Leftrightarrow \begin{cases} \text{either } (a, b) = (0, 0) & \text{or } (a', b') = (0, 0) \\ \text{either } (a, b) = (a', b') \end{cases} \end{aligned}$$

$(a, b) = (a', b')$ is impossible because $(c + c', d + d')$ is the parity of the segments of $\Pi_1 \cap \Pi_2$, and a parity of a segment is never even. So the system is degenerate if and only if $(a, b) = (0, 0)$ or $(a', b') = (0, 0)$. In that case $e = 0$ and we can write $(e, f, g) = ((ab' + a'b), (b + b'), (a + a'))$ which is different from $(0, 0, 0)$ since (a, b) is different from (a', b') .

- Either the system 11 above is non-degenerate, i.e. $ab' + a'b = 1$. In that case:

- Either $e = 0$, so we get $f = g = 0$ which is impossible since we assumed $(e, f, g) \neq (0, 0, 0)$.
- Either $e = 1$, so we get $f = b + b'$ and $g = a + a'$.

So finally, we get that either $\theta = (0, 0, 0)$, and then $\theta_2 = \theta_1$, either $\theta \neq (0, 0, 0)$, and then $\theta = \theta(s)$ so $\theta_2 = \theta(s) + \theta_1$. \square

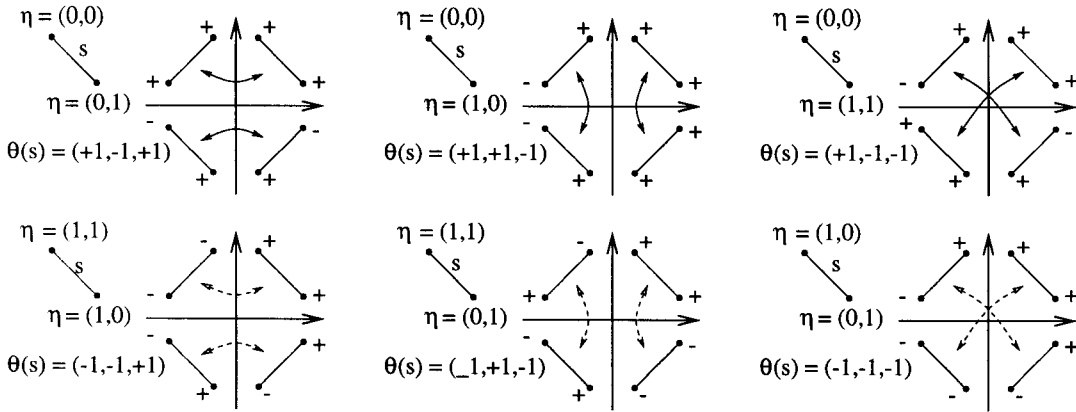


Figure 38: The total parity $\theta(s)$ of a primitive segment s , and its action as a symmetry on the distribution of signs on s . This action doesn't change the sign of s , although it may change the signs of the integral points of s (in that case the symmetry is represented with dotted arrows).

6.3 Zone decompositions, and Harnack zone-wise sign distributions

6.3.1 Zone decompositions

Let's recall the definition of a zone given in section 2.5.

6.3.1.1 Definition

A *zone* will be an integral polygon $Z \subset \Pi$ such that its boundary is a union of primitive segments having each at least one end on $\partial\Pi$. A *zone decomposition* of Π is a cell decomposition of Π such that the two dimensional cells are zones.

6.3.1.2 Lemma

Let \mathcal{T} be a primitive triangulation of an integral polygon Π , and let Z and Z' be two zones of Π which are union of triangles of \mathcal{T} . Then $Z \cap Z'$ is the union of some integral points, some primitive edges, and some zones of Π .

proof. Indeed the intersection of a primitive segment of ∂Z with Z' is either empty, either an integral point, either the segment itself. Since the boundary of $Z \cap Z'$ is a union of intersections of primitive segments of ∂Z with Z' and of intersections of primitive segments of $\partial Z'$ with Z , it is a union of integral points, and primitive segments having each at least one endpoint on $\partial\Pi$. So

if $\text{int}(Z) \cap \text{int}(Z') \neq \emptyset$, then the two dimensional part of $Z \cap Z'$ is a union of zones of Π . \square

6.3.1.3 Definition

The *intersection* $\Delta \cap \Delta'$ of two zone decompositions of an integral polygon Π is the cell decomposition of Π with all the possible intersections of zones of Δ with zones of Δ' as cells.

6.3.1.4 Corollary

Let \mathcal{T} be a primitive triangulation of an integral polygon Π , and let Δ and Δ' be two zone decompositions of Π , such that every zone is a union of triangles of \mathcal{T} . Then $\Delta \cap \Delta'$ is a zone decomposition of Π .

proof. Indeed this assertion follows by applying lemma 6.3.1.2 to every zone of Δ successively with every zone of Δ' . \square

6.3.1.5 Definition

A sign distribution on an integral polygon will be called a Harnack zone-wise distribution, if it is a Harnack sign distribution on any zone of a zone decomposition of the polygon.

6.3.2 Harnack zone-wise decomposition

6.3.2.1 Lemma

Let Π be an integral polygon, let Δ be a zone decomposition of Π , let δ be a Harnack zone-wise distribution (with respect to Δ), and let \mathcal{T} and \mathcal{T}' be two arbitrary primitive triangulation of Π which are sub-decompositions of Δ . Then $K(\Pi, \mathcal{T}, \delta)$ and $K(\Pi, \mathcal{T}', \delta)$ are congruent.

proof. Indeed let Z_1, \dots, Z_r be the zones of Δ , let δ_i be the sign distribution δ restricted to Z_i , let \mathcal{T}_i and \mathcal{T}'_i be the restrictions of \mathcal{T} and \mathcal{T}' to Z_i and let $K_i = K(Z_i, \mathcal{T}_i, \delta_i)$, and $K'_i = K(Z_i, \mathcal{T}'_i, \delta_i)$. From corollary 5.3.2.6 we get that K_i and K'_i are congruent by homeomorphism which is the identity on the boundary ∂Z_i . Therefore, since $K = \# K_i$ and $K' = \# K'_i$ (i.e. K is the gluing of all the K_i and K' is the gluing of all the K'_i), the curves $K(\Pi, \mathcal{T}, \delta)$ and $K(\Pi, \mathcal{T}', \delta)$ are congruent. \square

6.3.2.2 Proposition

For any maximal lattice T-curve $K(\Pi, \mathcal{T}, \delta)$, the triangulation \mathcal{T} is a sub-decomposition of some zone decomposition Δ of Π , and δ is a Harnack zone-wise sign distribution with respect to Δ .

proof. From prop. 6.2.2.1 we know that the algorithm of section 6.2 decomposes Π into two polygons Π_1 and Π_2 which have only one or two edges in common. Therefore it is clear that Π_1 and Π_2 are zones of Π . In this algorithm, the twists are chosen with some degree of freedom. So a particular progression of the algorithm is characterized by an ordered sequence of twists. Let I_1, \dots, I_r be all the indexations of the possible sequences of twists characterizing a progression of the algorithm.

So to each I_i corresponds a decomposition of Π into two polygons Π_{2i} and Π_{2i+1} , and since those polygons are zones, to each I_i correspond a zone decomposition Δ_i of Π . From corollary 6.3.1.4 we get that the intersection of all the Δ_i is a zone decomposition Δ of Π . Let $(\mathcal{T}_Z, \delta_Z)$ be the restriction of (\mathcal{T}, δ) to a zone Z of Δ , and let $K_Z = K(Z, \mathcal{T}_Z, \delta_Z)$.

Since the algorithm of section 6.2 has been used as much as possible, all the twists of $F(K)$ have been cut at some stage. So for every zone Z of Δ , the T-filling $F(K_Z)$ contains no twist. From prop. 6.1.0.6 we get that K_Z is a Harnack T-curve. So $K = \# K_Z$ and δ is a Harnack zone-wise sign distribution with respect to Δ . \square

7 From zone decompositions to Maximal T-Curves

7.1 Minimal and odd-cycle-free zone decompositions

Let Π be an integral polygon and Δ be a zone decomposition of Π .

7.1.0.3 Definition

A zone decomposition will be called a *minimal zone decomposition* if there exist a zone-wise Harnack distribution of signs δ on Π , with the property that for any two adjacent zones Z_i and Z_j of Δ , the restrictions δ_{Z_i} and δ_{Z_j} are of different type.

7.1.0.4 Definition

The *incidence graph of a zone decomposition* Δ of an integral polygon Π is the 1-skeleton Γ of a cell decomposition of Π dual to Δ . So Γ is a graph, its vertices represent the zones of Δ , and two vertices are linked by a number of (graph-)edges equal to the number of (zone decomposition)-edges shared by the two corresponding zones.

7.1.0.5 Definition

A set of zones Z_1, \dots, Z_r of a zone decomposition Δ of an integral polygon will be called a *cycle of zones* if they are represented by the vertices of a (graph-)cycle on the incidence graph of Δ . We will assume in our notations that the zones are indexed always in the same direction, say counterclockwise. We will call an *edge of the cycle*, and we will denote it e_i the edge shared by Z_i and Z_{i+1} , with i modulo r (if $r = 2$ there is two edges e_1 and e_2 shared by both Z_1 and Z_2). We will also note usually S the vertex common to all the zones Z_i .

Notice that if Δ is an arbitrary zone decomposition of Π , it is possible to make a minimal zone decomposition Δ' out of Δ , by the following algorithm:

- If Z_1, \dots, Z_r is a cycle of zones of Δ , let's fix a Harnack distribution δ_1 of arbitrary type θ_1 in Z_1 , and let δ_i be the Harnack distribution in Z_i , $i = 2, \dots, r$, of type $\theta_i = \theta_1 + \sum_{j=1}^{i-2} \theta(e_j)$. Thanks to lemma 6.2.2.3 we have $\theta_{i-1} \neq \theta_i$ and $\delta_{i-1} = \delta_i$ on e_{i-1} .
- If $\theta_r + \theta(e_r) \neq \theta_1$, then let's remove the edge(s) of $Z_1 \cap Z_r$, and consider $Z_1 \cup Z_r$ as a new zone Z'_1 . By doing this operation as many times

as necessary, we get a new cycle of zones Z'_1, Z_2, \dots, Z_s , where $Z'_1 = Z_{s+1} \cup \dots \cup Z_r \cup Z_1$ (s may be equal to 1), such that $\theta_{s+1} = \theta_1$, i.e. $\sum_{i=1}^s \theta(e_i) = (0, 0, 0) \pmod 2$.

- By doing the operation above simultaneously on all cycles of Γ , we get from Δ a new zone decomposition Δ' .

7.1.0.6 Lemma

The new zone decomposition Δ' is minimal.

proof. Indeed, let's choose a type θ_1 of Harnack distribution in an arbitrary initial zone Z_1 . For any zone Z of Δ , let θ_Z be the type of the Harnack distribution in Z defined from θ_1 as follows: Since the incidence graph Γ' of Δ' is connected, there is a path on Γ' from the vertex representing Z_1 to the vertex representing Z . Let e_1, \dots, e_r be the edges of zones of Δ' which are represented by the edges of this path. Then $\theta_Z = \theta_1 + \sum_{i=1}^r \theta(e_i)$.

The result doesn't depend on the path chosen. Indeed let θ'_Z be the type found with another path. The difference of the two paths is a union of cycles. From the construction of Δ' we get that the sum of the total parities of the edges of each cycle is equal to $(0, 0, 0)$. This implies that $\theta'_Z = \theta_Z$. So from this construction we get that for any two adjacent zones $Z_i, Z_j \in \Delta'$, the Harnack distributions δ_{Z_i} and δ_{Z_j} have different types, and from lemma 6.2.2.3 we deduce that the two distributions are equal on $Z_i \cap Z_j$.

So the sign distribution δ which is equal to δ_Z on any zone $Z \in \Delta'$ shows that Δ' is a minimal zone decomposition. \square

We recall here the definition of an odd-cycle-free zone decomposition given in section 2.5 in slightly different terms.

7.1.0.7 Definition

An *odd-cycle-free zone decomposition* of an integral polygon is a zone decomposition of that polygon such that, for any cycle of zones of that zone decomposition, and for any parity, the number of edges of the given cycle and of the given parity is even.

7.1.0.8 Lemma

An odd-cycle-free zone decomposition is a minimal zone decomposition.

proof. Indeed let Δ be an odd-cycle-free zone decomposition. If we apply the algorithm described above we must get $\Delta = \Delta'$. It is clear that a necessary and sufficient condition for this is the following: For every cycle of zones

Z_1, \dots, Z_r of Δ , the sum $\sum_{i=1}^r \theta(e_i)$ is equal to $(0, 0, 0)$ (with the notations of definition 7.1.0.5). Since all the segments e_1, \dots, e_r have a common endpoint, S , the total parity $\theta(e_i)$ of an edge e_i depends only on the parity of the other endpoint, and therefore depends only on the parity (a, b) of e_i . Since for each parity, the number of segments e_i of that parity is even, for each total parity, the number of segments e_i of that total parity is also even. Therefore $\sum_{i=1}^r \theta(e_i) = (0, 0, 0)$. \square

Notice that the converse of this lemma is not true. We exhibit in fig. 39 a minimal zone decomposition which is not an odd-cycle-free zone decomposition.

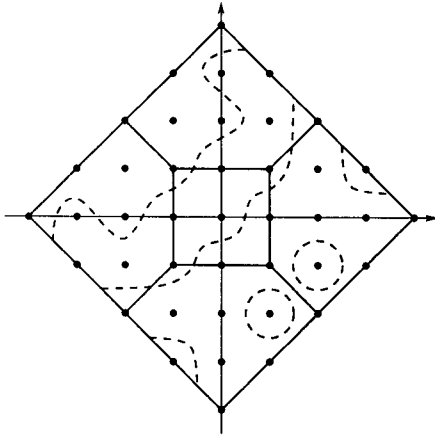


Figure 39: A minimal zone decomposition of the triangle $\mathbf{T}(4)$ which is not an odd-cycle-free zone decomposition. Notice that the lattice T-curve on $\mathbb{R}P^2$ constructed from it is not maximal.

7.2 From minimal zone decompositions to T-curves

Now we describe in two steps a construction of a T-curve K out of the data (Π, Δ) where Π is an integral polygon (the carrier polygon of K), and Δ is a minimal zone decomposition of Π .

- Let complete arbitrarily the zone decomposition Δ into a primitive triangulation \mathcal{T} of Π .
- Since Δ is minimal, let δ be a zone-wise Harnack distribution of signs, such that for any two adjacent zones $Z_i, Z_j \in \Delta$, the restrictions δ_{Z_i}

and δ_{Z_j} have different types.

7.2.0.9 Lemma

Let Π be an integral polygon in $\mathbb{R}_{\geq 0}^2$, let Δ be a minimal zone decomposition, and let $K = K(\Pi, \mathcal{T}, \delta)$ be the lattice T-curve constructed as above from the data (Π, Δ) . Then K depends, up to congruence, neither on the choice of the triangulation \mathcal{T} which completes Δ , neither on the choice of the zone-wise Harnack distribution of signs δ .

proof. Let $K' = K(\Pi, \mathcal{T}', \delta)$ be a lattice T-curve constructed as above from the data (Π, Δ) with the same choice of sign distribution δ but with an arbitrary other choice of triangulation \mathcal{T}' .

We get from cor. 5.3.2.6 that for any zone $Z \in \Delta$, the Harnack T-curve $K_Z = K(Z, \mathcal{T}_Z, \delta_Z)$ (where $(\mathcal{T}_Z, \delta_Z)$ is the restriction of (\mathcal{T}, δ) to Z) is congruent by a homeomorphism which is the identity on the boundary of the quadrants of $S(Z)$, to $K'_Z = K(Z, \mathcal{T}'_Z, \delta_Z)$. Since K is the gluing of the Harnack T-curves K_Z for all the zones Z of Δ , we deduce that K is congruent to K' .

Now let $K' = K(\Pi, \mathcal{T}, \delta')$ be a lattice T-curve constructed as above from the same data (Π, Δ) with the same choice of triangulation \mathcal{T} but with another choice of sign distribution δ' , such that for a given zone Z of Δ , the restriction δ'_Z is of type $(1, 0, 0)$.

Since for any two adjacent zones $Z_i, Z_j \in \Delta$, the restrictions δ_{Z_i} and δ_{Z_j} have different types, we get from lemma 6.2.2.3, that the type of δ_{Z_i} is determined by the type of δ_{Z_j} . Since the adjacency graph of Δ is connected and since Δ is a minimal zone decomposition, δ is determined by the type of δ_Z .

From lemma 5.3.2.4 we get that all the types of δ_Z can be obtained from the type $(1, 0, 0)$ by letting $(\mathbb{Z}_2)^3$ act on δ_Z . Moreover it is clear that for any $\theta \in (\mathbb{Z}_2)^3$, an initial distribution $(\theta \cdot \delta_Z)$ gives rise to the distribution $(\theta \cdot \delta)$ on Π . So we deduce from lemma 5.3.2.4 that K and K' are symmetric to one another, hence they are congruent. \square

7.3 odd-cycle-free zone decomposition and maximal T-curves

7.3.0.10 Theorem

- (1) Every lattice T-curve constructed as in section 7.2 from a data (Π, Δ) , where Δ is an even zone decomposition, is a maximal lattice T-curve.
- (2) Every maximal T-curve can be constructed as in section 7.2 from a data (Π, Δ) , where Δ is an odd-cycle-free zone decomposition.

7.3.1 Proof of the part (1) of theorem 7.3.0.10**7.3.1.1 Definition**

Let Π be an integral polygon and let Z_1, \dots, Z_r be a cycle of zones of a zone decomposition of Π . The *completed zone* \hat{Z}_i is the piece of Π which is delimited by the edges $Z_{i-1} \cap Z_i$ and $Z_i \cap Z_{i+1}$, and by $\partial\Pi$, and which contains Z_i .

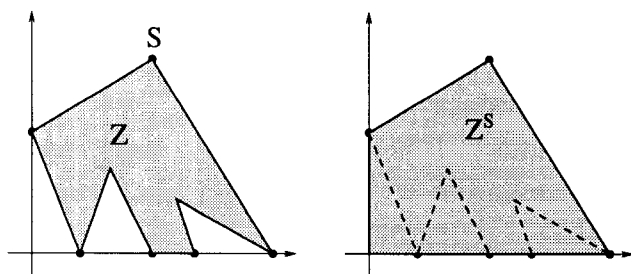


Figure 40: A zone and its completed zone.

Let Δ be an odd-cycle-free zone decomposition of an integral polygon Π , and let $K = K(\Pi, \mathcal{T}, \delta)$ be a lattice T-curve constructed as in section 7.2 from the data (Π, Δ) . We will give now a reduction algorithm which will output a sequence of zone-wise Harnack T-curves, $K = K^0, K^1, \dots, K^r$, where $K^i = K(\Pi, \mathcal{T}, \delta^i)$, and a sequence $\Delta = \Delta^0, \Delta^1, \dots, \Delta^r$ of odd-cycle-free zone decompositions, such that K^i is constructed as in section 7.2 from the data (Π, Δ^i) , such that Δ^{i+1} contains less zones than Δ^i , such that Π is the only zone of Δ^r (so K^r is a Harnack T-curve), and such that all the K^i have homeomorphic T-filling. Let Γ^i be the incidence graph of Δ^i .

(a) Assume first that Γ^i has a vertex of multiplicity one (i.e. it is the endpoint of only one edge of Γ^i), let Z_1 be the zone of Δ^i represented by this endpoint. So Z_1 is adjacent to only one zone $Z_2 \in \Delta^i$ and only by one primitive segment. Let θ be the total parity of that segment.

The completed zones \hat{Z}_1 and \hat{Z}_2 decompose Π . Let δ_{i+1} be defined by its restrictions to \hat{Z}_1 and to \hat{Z}_2 in the following way:

$$\begin{aligned}\delta_{\hat{Z}_1}^{i+1} &= \delta_{\hat{Z}_1}^i \\ \delta_{\hat{Z}_2}^{i+1} &= (\theta \cdot \delta_{\hat{Z}_2}^i)\end{aligned}$$

So $\delta_{\hat{Z}_1}^{i+1}$ and $\delta_{\hat{Z}_2}^{i+1}$ have same type. Let $K^{i+1} = K(\Pi, \mathcal{T}, \delta^{i+1})$. So $K_{Z_1 \cup Z_2}^{i+1}$ is a Harnack T-curve. The curve K^i is the gluing of the curves $K_{\hat{Z}_1}^i$ and $K_{\hat{Z}_2}^i$, and the curve K^{i+1} is the gluing of the curves $K_{\hat{Z}_1}^{i+1} = K_{\hat{Z}_1}^i$ and $K_{\hat{Z}_2}^{i+1} = (\theta \cdot K_{\hat{Z}_2}^i)$.

From prop. 6.2.2.1, we get that $F(K_i)$ is the gluing of $F(K_{\hat{Z}_1}^i)$ and $F(K_{\hat{Z}_2}^i)$ by one twists only (upon the segment $Z_1 \cap Z_2$), and from lemma 5.5.3.1 we get that $F(K^{i+1})$ is the gluing of $F(K_{\hat{Z}_1}^i)$ and $F(\theta \cdot K_{\hat{Z}_2}^i) = F(K_{\hat{Z}_2}^i)$ upon the same segment but with no twists. Therefore $F(K^i) \sim F(K^{i+1})$ (see for instance the first diagram in fig. 37).

Since Z_1 and Z_2 are adjacent, it is clear that $Z_1 \cup Z_2$ is a zone in Π . So let Δ^{i+1} be the zone decomposition obtained from Δ^i by taking $Z_1 \cup Z_2$ as a new zone (and keeping the other zones). It is clear that Δ_{i+1} is again an odd-cycle-free zone decomposition, and since K^i is the T-curve constructed as in section 7.2 from the data (Π, Δ^i) , it is clear that K^{i+1} is the T-curve constructed as in section 7.2 from the data (Π, Δ^{i+1}) .

(b) Assume now that Γ^i has no endpoint, but has some cycle of zones Z_1, \dots, Z_r . The completed zones $\hat{Z}_1, \dots, \hat{Z}_r$ decompose Π . Let δ^{i+1} be defined from its restrictions to the completed zones \hat{Z}_j in the following way:

$$\begin{aligned}\delta_{\hat{Z}_1}^{i+1} &= \delta_{\hat{Z}_1}^i \\ \delta_{\hat{Z}_j}^{i+1} &= \left(\left(\sum_{k=1}^{j-1} \theta(e_k) \right) \cdot \delta_{\hat{Z}_j}^i \right) \quad \text{for } j = 2, \dots, r\end{aligned}$$

Where $\theta(e_k)$ is the total parity of the edge of the cycle of zones $e_k = Z_{k-1} \cap Z_k$ (see def. 7.1.0.5 for more precisions on the notations). Let $K^{i+1} = K(\Pi, \mathcal{T}, \delta^{i+1})$.

From lemma 6.2.2.3 we get that the distributions $\delta_{\hat{Z}_j}^{i+1}$ have same type θ_1 , therefore δ^{i+1} restricted to $Z_1 \cup \dots \cup Z_r$ is a Harnack distribution of signs, and $K_{\bigcup Z_j}^{i+1}$ is a Harnack curve.

From prop. 6.2.2.1, we know that $F(K_i)$ is the gluing of the surfaces $F(K_{\hat{Z}_j}^i)$ by twists upon the edges e_j , and that $F(K^{i+1})$ is the gluing of the

same surfaces upon the same edges but with no twists. Since Δ^i is an odd-cycle-free zone decomposition, the number r of zones in the cycle of zones is even. So by flipping, for one index j over two, the surfaces $F(K_{Z_j}^i)$ (which are each attached to the rest of $F(K^i)$ by two twists) in the hole where lies S (the vertex common to all the zones Z_j), we undo the twists two by two (see fig. 41). Therefore the resulting surface is homeomorphic to $F(K^{i+1})$.

Since the zones Z_1, \dots, Z_r form a cycle of zones, it is clear that their union, is also a zone of Π , so let Δ^{i+1} be the zone decomposition obtained from Δ^i by taking $Z_1 \cup \dots \cup Z_r$ as a new zone (and keeping the other zones). It is clear that Δ^{i+1} is again an odd-cycle-free zone decomposition. Since K_i is constructed as in section 7.2 from the data (Π, Δ^i) , it is clear that K^{i+1} is constructed as in section 7.2 from the data (Π, Δ^{i+1}) .

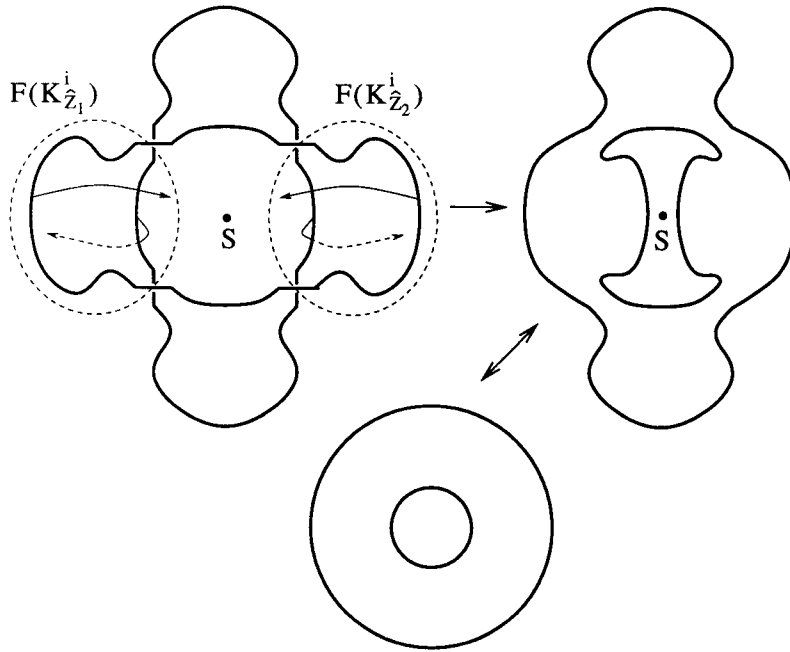


Figure 41: How to undo the twists of $F(K^i)$ to get $F(K^{i+1})$.

(c) By doing steps (a) and (b) alternatively as much as possible, we decrease the number of zones in the sequence Δ^i until we get just one zone, Π itself, in Δ^r . So the last curve K^r is a Harnack curve. Therefore $F(K^r)$ is a sphere with holes, and since $F(K^r) = F(K^{r-1}) = \dots = K(K^0)$, we get from lemma 5.3.1.3 that $K^0 = K$ is a maximal T-curve. \square

7.3.2 Proof of the part (2) of theorem 7.3.0.10

(a) Let $K = K(\Pi, \mathcal{T}, \delta)$ be a maximal T-curve. From prop. 6.3.2.2 we get that the triangulation \mathcal{T} is a sub-decomposition of some zone decomposition Δ of Π . From the proof of prop. 6.3.2.2, we deduce easily that Δ is a minimal zone decomposition: Indeed if e is an edge of two adjacent zones of Δ which were to have Harnack distributions of same type, there would be no twist upon e , so the cutting algorithm of section 6.2.1 wouldn't have separated these two zones. Hence K is congruent to a T-curve constructed as in section 7.2 from the data (Π, Δ) .

(b) Let's show now that Δ is in fact an odd-cycle-free zone decomposition. Let Z_1, \dots, Z_r be a cycle of zones of Δ .

Let's show first that r is even. Let γ be a loop on $F(K)$ around the vertex S common to all the zones Z_i (see fig.42). The only twists through which γ passes are situated upon the edges e_1, \dots, e_r of the cycle (because K restricted to each Z_i is a Harnack curve). Since K is maximal, $F(K)$ is orientable. This implies that γ passes through an even number of twists, so r is even.

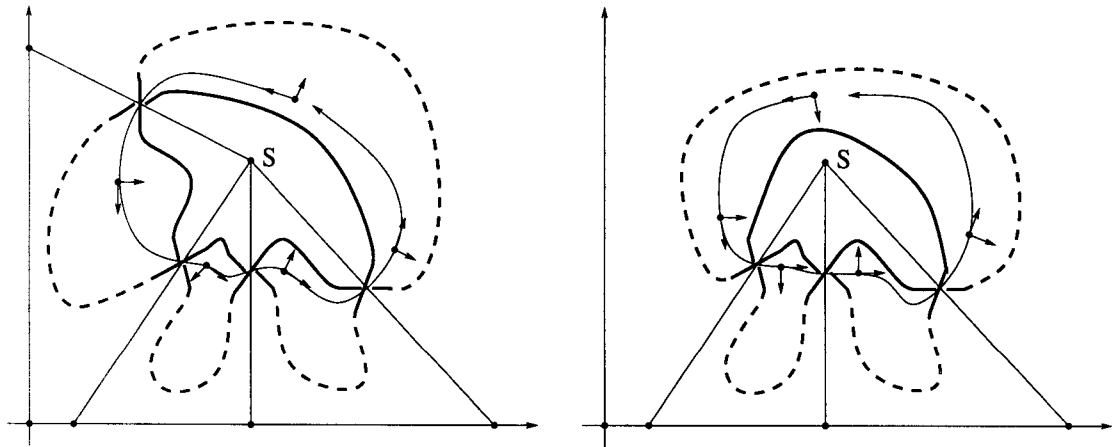


Figure 42: If K is maximal, then the number of zones in a cycle of zones must be even, otherwise $F(K)$ wouldn't be orientable. Here the orientation on $F(K)$ is not reversed along a loop when the cycle has four zones, but it is reversed when the cycle has three zones.

Recall that a segment has never even parity, so the parity of a segment can be $(1, 0)$, $(1, 1)$ or $(0, 1)$. Let $N_{a,b}$ be the number of edges e_i of parity

(a, b) . From the last paragraph we get that

$$N_{1,0} + N_{1,1} + N_{0,1} = 0 \pmod{2} \quad (12)$$

Since Δ is minimal, we have also

$$\sum_{k=1}^r \theta(e_k) = (0, 0, 0) \quad (13)$$

Recall that the parity (a, b) of a segment is included as the two last coordinates in the total parity $\theta = (c, a, b)$ of the segment. So the equation 13 above can be restated with the parity of the edges (instead of their total parity) in the following way:

$$N_{1,0} \cdot (1, 0) + N_{1,1} \cdot (1, 1) + N_{0,1} \cdot (0, 1) = (0, 0) \pmod{2}$$

Which is equivalent to

$$N_{1,0} + N_{1,1} = 0 \pmod{2} \quad (14)$$

$$N_{1,1} + N_{0,1} = 0 \pmod{2} \quad (15)$$

Putting equations 12, 14, and 15 we get that $N_{1,0} = N_{1,1} = N_{0,1} = 0$. Hence the zone decomposition is even. \square

Part II

The Ragsdale Conjecture for Maximal Lattice T-curves

8 Introduction.

Part II of this text is only concerned with lattice \mathbf{T} -curves on $\mathbb{R}P^2$, therefore from now on to avoid too many repetitions we will always assume, unless explicitly stated, that lattice \mathbf{T} -curves are on $\mathbb{R}P^2$. We will keep the notations and definitions of part I. So, as in part I, we denote by $\mathbf{T} = \mathbf{T}(d)$ the triangle in \mathbb{R}^2 with vertices $A_0 = (0,0)$, $A_1 = (d,0)$, and $A_2 = (0,d)$. Recall that $\mathbb{R}P^2$ has a fourfold ramified covering structure on \mathbf{T} , given by $\mu : \mathbb{R}P^2 \rightarrow \mathbf{T}$, $(x_0 : x_1 : x_2) \mapsto (\frac{|x_1|}{\sum |x_i|}, \frac{|x_2|}{\sum |x_i|})$. We denote too by $l_0 = A_1A_2$, $l_1 = A_2A_0$, and $l_2 = A_0A_1$ the segments forming the edges of \mathbf{T} . So the lifts $\mu^{-1}(l_i)$ are the lines $x_i = 0$ of $\mathbb{R}P^2$.

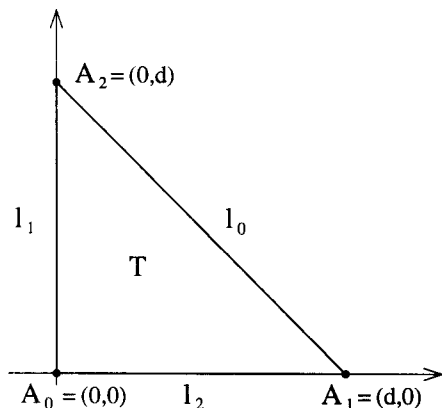


Figure 43: The ambient triangle.

For short we will write simply *algebraic curve* for “real projective non-singular algebraic curve”. We will use the letter K for curves. So if K is an algebraic curve, and if it is defined by a polynomial f , we will denote it by $K(f)$.

Recall (in slightly different words than in def. 7.1.0.5) that a *cycle of zones* of a zone decomposition Δ of \mathbf{T} is the sequence of all the zones Z_1, \dots, Z_r of Δ which share an integral point S lying in the interior of \mathbf{T} . The zones are assumed to be always indexed in the same way (say counterclockwise around S). An *edge of a cycle of zones* is a primitive segment of $Z_i \cap Z_{i+1}$ (this intersection is exactly one primitive segment when $r > 2$).

Recall (see def. 7.1.0.7) that an odd-cycle-free zone decomposition of \mathbf{T} is a zone decomposition Δ such that for every parity, and for every cycle of

zones of Δ , the number of edges of the given cycle of zone, which have the given parity, is even.

Recall the construction of 7 of a lattice T-curve from an odd-cycle-free zone decomposition Δ of \mathbf{T} . Since Δ is odd-cycle-free we can choose a zone-wise Harnack distribution of signs δ on \mathbf{T} such that for any two adjacent zones Z_i, Z_j of Δ , the Harnack distributions δ_{Z_i} and δ_{Z_j} (i.e. the restrictions of δ to Z_i and Z_j) have different types (see lemma 7.1.0.8). Then we choose a primitive triangulation \mathcal{T} of \mathbf{T} which completes Δ . Let $K = K(\mathbf{T}, \mathcal{T}, \delta)$.

Any other choice δ' for the zone-wise Harnack distribution of signs, and any other choice \mathcal{T}' for the triangulation completing Δ would have led to a lattice T-curve $K' = K(\mathbf{T}, \mathcal{T}', \delta')$ which is congruent to K (see lemma 7.2.0.9). Since we are just interested in lattice T-curves up to congruence, we denote by $K(\Delta)$ any lattice T-curve which is constructed that way from an odd-cycle-free zone decomposition Δ .

Recall that a *maximal curve (of degree d)* is a curve with the maximum number of connected components. The Harnack theorems (see reference [3] in the case of algebraic curves, and theorem 5.3.1.1 for lattice T-curves) states that this number is equal to $\frac{(d-1)(d-2)}{2} + 1$.

Recall now the main theorem of part I (applied here to lattice T-curves on $\mathbb{R}P^2$):

Theorem: (see 7.3.0.10)

- (1) *Every lattice T-curve which is constructed from an odd-cycle-free zone decomposition of \mathbf{T} (as recalled above) is a maximal T-curve.*
- (2) *Every maximal T-curve can be constructed (as recalled above) from an odd-cycle-free zone decomposition of \mathbf{T} .*

Recall that the connected components of a lattice T-curve of even degree $2k$ are only ovals, and the connected components of a lattice T-curve of odd degree $2k + 1$ are all ovals but one which is one-sided.

We will denote, as in part I, by $\sigma_{a,b}$ the symmetry $(x, y) \mapsto ((-1)^a x, (-1)^b y)$, where $a, b \in \{0, 1\}$.

8.0.2.1 Definition (even/odd ovals, P and N)

An oval lying inside an even (an odd) number of other ovals is called an *even* (an *odd*) oval. We will write P (resp. N) for the number of even (of odd) ovals of a curve K .

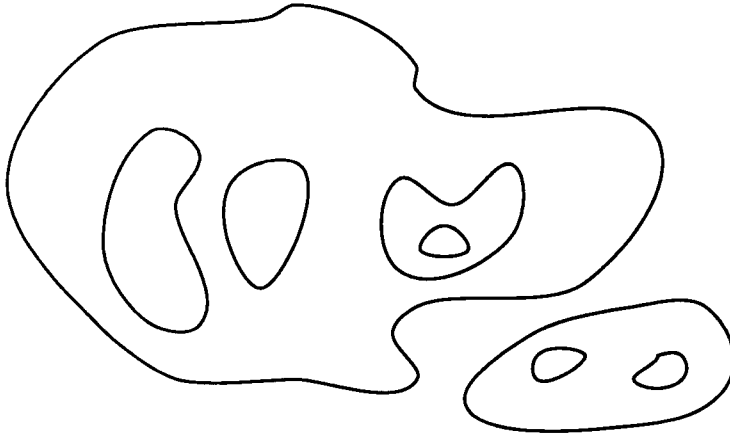


Figure 44: A curve with 3 even ovals and 5 odd ovals.

8.1 Some history.

In 1907 Virginia Ragsdale [9] wrote the following conjecture: Assume that the polynomial f defining an algebraic curve of even degree $K(f)$ takes negative values outside all the ovals, and denote by $\{f > 0\}$ and $\{f < 0\}$ the subsets of $\mathbb{R}P^2$ where f takes positive and negative values. Then

1. If $K = K(f)$ is a maximal curve of degree $2k$, then the number of connected components of $\{f > 0\}$ and of $\{f < 0\}$ are both greater or equal than $\frac{1}{2}(k-1)(k-2) + 1$.
2. If $K = K(f)$ is not a maximal curve, then the number of connected components of $\{f < 0\}$ and of $\{f > 0\}$ are both less or equal to $k^2 + \frac{1}{2}(k-1)(k-2)$.

Let's write $R(k)$ for the *Ragsdale bound* $\frac{3k(k-1)}{2} + 1$. It is easy to calculate that in both cases the two inequalities are equivalent to the following ones (notice that the number of connected components of $\{f > 0\}$ and $\{f < 0\}$ are respectively equal to P and $N + 1$).

$$N \leq R(k) - 1 \quad \text{and} \quad P \leq R(k)$$

In 1937 Petrowskii, who wasn't aware of Ragsdale work, concludes his paper [8] by pointing out that in all the known curves of degree $2k$ (the "known

curves" at that time were mainly the families of curves due to Harnack and to Hilbert), one has:

$$N \leq R(k) \quad \text{and} \quad P \leq R(k)$$

In 1980 Viro [7] constructed algebraic curves of even degree with $N = R(K)$, so the Ragsdale conjecture was reformulated since then like in Petrowskii's paper. In his paper Viro gave at the same time a possible generalization of Ragsdale conjecture in more modern terms: Let K be here the set of fixed points of an anti-holomorphic involution on a nonsingular simply connected compact complex surface $\mathbb{C}K$. Do the following inequality hold:

$$\dim H_1(K; \mathbb{Z}/2\mathbb{Z}) \leq h^{1,1}(\mathbb{C}K)$$

In 1993 Itenberg [4] disproved Ragsdale conjecture by constructing T-curves of degree $2k$ with:

$$\begin{aligned} N &= R(k) + \lfloor \frac{k^2 - 6k + 13}{8} \rfloor - 1 \quad \text{or} \\ P &= R(k) + \lfloor \frac{k^2 - 6k + 13}{8} \rfloor \end{aligned}$$

Where we denote by $\lfloor a \rfloor$ the greatest integer smaller than a .

In 1994 [2] I improved Itenberg result by constructing T-curves with:

$$\begin{aligned} N &= R(k) + \lfloor \frac{k^2 - 7k + 16}{6} \rfloor - 1 \quad \text{or} \\ P &= R(k) + \lfloor \frac{k^2 - 7k + 16}{6} \rfloor \end{aligned}$$

It is interesting to notice at this point that the conjunction of Harnack theorem (see theorem 2.2.0.3) $P + N \leq (2k - 1)(k - 1) + 1$ and of Petrowskii inequalities [8] $|P - N| \leq R(k) + 1$, shows that

$$P \leq R(k) + \frac{k^2 - 9k + 6}{4} \quad \text{and} \quad N \leq R(k) + \frac{k^2 - 9k + 6}{4}$$

Therefore there may be still some gap to fill, and a sharp bound still remains to be found.

Being more careful at the way Ragsdale wrote her conjecture we see that she stated two different forms of her conjecture, **(1)** a weak form (for maximal

curves), and **(2)** a strong form (for all the curves). Finally it is the strong form which has been disproved and the weak form still remains open, namely do the following inequalities:

$$N \leq R(k) \quad \text{and} \quad P \leq R(k)$$

hold for all maximal curves of degree $2k$?

8.2 The main theorems.

Let $R(k)$ be, as previously, the Ragsdale bound $\frac{3k(k-1)}{2} + 1$, and let $M(k)$ be the maximum number of connected components of a curve of even degree $2k$. It is interesting to notice that Itenberg's counterexamples are T-curves with $M(k) - \frac{k^2}{8} + \dots$ ovals, where the dots represent some term of lower degree in k , but my counterexamples are T-curves with $M(k) - k + \dots$ ovals. I constructed also T-curves with N or P equal to $R(k) + k/3 + \dots$, and with just $M(k) - 2$ ovals. So it seemed very possible that there exist maximal T-curves with N or P passing $R(k)$ at least by a nonzero linear term in k . The main theorem of this section shows that this is not the case, namely:

Theorem: (see 12.4.0.12)

The following inequalities hold:

$$N \leq R(k) + 3 \quad \text{and} \quad P \leq R(k)$$

for every maximal lattice T-curve of even degree $2k$.

In the proof of this theorem appears an intermediate theorem. Let Δ be an odd-cycle-free zone decomposition of \mathbf{T} , let $K = K(\Delta)$, and let Δ' be the decomposition of \mathbf{T} obtained from Δ by removing all the edges of zones, which have an endpoint of even parity. It is easy to check that Δ' is again an odd-cycle-free zone decomposition, so let $K' = K'(\Delta')$.

Theorem: (see 10.6.0.5)

The number of even (odd) ovals of K is equal to the number of even (odd) ovals of K' .

8.3 Some new definitions

Some integral points of the boundary of a zone are of particular interest. They are mainly the vertices of the zone, but in some cases an interesting

integral point can belong to the interior of an edge of the zone (see fig 45). Since the term “vertex” is already over-used, we will use some new term, and give at the same time a precise definition of the integral points of the boundary of a zone, which are of interest:

8.3.0.2 Definition (the nodes of a zone)

A *node* of a zone is an integral point which belongs to the boundary of the zone, but doesn't belong to the interior of the intersection of the zone with $\partial\mathbf{T}$ (see fig. 45).

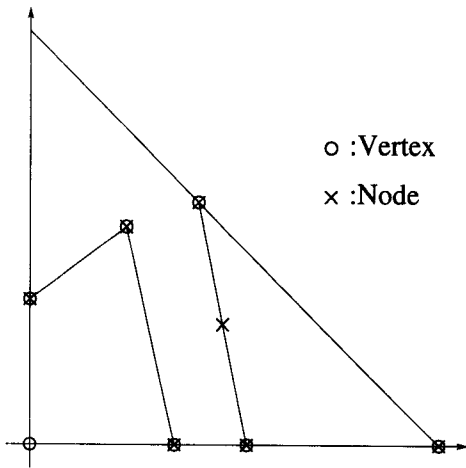


Figure 45: nodes and vertices of a zone.

8.3.0.3 Definition (inner-node and boundary-node)

An *inner-node* of a zone is a node of the zone, which lies in the interior of \mathbf{T} . A *boundary-node* of a zone is a node of the zone, which lies on $\partial\mathbf{T}$.

8.3.0.4 Definition (consecutive boundary-nodes)

Let Δ be a zone decomposition of \mathbf{T} . Two boundary-nodes (of zones) in Δ are *consecutive* if one is met after the other one when following $\partial\mathbf{T}$ in clockwise or counterclockwise direction.

8.3.0.5 Definition (separating segments and edges)

A *separating edge* of a zone is an edge of the zone, which is a primitive segment separating \mathbf{T} into two components.

8.3.0.6 Definition (Pie diagram)

Let Δ be an odd-cycle-free zone decomposition of \mathbf{T} , let $K = K(\Delta)$, and let h be a homeomorphism transforming \mathbf{T} into a disk, and transforming the edges of the zones of Δ which do not lie in $\partial\Pi$, into segments. A *Pie diagram* of K (or just of a part of K) is the image of K under the composition $h \circ \mu$ (recall that μ is the projection $\mathbb{R}P^2 \rightarrow \mathbf{T}$), (see an example on fig 47).

8.3.0.7 Lemma

Let Δ be an odd-cycle-free zone decomposition of \mathbf{T} and let $K = K(\Delta)$. Let P and P' be two consecutive boundary-nodes in Δ (P and P' may be on different edges of \mathbf{T}). Then

- the segment PP' belongs to one zone.
- In the pie diagram, it is the same arc of K which surrounds P and P' in this zone.

proof. That P and P' are consecutive implies clearly that PP' belongs to one zone. Since the distribution of signs in this zone is a Harnack distribution, the oval surrounding P in the pie diagram surrounds all the integral points of $\partial\mathbf{T}$ between P and P' (see fig. 46). \square

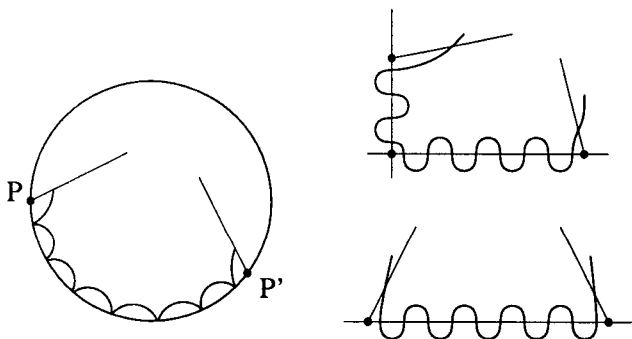


Figure 46: Shape of the arc between two consecutive boundary-nodes.

8.3.0.8 Definition (sector)

Let Δ be a zone decomposition of \mathbf{T} having some zones with an inner-node S . Let P and P' be two boundary-nodes linked by two edges of zones of Δ to S . The *sector* $\widehat{PSP'}$ is the subset of \mathbf{T} swept by a half line with origin S rotating counterclockwise from SP to SP' .

Now we can reformulate and complete def. 7.3.1.1 of a completed zone:

8.3.0.9 Definition (Completed zones Z^S and Z^e)

Let Δ be a zone decomposition of \mathbf{T} having a zone Z with an inner-node S , and let P and P' be the boundary-nodes such that SP and SP' are edges of Z . The *completed zone* Z^S is the one sector $\widehat{PSP'}$ or $\widehat{P'SP}$ containing Z .

Let Δ be a zone decomposition of \mathbf{T} having a zone Z with separating edge e . So e splits \mathbf{T} into two (open) components. The completed zone Z^e is the closure of the component containing Z .

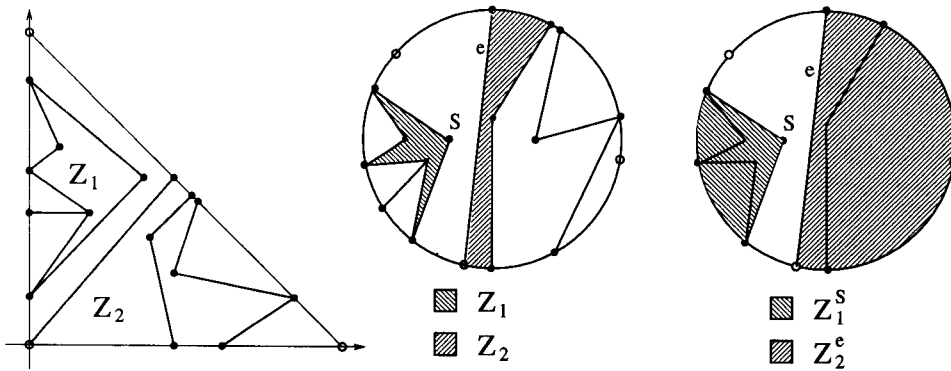


Figure 47: Examples of Pie-diagrams and of completed zones.

8.3.0.10 Definition (neighborly in/out-side of an oval)

Let K be a nonsingular curve on $\mathbb{R}P^2$. We say that a point P lies *neighborly inside (outside)* of an oval O of K , if P lies inside (outside) of O and outside of any oval lying inside (outside) of O .

So the sign of an oval, lying entirely in a quadrant of $\mathbb{R}P^2$, of a lattice T-curve K on $\mathbb{R}P^2$ (see def. 4.3.0.7) is the sign of the points which lie neighborly inside the oval.

9 The Point-Oval Correspondence.

9.1 Definition of the correspondence

Let Δ be an odd-cycle-free zone decomposition of \mathbf{T} , and let $K = K(\Delta)$. Since K is a maximal lattice T-curve, the number of connected components of K is equal to $(2k - 1)(k - 1) + 1$. The number of integral points in the interior of \mathbf{T} is equal to $(2k - 1)(k - 1)$. So let $*$ be an arbitrary point and let's define now a one-to-one correspondence α between the set $(\text{int } \mathbf{T} \cap \mathbb{Z}^2) \cup \{*\}$ and the set of connected components of K in the following way:

9.1.0.11 Definition (1 — Correspondence in the interior of a zone)

Since $K = K(\Delta) = K(\mathbf{T}, \mathcal{T}, \delta)$ is the gluing of the T-curves $K(Z, \mathcal{T}_Z, \delta_Z)$ for all the zones Z of Δ , we get from the proof of prop. 5.3.2.5, that there is an empty oval surrounding some symmetric copy $(\sigma_{a,b} \cdot P)$, for every integral point P which is not an inner-node for Δ . So let $\alpha(P)$ be this oval.

Let S be an inner-node of a zone of Δ , and let Z_1, \dots, Z_m be all the zones of Δ sharing S as inner-node. Assume that the Z_i are indexed counterclockwise around S , and let $SP_i = Z_i \cap Z_{i+1}$ (or $SP_1 \cup SP_2 = Z_1 \cap Z_2$ if $m = 2$).

Let's have a closer look of K in the pie diagram. From the proof of prop. 5.3.2.5, we get that an arc a_i of K surrounds S in Z_i , surrounds P_i in Z_{i+1} , and surrounds P_{i-1} in Z_{i-1} .

9.1.0.12 Lemma

The arcs a_{i+1} and a_{i-1} belong to the same connected component of K .

proof. Recall from lemma 5.0.1.2 that on the pie diagram, for each i , the edge SP_i is cut exactly twice by K . More precisely SP_i is cut once by a_i and once by a_{i+1} , and SP_{i-1} is cut once by a_{i-1} , and once by a_i . In $\mathbb{R}P^2$ the boundary of $\bigcup_{a,b}(\sigma_{a,b} \cdot Z_i^S)$ is equal to $\bigcup_{a,b}(\sigma_{a,b} \cdot (SP_{i-1} \cup SP_i))$. So, in the pie diagram, the only way for the arc a_{i+1} which "break in" Z_i^S through SP_i , to escape Z_i^S is to pass through SP_{i-1} . Hence a_{i+1} is connected to a_{i-1} (see fig. 48). \square

Notice that since Δ is odd-cycle-free, we get from the lemma 9.1.0.12 just above that there is two different connected components of K , one component surrounding S in the union $\bigcup Z_{2j+1}^S$, and one component surrounding S in the union $\bigcup Z_{2j}^S$.

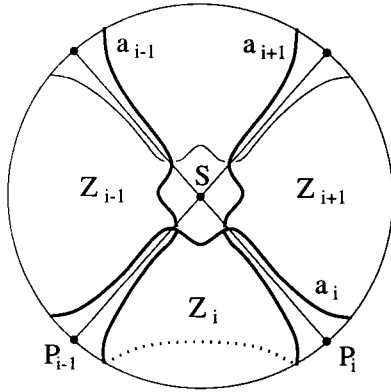


Figure 48: Two different connected components of K surround the inner-node S .

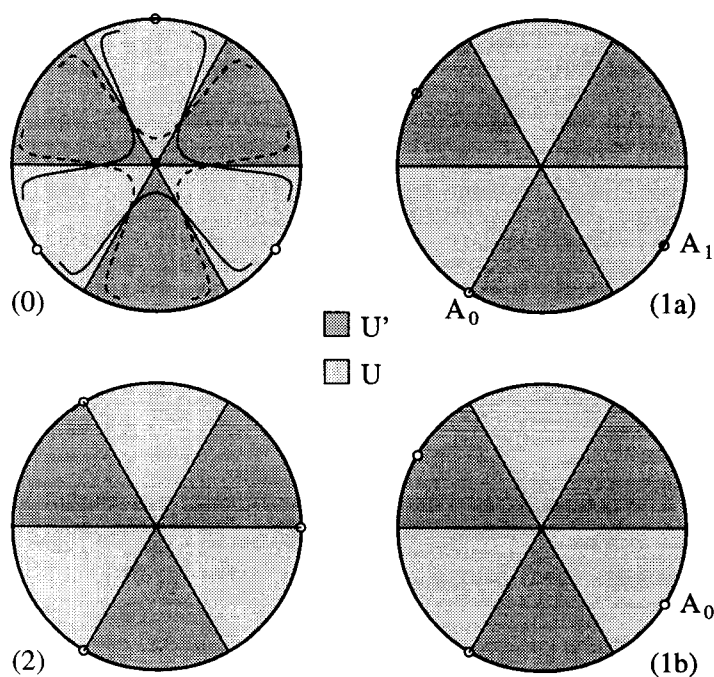
9.1.0.13 Definition ($U(S)$ and $U'(S)$)

1. If the two unions $\bigcup Z_{2j}^S$ and $\bigcup Z_{2j+1}^S$ don't contain the same number of points among A_0, A_1 and A_2 , then let $U(S)$, or simply U , be the union which contains the largest number of those points, and let $U'(S)$, or simply U' , be the union which contains the smallest number.
2. If the two unions contain the same amount of A_i 's, consider the two following cases (see illustrations on fig. 49 (1.a), (1.b), and (2)):
 - (a) Just one A_i , belongs to the intersection of the two unions. Then two sub-cases arise.
 - i. A_0 belongs to the intersection, then U is the union containing A_1 and U' is the other union.
 - ii. A_0 doesn't belong to the intersection, then U is the union containing A_0 and U' is the other one.
 - (b) The three A_i 's belong to the intersection, then U will be any of the union and U' the other one.

Notice that in both cases 2a and 2b, U contains A_0 .

9.1.0.14 Definition (2 — Correspondence for inner-nodes)

For an inner-node S , let $\alpha(S)$ be the connected component of K surrounding S in U . Now in order to see that α is injective one

Figure 49: The four cases arising in the definition of U .

should skip to the prop. 9.2.0.15. Assume now this is true, so one connected component should be left. Let $\alpha(*)$ be this connected component.

9.2 Properties of the correspondence

Let Δ be an odd-cycle-free zone decomposition of \mathbf{T} , let $K = K(\Delta)$ and let α be the point-oval correspondence defined in subsection 9 above.

9.2.0.15 Proposition

If S and R are two different inner-nodes, then $\alpha(S)$ and $\alpha(R)$ are two different connected components of K .

proof. Assume that $\alpha(S) = \alpha(R)$ for some $S \neq R$. Let Z_0, Y_0 be the zone of Δ such that $Z_0^S \supset R$ and $Y_0^R \supset S$. We prove now that the assumption cannot hold.

1. If the oval $\alpha(S)$ surrounds S in Z_0 then $\alpha(S)$ cannot surround R , so $\alpha(S) \neq \alpha(R)$. Therefore $Z_0^S \subset U'(S)$, and similarly $Y_0^R \subset U'(R)$.

Moreover Z_0^S contains all the zones Y^S other than Y_0^R , and similarly Y_0^R contains all the zones Z_S other than Z_0^S . Therefore we have:

$$U(R) \subset U'(S) \quad \text{and similarly} \quad U(S) \subset U'(R) \quad (16)$$

2. Let $a(S)$ and $a'(S)$ (let $a(R)$ and $a'(R)$) be the number of points among A_0, A_1 and A_2 which lie in $U(S)$ and $U'(S)$ (in $U(R)$ and $U'(R)$). From the inclusions 16 above, one gets that $a(R) \leq a'(S)$ and that $a(S) \leq a'(R)$. From the definition 9.1.0.13 of U and U' , one gets that $a'(R) \leq a(R)$ and that $a'(S) \leq a(S)$, so these numbers are all equal to a same number a . Since there are three points A_i , the number a cannot be 1, but must be 3 or 2.
3. Assume that $a = 3$. Then $U(S) \cap U'(S)$ as well as $U(R) \cap U'(R)$ contains the three A_i 's. But this is impossible since $U(S) \cap U'(S) \cap U(R) \cap U'(R)$ contains at most two points (two boundary-nodes), (see fig. 50).

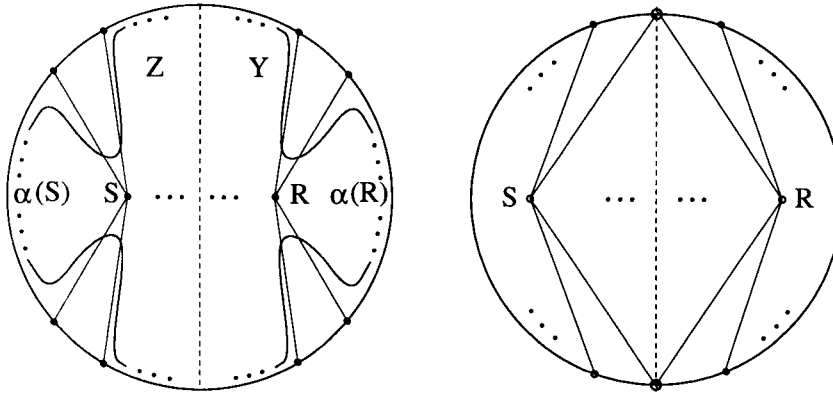


Figure 50: The ovals $\alpha(S)$ and $\alpha(R)$ are represented on the left pie-diagram. On the right diagram, we see that $U(S) \cap U'(S) \cap U(R) \cap U'(R)$ contains at most two points.

4. Assume that $a = 2$. Then $U(S) \cap U'(S)$ contains only one A_i . Let's write it $A(U(S) \cap U'(S))$. Also $\text{int}U(S)$ and $\text{int}U'(S)$ contain each one A_i . Let's write them $A(\text{int}U(S))$ and $A(\text{int}U'(S))$. With R instead of S we relabel the three A_i 's in a similar way: $A(U(R) \cap U'(R))$, $A(\text{int}U(R))$ and $A(\text{int}U'(R))$.

- (a) From the inclusions 16 above we get that $A(\text{int}U(S))$ and $A(U(S) \cap U(S'))$ belong to $U'(R)$, so $A(\text{int}U'(S)) = A(\text{int}U(R))$.
- (b) Similarly $A(\text{int}U'(R)) = A(\text{int}U(S))$.
- (c) Since $\text{int}U(S)$ and $\text{int}U(R)$ are disjoint, $A(\text{int}U(S))$ and $A(\text{int}U(R))$ are different points.
- (d) Since there is three points A_i we get that $A(U(S) \cap U'(S)) = A(U(R) \cap U'(R))$.
- (e) From the definition 9.1.0.13 of U and of U' , $A(\text{int}U'(S))$ and $A(\text{int}U'(R))$ are different than A_0 . Therefore $A_0 = A(U(S) \cap U'(S))$.
- (f) From argument 4c we get that A_1 is equal either to $A(\text{int}U(S))$, either to $A(\text{int}U(R))$.

But the last assertion contradicts the definition of U and U' . Indeed for both $U(S)-U'(S)$ and $U(R)-U'(R)$ we are in case 2(a)i of the definition, so A_1 should be equal to both $A(\text{int}U(S))$ and $A(\text{int}U(R))$.

□

10 Removing even edges

Let Δ be an odd-cycle-free zone decomposition of \mathbf{T} .

If Δ contains some zone with an inner-node S , let Z_1, \dots, Z_r be the cycle of zones of Δ around S . We assume without loss of generality that the completed zone Z_1^S is in U and is one of the completed zones Z_i^S which contain the largest number of the points among A_0, A_1 and A_2 . We will denote $a_i = (S, P_i)$ the edge met first from Z_{i-1} when turning around S counterclockwise (if $r > 2$ then a_i is just $Z_{i-1} \cap Z_i$).

Similarly if Δ contains some zone with a separating edge e , let Z_1 and Z_2 be the two zones adjacent along e . If they don't contain the same number of points A_i , then we assume without loss of generality that the completed zone Z_1^e contains more points A_i than Z_2^e .

10.0.0.16 Definition

We will say that an integral segment is *even* $(c, a, b) \in (\mathbb{Z}_2)^3$ if $c = 0$.

Notice that since the parity of the integral points of an integral segment takes exactly two values, we get from the definition 6.2.2.2 of the total parity, that a segment is even if and only if it contains an integral point of even parity.

10.1 Which point inside which oval

10.1.1 Local deformation of a lattice T-curve

Recall that the four quadrants of $\mathbb{R}P^2$ are represented by the four symmetric copies $(\sigma_{a,b} \cdot \mathbf{T})$, for all $a, b \in \{0, 1\}$.

An arc a of K lying inside a disk in $\mathbb{R}P^2$ can be moved and deformed by any sequence of the following operations (represented on figure 51):

1. If a has its two end points in a given quadrant then it can be shrunk, with endpoints fixed, into an arc inside this quadrant.
2. If a has its two endpoints in two given quadrants which are adjacent in the disk, then it can be shrunk, with endpoints fixed, into a segment.
3. If a has its two endpoints in two given quadrants which are opposite in the disk, then it can be deformed into an arc avoiding any one of the remaining two quadrants.

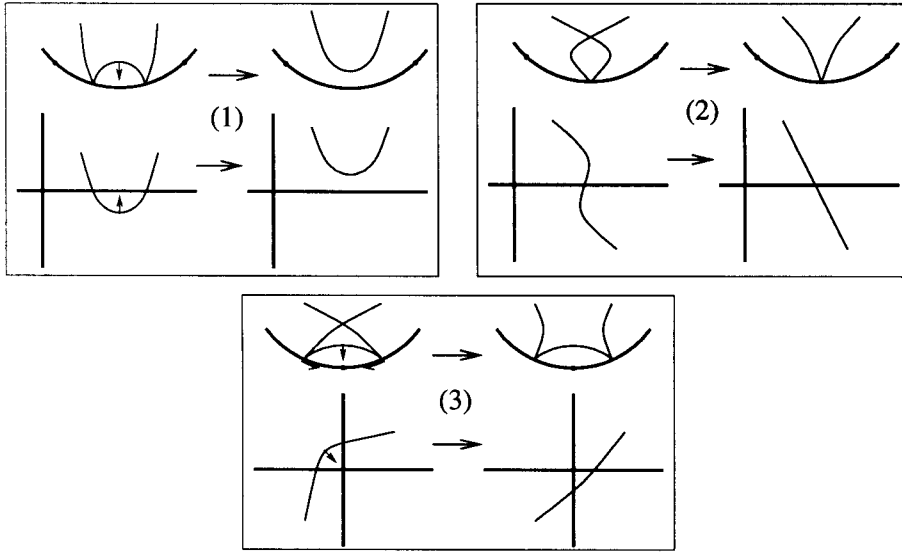


Figure 51: The three basic deformations of an arc of the curve viewed on a pie diagram.

10.1.2 Points inside their corresponding ovals

10.1.2.1 Lemma

For every point $P \in ((\text{int } \mathbf{T}) \cap \mathbb{Z}^2)$, some symmetric copy $(\sigma_{a,b} \cdot P)$ lies neighborly inside $\alpha(P)$.

proof. If P is not an inner-node, then this is clear since the distribution of signs in the zone containing P is a Harnack distribution. Assume then that $P = S$ is an inner-node and let's keep track on the Pie diagram of the inside of the ovals by drawing small arrows directed inside.

Now assume that the copies $(\sigma_{a,b} \cdot S)$, for all $a, b \in \{0, 1\}$, surrounded by $\alpha(S)$ in U are outside $\alpha(S)$ (see the coorientation of $\alpha(S)$ on the pie-diagram, fig. 52). Since $\text{int } U'$ contains at most one A_i , the lift $\mu^{-1}(Z^S)$, for any zone $Z \subset U'$ with inner-node S , is a disk or a union of two disks. So we can move and deform locally, inside U' , $\alpha(S)$ by a finite sequence of the operations of 10.1.1 into

1. Either an oval surrounding completely the point S in the Pie diagram (see fig. 52 (1)).
2. Either an oval surrounding the point S and a point A_i in the pie diagram

(see fig. 52 (2)).

These two cases are impossible. Indeed, since we didn't move or deform the oval inside U , we see on the diagram that in case 1 the inside is in fact outside. In case 2 the two arcs of $\alpha(S)$ cutting $\partial\mathbf{T}$ on each side of a point A_i should belong to three different quadrants, and at the same time we see on the diagram that $\alpha(S)$ should belong to no more than two quadrants.

So the assumption cannot hold, and one of the symmetric copy $(\sigma_a, b \cdot S)$ must lie (neighborly) inside $\alpha(S)$. \square

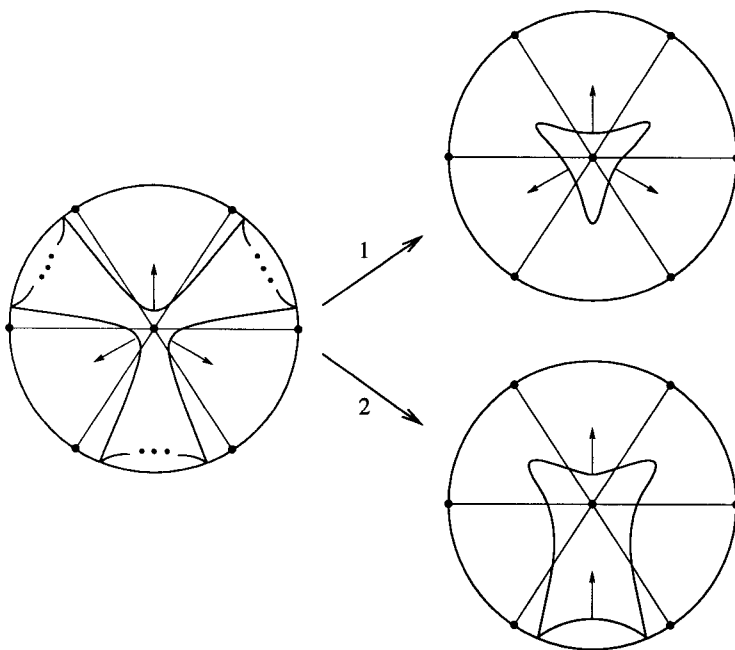


Figure 52: Impossible shrinking of an oriented oval.

10.2 Where $\alpha(*)$ is not

Let Δ be an odd-cycle-free zone decomposition of $\mathbf{T}(d)$, and let $K = K(\Delta)$. A separating edge of a zone of Δ or two edges of zones of Δ meeting in an inner-node, split $\mathbf{T}(d)$ into two connected components V_1 and V_2 . Assume that V_1 is the one with the interior that contains the largest number of points among A_0, A_1 , and A_2 . So the interior of V_2 doesn't intersect at least one of the segments among l_0, l_1, l_2 . We assume that it is l_0 that $\text{int } V_2$ doesn't

intersect. Let W_i be the lift $\mu^{-1}(V_i)$, for $i = 1, 2$. So the interior of W_2 is homeomorphic to an open disk or to the union of two open disks.

10.2.0.2 Lemma

The oval $\alpha(*)$ of K doesn't lie entirely in W_2 .

proof. Let U'_1 be the closure of the complementary of V_2 in $\mathbf{T}(2d+1)$, and let Δ' be the zone decomposition of $\mathbf{T}(2d+1)$ obtained in the following way:

- Take as zone of Δ' all the the zones of Δ in V_2 .
- If $V_1 \cap V_2$ contains an inner-node S , then, for each edge SQ of Δ with Q of even parity on the segment $l_0(d)$, place an edge SQ' (each time a different one) of zone of Δ' with Q' of even parity on $l_1(2d+1)$ or on $l_2(2d+1)$.

All the points of parity $(1, 1)$ on $\partial\mathbf{T}$ lie on l_0 . Since Δ is odd-cycle-free, the number of edges SQ of zones of Δ , with Q of parity $(1, 1)$, is even. Therefore the number of edges SQ of Δ' , with Q of a given parity, is even. So Δ' is odd-cycle-free. Let K' be the maximal T-curve $K(\Delta')$, and let α and α' be the point-oval correspondence of K and K' respectively.

Since the piece of K' and the piece of K in W_2 are equal, we get that $\alpha(P) = \alpha'(P)$ if $P \in U_2$. Since K' has odd degree, the oval $\alpha'(*)$ is one-sided, and therefore doesn't lie entirely in the interior of W_2 . So all the ovals lying entirely in W_2 are of the kind $\alpha'(P)$. Hence $\alpha(*)$ doesn't lie entirely in W_2 . \square

10.3 The sign of an oval

Let K be a T-curve. Recall that the *sign of an oval of K* lying inside a quadrant of $\mathbb{R}P^2$ is the sign of the points lying neighborly inside the oval. If K has even degree, then this definition is naturally extended to any oval. Indeed if an oval of K intersects two quadrants, then the points lying neighborly inside the oval have same signs in both quadrants (this is not automatically the case if the degree is odd).

10.4 Removing one even edge

Let Δ be an odd-cycle-free zone decomposition of $\mathbf{T}(2k)$ having a separating edge e which is an even segment, and let $\theta(e)$ be the total parity of e . Let

Δ' be the zone decomposition obtained from Δ by removing the edge e . It is obvious that Δ' is again an odd-cycle-free zone decomposition. So let K and K' be the maximal lattice T-curves $K(\Delta)$ and $K(\Delta')$ (so K and K' have even degree). Let δ and δ' be the zone-wise Harnack distribution of signs defining K and K' , and let α and α' be the point-oval correspondences for K and for K' .

10.4.0.3 Proposition

The sign distribution δ' can be chosen so that, for all $P \in \text{int } \mathbf{T} \cap \mathbb{Z}^2$, the sign of $\alpha'(P)$ is equal to the sign of $\alpha(P)$, and the sign of $\alpha()$ is equal to the sign of $\alpha'(*)$.*

proof. Let δ' be equal to δ on Z_1^e . So δ' is equal to $(\theta(e) \cdot \delta) = ((0, a, b) \cdot \delta) = \delta \circ \sigma_{a,b}$ on Z_2^e (see fig. 54). Since for every $P \in Z_1^e$, a copy $(\sigma_{c,d} \cdot P)$ is surrounded by an oval $\alpha(P)$, the copy $(\sigma_{a+c,b+d} \cdot P)$ is surrounded by the oval $\alpha'(P)$ and is of sign $\delta'(P) = \delta(P)$.

Let W_i be the lift $\mu^{-1}(Z_i^e)$ for $i = 1, 2$. From lemma 5.0.1.2 we get that there is exactly one connected component O of K (resp. O' of K') which intersects the lift $\mu^{-1}(e) = W_1 \cap W_2$. Since the piece of O and the piece of O' in W_1 are equal, and since the interior of W_2 is homeomorphic to an open disk, the points of $W_1 \cap W_2$ neighborly interior to O remain neighborly interior to O' . So the sign of O is equal to the sign of O' .

- If $\alpha(*)$ is equal to O , then we get as a consequence of lemma 10.2.0.2 that $\alpha'(*)$ is equal to O' . In this case we just proved that the sign of $\alpha(*)$ is equal to the sign of $\alpha'(*)$.
- If $\alpha(*)$ is not equal to O , we get from lemma 10.2.0.2 that $\alpha(*) \subset W_1$. So $\alpha'(*) \subset W_1$ and the sign of $\alpha(*)$ is equal to the sign of $\alpha'(*)$.

□

10.5 Removing two even edges

Let Δ be an odd-cycle-free zone decomposition of $\mathbf{T}(2k)$ having a cycle of zones, around an inner-node S , with two edges of the cycle SP and SP' which are both even and both of same total parity θ . Let Δ' be the zone decomposition obtained from Δ by removing SP and SP' . It is obvious that Δ' is again an odd-cycle-free zone decomposition. So let K and K' be the

maximal lattice T-curves $K(\Delta)$ and $K(\Delta')$. Let δ and δ' be the zone-wise Harnack distributions of signs defining K and K' , and let α and α' be the point-oval correspondence for K and K' .

If the two sectors $V_1 = \widehat{PSP}$ and $V_2 = \widehat{P'SP}$ don't contain the same amount of A_i 's, then we assume without loss of generality that V_1 is the one containing the most of the A_i 's.

Thanks to lemma 5.3.2.4 we assume without loss of generality that S itself is surrounded by the oval $\alpha(S)$. For $i = 1, 2$, let W_i be the lift $\mu^{-1}(V_i)$ and let T_i (resp. T'_i), $i = 1, 2$, be the subsets of W_i containing S and bounded by $\alpha(S)$ (by $\alpha'(S)$).

Since S lies inside $\alpha(S)$, the union $T_1 \cup T_2$ is homeomorphic to a disk, and T_1 and T_2 are homeomorphic to two disk sectors (see the shrinking of $\alpha(S)$ on a pie-diagram fig. 54).

10.5.0.4 Proposition

The sign distribution δ' can be chosen so that for all $P \in (\text{int } \mathbf{T} \cap \mathbb{Z}^2)$, the sign of $\alpha'(P)$ is equal to the sign of $\alpha(P)$, and the sign of $\alpha'()$ is equal to the sign of $\alpha(*)$.*

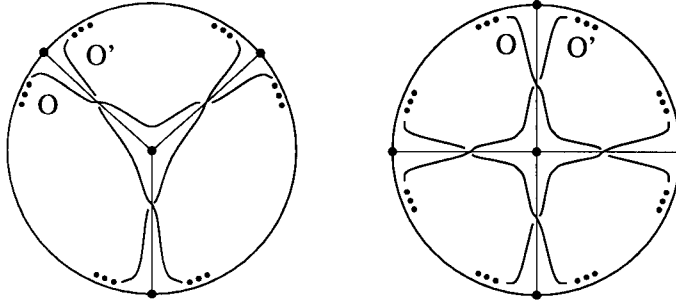
proof. Let δ' be equal to δ on V_1 . So δ' is equal to $(\theta \cdot \delta)$ on V_2 .

The assertion restricted to the points $P \neq S$ is obvious (same as in 10.4.0.3). Let's see for $P = S$. Since we assumed that S lies neighborly inside $\alpha(S)$, we know that S lies either neighborly inside or neighborly outside $\alpha'(S)$, so it suffices to show that S lies inside $\alpha'(S)$. Observe that the subset T'_1 is equal to T_1 and that W_2 is an open disk or the union of two open disks.

Because the number of edges of the cycle of zones around S in Δ (and in Δ') is even, there are exactly two connected components of K (and of K') that cut the edges of the cycle of zones (see section 9.1 and the remark right after lemma 9.1.0.12), (see also fig. 53). Therefore $\alpha(S)$, (and $\alpha'(S)$), cuts the boundary of W_2 exactly twice.

Hence T'_2 must be homeomorphic to a disk sector, like T_2 (see fig. 54). So the side of $\alpha'(S)$ containing T_1 (and containing S) is homeomorphic to a disk. Therefore it is the inside of $\alpha'(S)$. Moreover, as $\delta(S) = \delta'(S)$, the two ovals $\alpha(S)$ and $\alpha'(S)$ have the same sign.

Similar arguments than in prop. 10.4.0.3 show that the sign of $\alpha(*)$ is equal to the sign of $\alpha'(*)$. \square



If the number of edges is odd then $O = O'$, otherwise $O \neq O'$

Figure 53: One or two connected component according to the parity of the number of edges.

10.6 Removing all the even edges

Let Δ be an odd-cycle-free zone decomposition of $\mathbf{T}(2k)$, let Δ' be the zone decomposition obtained from Δ by removing all the even edges. Then it is obvious that Δ' is again an odd-cycle-free zone decomposition of \mathbf{T} . So let K and K' be the maximal lattice T-curves $K(\Delta)$ and $K(\Delta')$.

10.6.0.5 Theorem

The number of even (odd) ovals in K' is the same than in K .

proof. Thanks to lemma 5.3.2.4 we assume without loss of generality that the even (odd) ovals of K are the ovals of positive (negative) signs. Then applying prop. 10.4.0.3 and 10.5.0.4 enough times, one gets rid of all even edges without changing the signs of the ovals. Hence K and K' have the same number of positive (negative) ovals.

Let's take the same notations than in prop. 10.4.0.3 and in prop. 10.5.0.4. So the interior of W_2 is homeomorphic to an open disk or to the union of two open disks. Since $\mathbb{R}P^2$ is decomposed into W_1 and W_2 , the subset W_2 is non-orientable. In each application of prop. 10.4.0.3 and prop. 10.5.0.4 the sign distribution in V_2 doesn't change. Therefore the sign distribution defining K in the non-orientable subset of $\mathbb{R}P^2 \setminus K$ has same type than the sign distribution defining K' in the non-orientable subset of $\mathbb{R}P^2 \setminus K'$. Since the positive (negative) ovals of K are the even (odd) ovals, the positive (negative) ovals of K' are also the even (odd) ovals. Hence K and K' have the same number of even (odd) ovals. \square

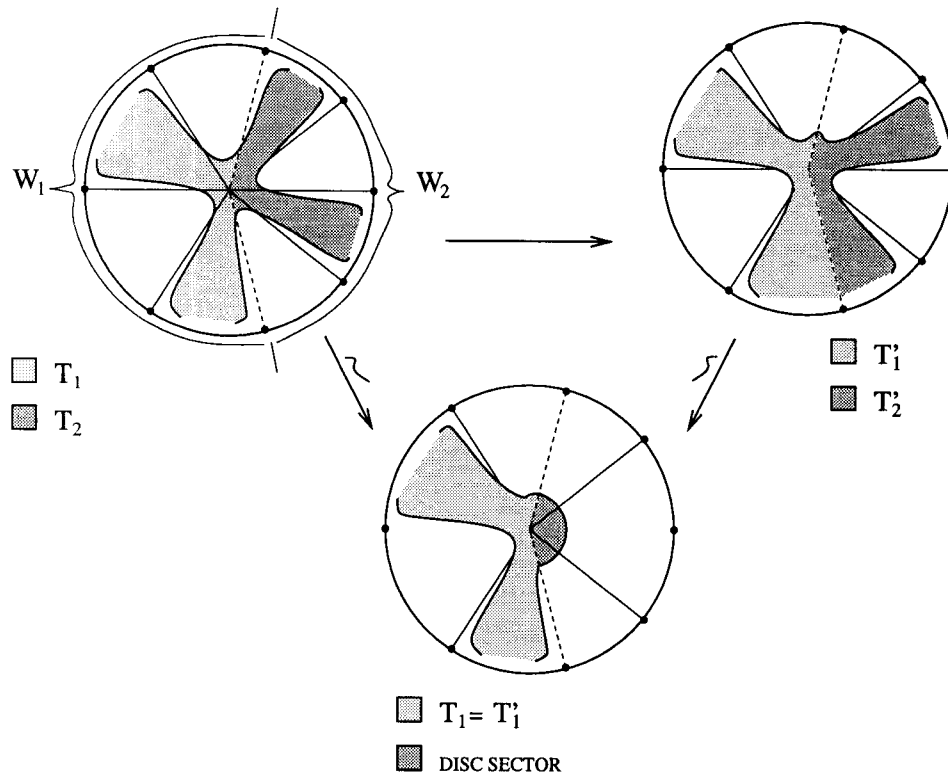


Figure 54: Removing two even edges.

11 Properties of even-node-free zone decompositions

Thanks to theorem 10.6.0.5 to study Ragsdale conjecture for maximal lattice T-curves, it is enough to study the conjecture for lattice T-curves $K(\Delta)$ where Δ is an odd-cycle-free zone decomposition of $\mathbf{T}(2k)$ with no even inner-nodes and no even boundary-nodes. We will consider mainly such decompositions from now on.

11.0.0.6 Definition (even-node-free zone decomposition)

We will call an *even-node-free zone decomposition* of $\mathbf{T}(2k)$ a zone decomposition of \mathbf{T} with no nodes of even parity.

We will study now more precisely the point-oval correspondence in even-node-free odd-cycle-free zone decompositions of $\mathbf{T}(2k)$ to find in prop. 12.3.0.11

and its corollary a relation between the parity of the points and the property of the ovals of being even or odd. Thus we will be able to count the number of even and odd ovals by counting integral points.

11.1 Basic observations

Let Δ be an even-node-free odd-cycle-free zone decomposition of $\mathbf{T}(2k)$.

11.1.0.7 Observation:

Since the three segments l_i (the edges of \mathbf{T}) are of even length $2k$, all the odd points of $\partial\mathbf{T}$ of a given parity lie on the same l_i . More precisely, points of parity $(1,1)$ lie on l_1 , points $(0,1)$ lie on l_2 and points $(1,0)$ lie on l_3 . In particular all boundary-nodes of Δ of a given parity lie on the same l_i .

11.1.0.8 Observation:

Since the nodes of Δ can be only of three parities, it is clear from the previous observation (11.1.0.7) that an inner-node S cannot be connected by some edges of zones of Δ to the three segments l_i .

11.1.0.9 Observation:

Since Δ is an odd-cycle-free zone decomposition it is clear from observation 11.1.0.7 that the number of boundary-nodes lying on a given l_i and connected to a given inner-node is even.

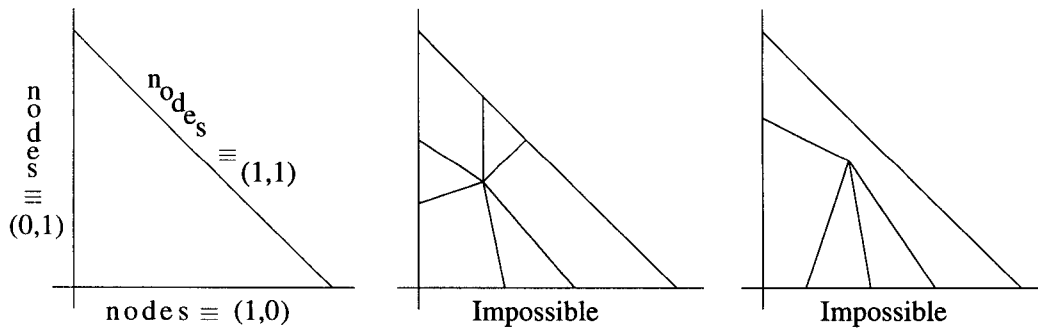


Figure 55: Three observations specific to even-node-free odd-cycle-free zone decompositions of $\mathbf{T}(2k)$.

11.2 Two important zone-definitions

11.2.0.10 Lemma

Let Δ be an even-node-free odd-cycle-free zone decomposition of $\mathbf{T}(2k)$. Then there exist a unique zone $Z \in \Delta$ such that the lift $\mu^{-1}(Z)$ contains a nontrivial homology cycle of $\mathbb{R}P^2$.

proof. It is clear that “The lift $\mu^{-1}(Z)$ contains a nontrivial homology cycle” can be restated into “The zone Z intersects the three segments $l_1, l_2,$ and l_3 ”. Let V_i be the union of zones of Δ not intersecting l_i , and let $V = V_0 \cup V_1 \cup V_2$. If V is not equal to \mathbf{T} then $\mathbf{T} \setminus V$ is a union of zones intersecting the three l_i 's. Since each A_i (which is equal to $l_j \cap l_k$) cannot belong to the boundary of a zone (because it is even), there cannot be more than one zone intersecting the three segments l_i . If $V = \mathbf{T}$, then $V_i \cap V_j$ is the edge SP_k of a zone of Δ , with $P_k \in l_k$. But then S connects the three l_i 's which contradicts observation 11.1.0.8. \square

11.2.0.11 Definition (the special zone)

Let Δ be an even-node-free odd-cycle-free zone decomposition of $\mathbf{T}(2k)$. The unique zone which, according to the preceding lemma (11.2.0.10), intersects the three segments l_1, l_2 and l_3 will be called the *special zone* of Δ .

11.2.0.12 Definition (separating union of zones)

Let Δ' be the decomposition obtained from Δ by removing all the edges of zones which are not separating edges. The zones of Δ' (view as unions of zones of Δ), will be called a *separating union of zones* of Δ . We will write usually Y for the separating union of zones.

11.3 Characterization of $\alpha(*)$

Let Δ be an even-node-free odd-cycle-free zone decomposition of $\mathbf{T}(2k)$ having an inner-node S , and let P_1, \dots, P_m be all the boundary-nodes of zones of Δ , which are connected to S and which lie on a given edge l_j . We assume that the P_i 's are indexed counterclockwise around S , and let Z_0, \dots, Z_m be the zones of Δ such that the segments SP_i and SP_{i+1} are edges of the zone Z_i . So Z_0 shares edge SP_1 with Z_1 and Z_m shares edge SP_m with Z_{m-1} (if S is not connected to any other line than l_j , then $Z_0 = Z_m$), (see fig 57).

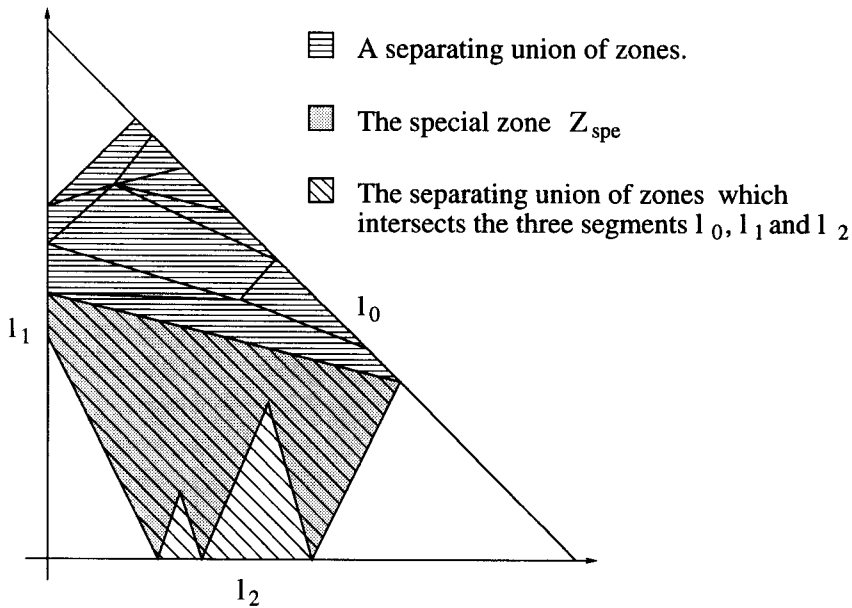


Figure 56: An example of a special zone and separating zones.

11.3.0.13 Lemma

- In the pie diagram of K , the arc of K which surrounds P_1 in Z_0 belong to the same connected component of K than the arc which surrounds P_m in Z_m .
- These two arcs surround P_1 and P_m in the same quadrant.

proof. Since neither S nor P_i is even, we get from observation 11.1.0.7 that the total parity of the segment SP_i will be equal to $(1, a, b)$ for some $a, b \in \{0, 1\}$ for all $i = 1, \dots, m$. So the type of the Harnack distributions of signs in all the Z_i must alternate. It will be equal to some θ in Z_0, Z_2, \dots, Z_m (we know that m is even from observation 11.1.0.9) and it will be equal to $((1, a, b) + \theta)$ in Z_1, Z_3, \dots, Z_{m-1} . So let's follow the arc, on the pie diagram,

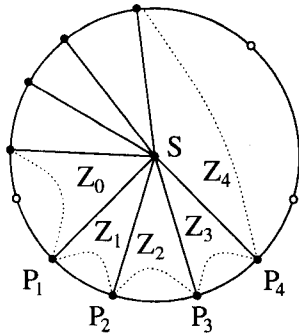


Figure 57: The notations for subsection 11.3 (view on a pie diagram).

surrounding P_1 in Z_0 (see fig. 58): For some $c, d \in \{0, 1\}$ this arc surrounds S in $(\sigma_{c,d} \cdot Z_j)$, for $j = 1, 3, \dots, m - 1$, and surrounds the boundary-nodes in $(\sigma_{c,d} \cdot Z_k)$, for $k = 0, 2, \dots, m$. \square

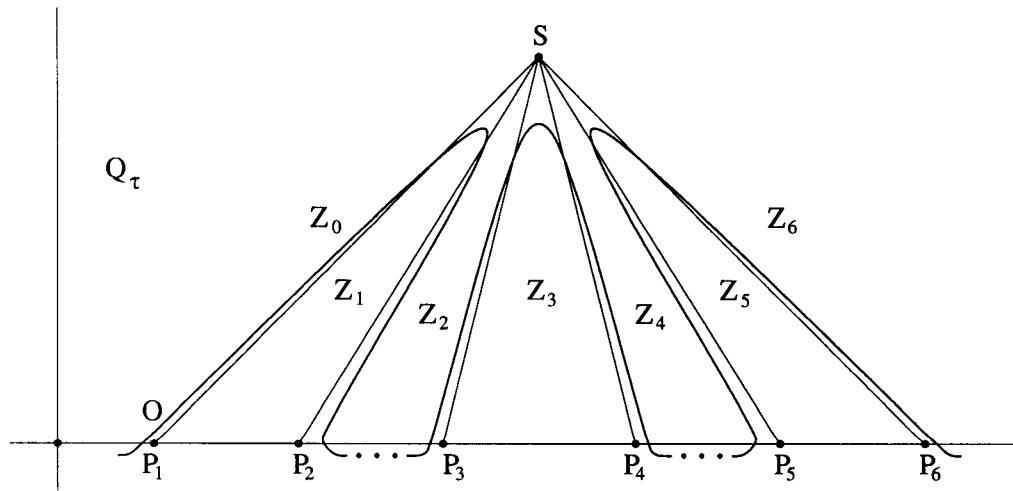


Figure 58: The arc surrounding all the P_i 's.

11.3.0.14 Lemma

The oval surrounding P_1 in Z_0 is not $\alpha(S)$.

proof. It is clear from observation 11.1.0.8 that either Z_0^S or Z_m^S contains at least two A_i 's, so all the Z_{2i+1} belong to $U'(S)$. But the oval surrounding P_1 in Z_0 is precisely the oval surrounding S in all the Z_{2i+1} , so from definition 9.1.0.14, this oval is not the oval $\alpha(S)$. \square

11.3.0.15 Lemma

The oval O surrounding P_1 in Z_0 is none of the $\alpha(R)$ for the inner-nodes R in the sector $\widehat{P_1 S P_m}$.

proof.

1. Since O surrounds S in all the Z_{2i+1} , it is clear that O is none of the $\alpha(R)$ for any R in any Z_{2i+1} .
2. Let Z be any Z_{2i} and let's write P and P' for P_{2i} and P_{2i+1} . If $Z^S = Z$, then Z contains no other inner-node than S . If $Z^S \neq Z$ then $Z^S \setminus Z$ is a union of sectors $Q_i S_i Q'_i$ (ordered counterclockwise around S , see fig. 59). Since O surrounds P in Z , lemma 8.3.0.7 and lemma 11.3.0.13 show that O surrounds all the Q_i , surrounds all the Q'_i and surrounds P' in Z . Then lemma 11.3.0.14 shows that O is none of the $\alpha(S_i)$. This is true for all the $Z = Z_{2j}$, so the lemma follows by induction on the inclusion-depth of the sectors.

□

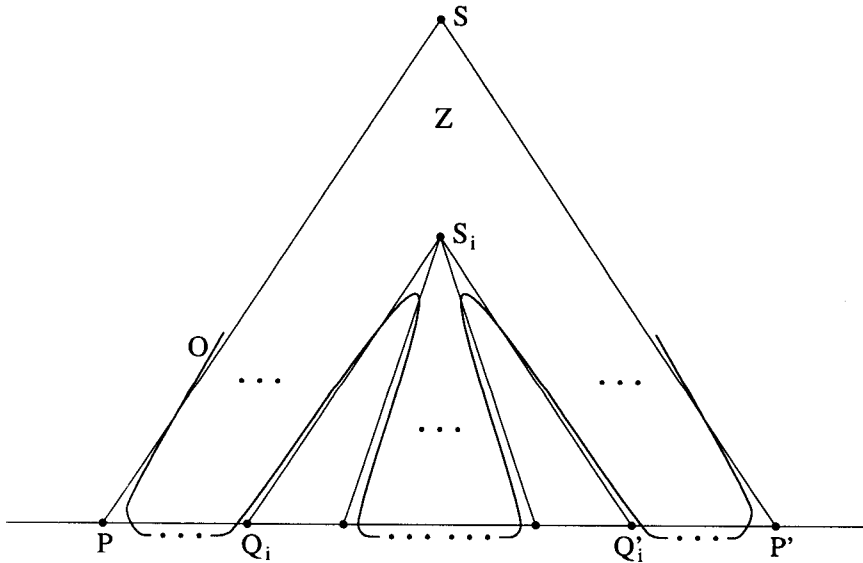


Figure 59: The arc surrounding all the P_i 's and Q_i 's.

11.3.0.16 Lemma

The two arcs of K passing through a separating edge belong to one connected component of K .

proof. Let e be a separating edge. Since e is primitive, the lift $\mu^{-1}(e)$ is cut exactly twice by K . Since the lift $\mu^{-1}(\mathbf{T} \setminus e)$ is disconnected, and since the connected components of K are closed, the two arcs of K intersecting the lift $\mu^{-1}(e)$ must belong to the same connected component of K . \square

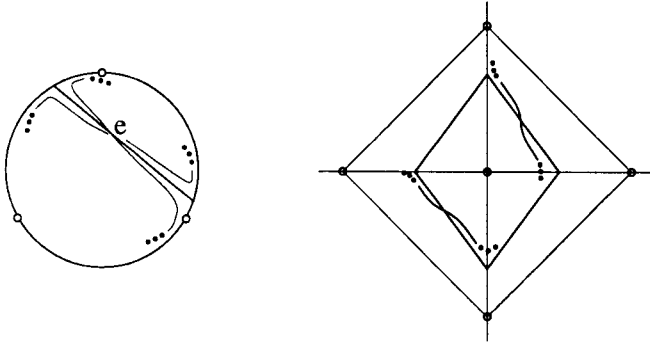


Figure 60: The two arcs cutting e are connected.

11.3.0.17 Lemma

Let Y be a separating union of zones of Δ , let $V = V(Y)$ be the union in Y of the zones of Δ intersecting more than one segment l_i , and let $K = K(\Delta)$. Then the oval $\alpha(*)$ of K surrounds in V all the boundary-nodes of zones of Δ in V .

proof. Let S_1, \dots, S_m (we may write $S_i = S_i(Y)$ if more precision is required) be all the inner-nodes in V (ordered counterclockwise). If $m = 0$, then V itself is a zone of Δ , so the only boundary-nodes in V are the endpoints of separating edges and lemmas 8.3.0.7 and 11.3.0.16 show that it is one connected component of K which surrounds these boundary-nodes.

If $m \geq 1$, then the complement $Y \setminus V$ is a union of sectors $\widehat{PSP'}$ with P and P' lying both on one edge l_j . Lemma 11.3.0.13 (or lemma 8.3.0.7 if P and P' are consecutive) shows that the arc surrounding P in V surrounds as well P' in V .

So it is one arc which surrounds all the P and the P' between two boundary-nodes of separating edges, but lemma 11.3.0.16 shows that the two arcs surrounding the boundary-nodes of a given separating edge belong to one oval, so the arcs surrounding all the boundary-nodes of the zones of Δ in V belong to the same oval O .

Moreover lemma 11.3.0.15 shows that O is none of the $\alpha(R)$ for any $R \in Y$. Since this is true for any Y and since O is the same oval for all the Y (again because of lemma 11.3.0.16), we get that $O = \alpha(*)$. \square

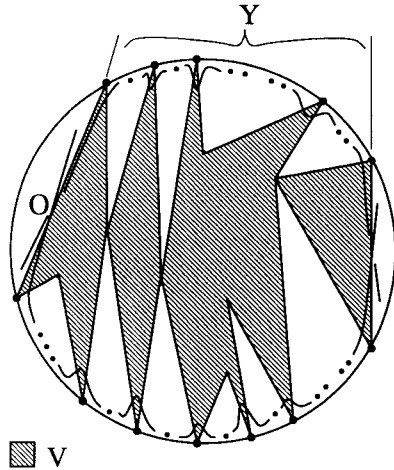


Figure 61: $\alpha(*)$ surrounds all the boundary-nodes of V .

11.3.0.18 Corollary

The separating edges of zones of Δ are all cut by (and only by) $\alpha()$.*

proof. This is an immediate consequence of prop. 11.3.0.17. Indeed the endpoints of a separating edge are boundary-nodes of some zones in a union V of zones of Δ (described in prop. 11.3.0.17). \square

11.3.0.19 Lemma

The oval $\alpha()$ of $K(\Delta)$ is an even oval.*

proof. Let Z be the special zone of Δ . Since Z intersects segments l_1, l_2 and l_3 , it lies in some union of zones $V(Y)$ (with the notation of prop. 11.3.0.17), so $\alpha(*)$ surrounds the boundary-nodes of Z . Let $P_0 \in l_0, P_1 \in l_1$, and $P_2 \in l_2$ be three boundary-nodes of Z . It is easy to find on a pie diagram a loop in Z

- which cuts $\partial\mathbf{T}$ only in P_0, P_1 , and P_2 ,
- which intersects $\alpha(*)$ near P_0 ,

- and which avoids all the other ovals of K intersecting Z .

This loop (see fig. 62) is the image on the pie diagram of four symmetric non trivial homology cycle on \mathbf{T}^* . Let $(\sigma_{a,b} \cdot P_0)$ be the copy of P_0 surrounded by $\alpha(*)$, and choose one among the two homology cycle passing through $(\sigma_{a,b} \cdot P_0)$. This cycle cuts $\alpha(*)$ at least once and at most three times. Since K has even degree all its components are ovals, so the loop must cut $\alpha(*)$ exactly twice. Since it doesn't cut any other oval, it means that $\alpha(*)$ is an outermost connected component. Hence $\alpha(*)$ is an even oval. \square

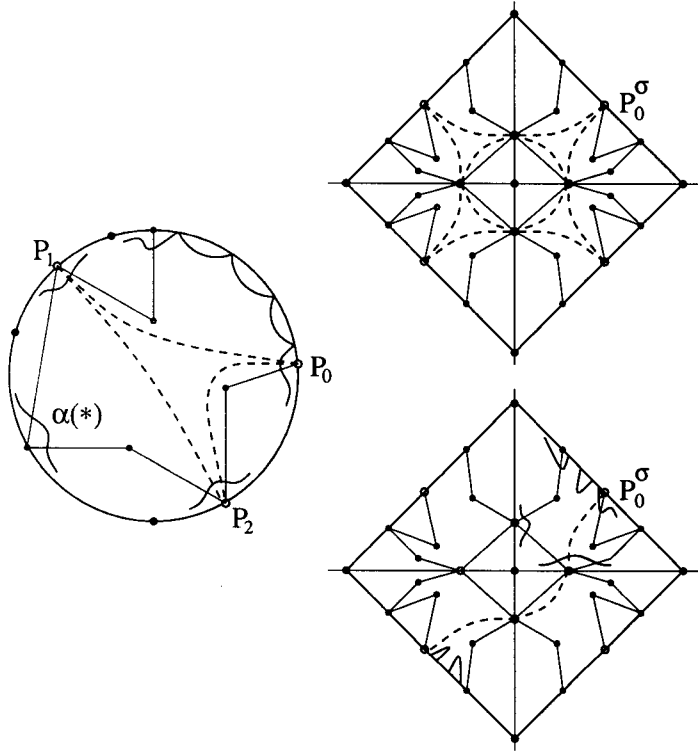


Figure 62: A nontrivial homology cycle cutting only $\alpha(*)$.

11.3.0.20 Lemma

Let K be a maximal lattice T -curve. If the Harnack distribution in the special zone is of type $(1, 0, 0)$, then the sign of the even ovals is $+1$.

proof. Because of lemma 11.3.0.19, it suffices to show that the sign of $\alpha(*)$ is $+1$. Let Z be the special zone, let $K = K(\mathbf{T}, \mathcal{T}, \delta)$ let K' be the Harnack

curve $K(\mathbf{T}, \mathcal{T}, \delta')$ where δ' is the Harnack distribution of signs on $\mathbf{T} \cap \mathbb{Z}^2$ of type $(1, 0, 0)$. So $\alpha'(*)$ is the nonempty oval of K' and is of sign $+1$. Therefore if $K = K'$ (i.e. if $Z = \mathbf{T}$), then the assertion of the lemma is clear. If $K \neq K'$, we compare the ovals $\alpha(*)$ and $\alpha'(*)$.

The lift of the complement $(\mathbf{T} \setminus Z)$ is a union of disks. Since δ_Z (the restriction to Z of δ) is a Harnack distribution, we know how $\alpha(*)$ intersects the boundary of the lift $\mu^{-1}(Z)$, which is also the boundary of the disks: The boundary of each disk is intersected by $\alpha(*)$ either twice either not at all. Since $\delta_Z = \delta'_Z$, the restrictions of K and K' to $\mu^{-1}(Z)$ are equal, and K' intersects the boundary of the disks at the same places than K does. Therefore the points of the boundary of $\mu^{-1}(Z)$ lying inside $\alpha(*)$ are also lying inside $\alpha'(*)$, so $\alpha(*)$ is also of sign $+1$. \square

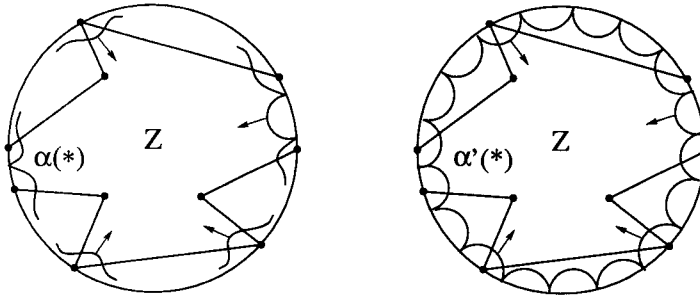


Figure 63: $\alpha(*)$ is, like $\alpha'(*)$, an even oval (the arrows represent the inside of the oval).

11.4 Counting points with signs

Let Δ be an even-node-free odd-cycle-free zone decomposition of \mathbf{T} , and let $K = K(\Delta)$. Assume that the distribution of signs is of type $(1, 0, 0)$ in the special zone.

11.4.1 The integral points of a zone

Notice that a zone in \mathbf{T} which is not the special zone has only one completed zone containing at most one A_i .

11.4.1.1 Definition (the top node)

The *top node* of a zone Z in \mathbf{T} is the inner-node S of Z such that Z^S contains at most one A_i .

Notice that all the completed zones of the special zone contain at least two A_i 's, so the special zone has no top vertex.

11.4.1.2 Definition ($|Z|$)

The set of integral points of a zone Z is the union of the integral points of $\text{int } Z$ and of the set of all its inner-nodes except its top one. It will be denoted $|Z|$.

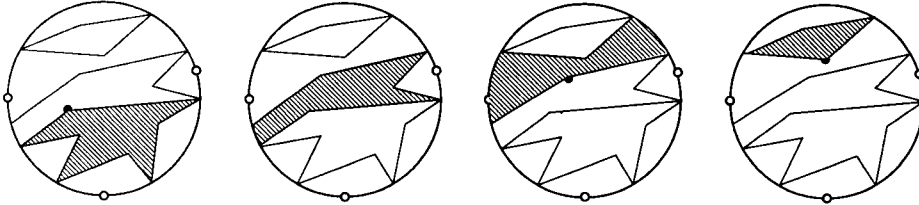


Figure 64: Examples of zones with their top node (black point).

11.4.1.3 Lemma

Let Δ be an even-node-free odd-cycle-free zone decomposition of \mathbf{T} . The family of subsets $|Z|$ for all $Z \in \Delta$ is a partition of $(\text{int } \mathbf{T}) \cap \mathbb{Z}^2$.

proof. Each point which is not an inner-node belongs to one and only one set $(\text{int } Z)$, hence to one and only one of the sets $|Z|$. If S is the inner-node of some zone of Δ , then from observation 11.1.0.8 we get that there is a zone Z of Δ with inner-node S such that Z^S contains at least two A_i 's. Therefore S belongs to this $|Z|$. Since there is only three A_i 's, there is only one such zone. □

11.4.1.4 Lemma

Let Δ be an even-node-free odd-cycle-free zone decomposition of \mathbf{T} , let $K = K(\Delta)$, let Z be a zone of Δ , let (c, a, b) be the Harnack type of the distribution of signs in Z , and let P be an arbitrary point of $|Z|$. Then the sign of $\alpha(P)$ is

- equal to $(-1)^c$ if P is a point of even parity.
- equal to $(-1)^{c+1}$ if P is a point of odd parity.

proof. If P is not an inner-node, this assertion follows from the definition 9.1.0.11 of $\alpha(P)$, and from the definition 5.3.2.1 of Harnack type.

Now let $P = S$ be an inner-node of parity (e, f) . Since the distribution in Z is of type (c, a, b) , we deduce from lemma 5.3.2.3 that an arc of K surrounds $(\sigma_{f+a,e+b} \cdot S)$ in $(\sigma_{f+a,e+b} \cdot Z)$. Since $S \in |Z|$, the completed zone Z^S contains at least two A_i 's. So $\alpha(S)$ is the oval surrounding S in Z (in the pie diagram), (see def. 9.1.0.14 of $\alpha(S)$). Therefore the arc of K surrounding $(\sigma_{f+a,e+b} \cdot S)$ in $(\sigma_{f+a,e+b} \cdot Z)$ belongs to $\alpha(S)$.

The set $(\mathbf{T} \setminus Z^S)$ contains at most one A_i , so its lift is homeomorphic to one or two (open) disks. Let e and e' be the two edges of Z meeting at S . Since $\alpha(S)$ intersects the lifts $\mu^{-1}(e)$ and $\mu^{-1}(e')$ each only once, the part of $\alpha(S)$ in $\mu^{-1}(\mathbf{T} \setminus Z^S)$ shrinks into an arc surrounding $(\sigma_{f+a,e+b} \cdot S)$ in the closure of $(\sigma_{f+a,e+b} \cdot (\mathbf{T} \setminus Z^S))$ (see fig. 65). Hence $(\sigma_{f+a,e+b} \cdot S)$ is neighborly inside $\alpha(S)$.

Let δ be the sign distribution defining K . Since the symmetry $\sigma_{f+a,e+b}$ is the composition of the symmetries $\sigma_{f,e}$ and $\sigma_{a,b}$, we have:

$$\delta(\sigma_{f+a,e+b} \cdot S) = (-1)^{\langle (e,f), (f,e) \rangle} \delta(\sigma_{a,b} \cdot S) = \delta(\sigma_{a,b} \cdot S)$$

The last term is equal, per definition (see def. 5.3.2.1), to $(-1)^c$ if S is a point of even parity, and to $(-1)^{c+1}$ if S is a point of odd parity. This finishes to prove the lemma since $(\sigma_{f+a,e+b} \cdot S)$ lies neighborly inside $\alpha(S)$. \square

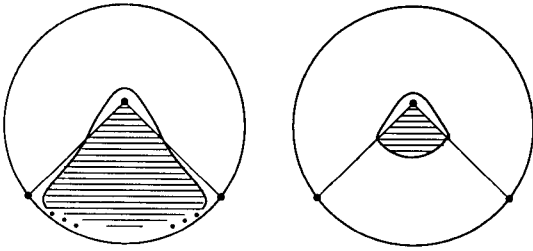


Figure 65: Shrinking of $\alpha(S)$ into a circle surrounding S .

11.4.2 Counting even and odd ovals via integral points

Recall from 11.3.0.18 that the only oval cutting the boundary of the lift of a separating union of zones Y in \mathbf{T} is $\alpha(*)$, so it is coherent to speak about the ovals in Y , keeping apart $\alpha(*)$.

Let Δ be an even-node-free odd-cycle-free zone decomposition of $\mathbf{T}(2k)$, let $K = K(\Delta)$, and let Y be a separating union of zones from Δ . Assume that the sign distribution δ defining K is of type $(1, 0, 0)$ in the special zone of Δ .

The set $|Y|$ is equal to $\text{int} Y \cap \mathbb{Z}^2$. It is partitioned into two sets V_0 and V_1 , where V_c is the union of the sets $|Z|$ such that $Z \subset Y$ and such that δ_Z is of type (c, a, b) for some $a, b \in \{0, 1\}$. Let $p_c|Y|$ be the number of points of even parity in V_c , let $n_c|Y|$ be the number of points of odd parity in V_c .

11.4.2.1 Proposition

The number of even ovals in Y is equal to $p_0|Y| + n_1|Y|$ and the number of odd ovals in Y is equal to $p_1|Y| + n_0|Y|$.

proof. Since the Harnack distribution in the special zone is of type $(1, 0, 0)$, the even ovals are of sign $+1$ and the odd ovals are of sign -1 (see 11.3.0.20). This proposition follows then directly from lemma. 11.4.1.4. \square

11.4.2.2 Corollary

The number of even ovals of K is equal to $\sum(p_0|Y| + n_1|Y|) + 1$ and the number of odd ovals of K is equal to $\sum(p_1|Y| + n_0|Y|)$, the two summations being on all the separating unions Y of zones of Δ .

proof. Indeed since $\alpha(*)$ is an even oval (see 11.3.0.19), we get the first assertion from prop. 11.4.2.1, and since the number of ovals is equal to the cardinal of $\mathbf{T} \cap \mathbb{Z}^2$ which is equal to $\sum(p_0|Y| + p_1|Y| + n_0|Y| + n_1|Y|) + 1$, the second assertion follows also from prop. 11.4.2.1. \square

12 Lattice geometry

Let Δ be an even-node-free odd-cycle-free zone decomposition of \mathbf{T} , let Y be a separating union of zones in Δ , and let $K = K(\Delta)$. Assume that the sign distribution defining K is of type $(1, 0, 0)$ in the special zone of Δ . We denote, like in 11.4.2, by $p_c|Y|$ (by $n_c|Y|$) the number of points of even (of odd) parity in the union $\bigcup |Z|$ for all the zone Z of Δ in Y in which the distribution of sign is of type (c, a, b) for some $a, b \in \{0, 1\}$. We will show in prop. 12.3.0.11 that

$$\begin{aligned} p_0|Y| - n_0|Y| &\leq 0 \\ p_1|Y| - n_1|Y| &\leq 0 \quad \left\{ \begin{array}{l} \text{if } Y \text{ intersects only two of the three} \\ \text{segments } l_0, l_1 \text{ and } l_2. \end{array} \right. \\ p_1|Y| - n_1|Y| &\leq 4 \quad \left\{ \begin{array}{l} \text{if } Y \text{ intersects the three} \\ \text{segments } l_0, l_1 \text{ and } l_2. \end{array} \right. \end{aligned}$$

The main theorem should then follow in section 12.4 from this result and from cor. 11.4.2.2.

12.1 Integral points in polygons

If A is a subset of \mathbb{R}^2 , we will write $p(A)$ and $n(A)$ for the number of even and non even points in A .

12.1.0.3 Proposition

Let Π be an integral convex polygon. If Π is degenerate, then $p(\Pi) - n(\Pi) \leq 1$. If Π is non-degenerate then $p(\Pi) - n(\Pi) \leq 0$.

proof.

- If Π is degenerate, then Π is
 - Either a segment. Then its two ends can have even parity, in which case $p(\Pi) - n(\Pi) = 1$, otherwise $p(\Pi) - n(\Pi) \leq 0$.
 - Either an integral point. Then it can have even parity, in which case $p(\Pi) - n(\Pi) = 1$, otherwise $p(\Pi) - n(\Pi) \leq 0$.
- If Π is non degenerate, let Π' be the convex hull of the even points of Π (so $p(\Pi') = p(\Pi)$ and $n(\Pi') \leq n(\Pi)$).

- If Π' is degenerate, then $p(\Pi') - n(\Pi') \leq 1$, but since Π is non degenerate $n(\Pi') < n(\Pi)$, so finally

$$p(\Pi) - n(\Pi) \leq 0$$

- If Π' is non degenerate, let \mathcal{T} be a triangulation of Π' such that its vertices are exactly the even points of Π' . Let v , e and f be respectively the number of vertices, edges and triangles of \mathcal{T} . Euler formula states that $v - e = 1 - f$. Since each end of an edge is even, each edge contains at least one non even point. It is clear then that $e \leq n(\Pi)$, $v = p(\Pi)$ and $f \geq 1$, so Euler formula shows that

$$p(\Pi) - n(\Pi) \leq v - e = 1 - f \leq 0$$

□

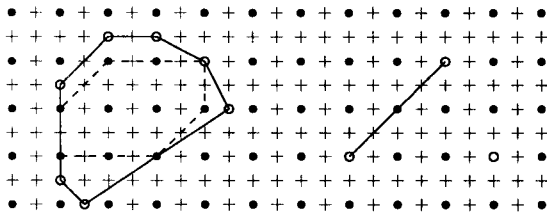


Figure 66: The convex hull of the set of even points of a non degenerate polygon and of two degenerate ones (a segment and a point).

12.1.0.4 Definition

A vertex of a polygon will be called an *obtuse vertex* if the angle inside the polygon, at this vertex, is greater than π .

12.1.0.5 Proposition

Let Π be a non-degenerate polygon (not necessarily integral) with k obtuse vertices. Then $p(int \Pi) - n(int \Pi) \leq k + 1$.

proof. Let's make an induction on k . If $k = 0$ then Π is convex and the convex hull of its interior points is also a convex polygon (may be degenerate), so from 12.1.0.3 we get that $p(int \Pi) - n(int \Pi) \leq 0 + 1$.

Let k be greater than 1 and assume that the proposition is true for any polygon with less than k obtuse vertices. Let P be an obtuse vertex, and

let's draw a line through P and through the angular sector outside Π at P . The segment carried by this line, which lies in Π and has endpoints P and Q on $\partial\Pi$, decomposes Π into two polygons Π_1 and Π_2 .

It is clear that we have enough degree of freedom to choose the line so that the segment PQ contains no integral point, except may be P itself, and so that Q is not a vertex of Π (see illustration on fig. 67). Therefore we get that $p(\text{int } \Pi_1) + p(\text{int } \Pi_2) = p(\text{int } \Pi)$ and $n(\text{int } \Pi_1) + n(\text{int } \Pi_2) = n(\text{int } \Pi)$.

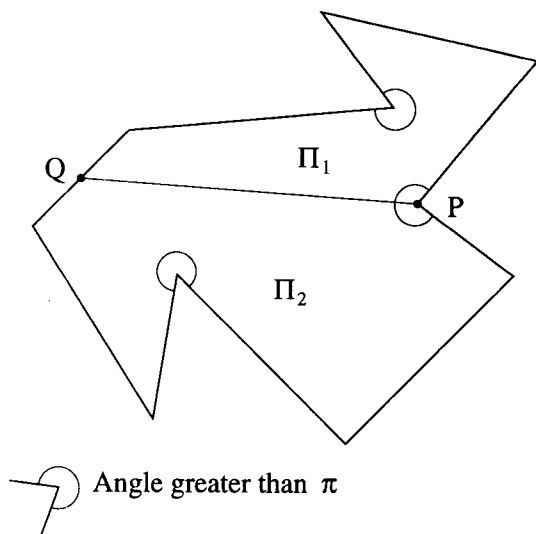


Figure 67: Partition of a non-convex polygon into two “more convex” polygons.

Let k_1 and k_2 be the numbers of obtuse vertices of Π_1 and Π_2 . The angles in Π_1 and Π_2 at P and at Q are clearly less than π . Therefore $k_1 + k_2 = k - 1$. Now with the hypothesis of induction $p(\text{int } \Pi_1) - n(\text{int } \Pi_1) \leq k_1 + 1$ and $p(\text{int } \Pi_2) - n(\text{int } \Pi_2) \leq k_2 + 1$. Summing these two inequalities we get

$$p(\text{int } \Pi) - n(\text{int } \Pi) \leq k_1 + k_2 + 2 = k - 1 + 2 = k + 1$$

□

12.2 Congruences in zones

If Z is a zone in \mathbf{T} , we write now $p|Z|$ and $n|Z|$ (instead of $p(|Z|)$ and $n(|Z|)$), for the number of points respectively of even and of odd parity in $|Z|$.

12.2.0.6 Lemma

Let Z be a zone in \mathbf{T} which is a triangle with vertices $P \in l_i$, $Q \in l_j$ and $A_k = l_i \cap l_j$ and such that PQ is a separating edge. Then $p|Z| - n|Z| \equiv 0 \pmod 4$.

This lemma is well known. It can be viewed for instance as a consequence of the congruence modulo 8 of Rokhlin for the maximal lattice T-curves with one nonempty oval (see [5] section 5). \square

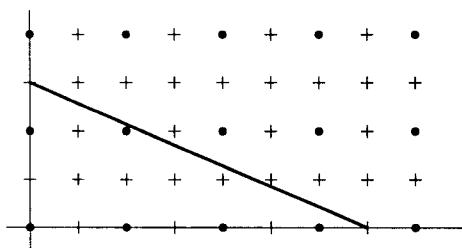


Figure 68: Simple nontrivial case illustrating $p - n \equiv 0 \pmod 4$.

12.2.0.7 Lemma

Let Z be a zone which intersects only one edge l of \mathbf{T} and which has only one inner-node S . Then $p|Z| - n|Z| \equiv 0 \pmod 4$.

proof. We assume without loss of generality that $l = l_2$. If Q is a point in \mathbf{T} , let $x_i(Q)$ be the distance from Q to l_i . Let P_0 and P_1 be the two boundary-nodes of Z , where P_i is closer to l_i . By a transformation $Q = (x, y) \mapsto Q' = (x, y + 2kx)$, $k \in \mathbb{Z}$, the zone Z is transformed into a zone Z' such that

1. If $S \equiv (0, 1)$, then $x_1(S') \leq x_1(P_1)$ (see fig. 69).
2. If $S \equiv (1, 1)$, then $x_0(S') \leq x_0(P_0)$

It is clear that $|Z|$ and $|Z'|$ have same cardinal and that the parity of a point is invariant under $Z \mapsto Z'$. We can translate Z' to a zone Z'' such that S'' belongs to l_2 (in case 1) or to l_0 (in case 2). Since in both cases S'' has same parity than S' the translation vector is even, so the parity of a point is invariant under $Z' \mapsto Z''$.

Now the zone Z'' can be written as the closure of the difference of two triangular zones like in lemma 12.2.0.6, $Z'' = \text{cl}(Z_1 \setminus Z_2)$ with the property

that $|Z''| = |Z_1| \setminus |Z_2|$ (see fig. 69). So

$$\begin{aligned} p|Z| - n|Z| &= (p|Z_1| - p|Z_2|) - (n|Z_1| - n|Z_2|) \\ &= (p|Z_1| - n|Z_1|) - (p|Z_2| - n|Z_2|) \end{aligned}$$

Therefore we get from lemma 12.2.0.6 that $p|Z| - n|Z| \equiv 0 \pmod 4$. □

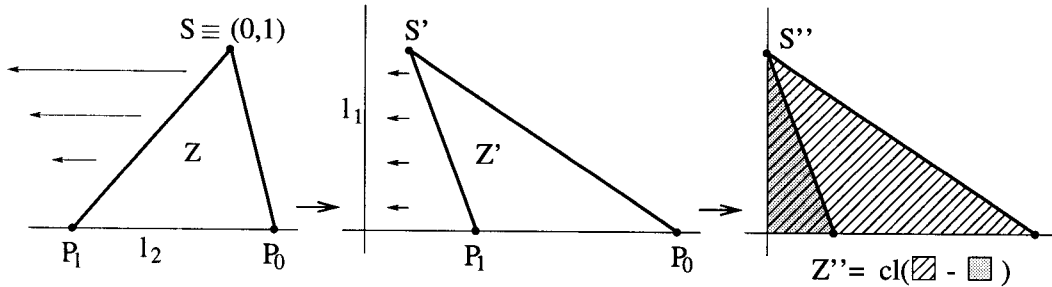


Figure 69: Squeezing and sliding a zone to see it as a difference of two simpler zones.

12.2.0.8 Lemma

Let Z be any zone intersecting only one edge l of \mathbf{T} , then $p|Z| - n|Z| \equiv 0 \pmod 4$.

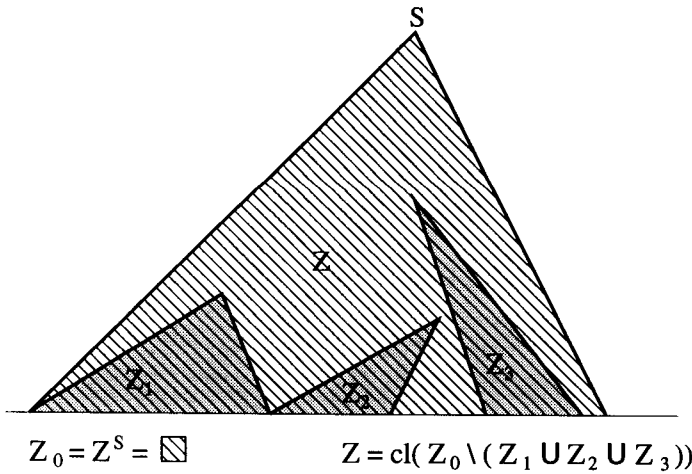


Figure 70: The zone Z seen as a difference of simpler zones.

proof. The zone Z can be written as a difference $Z = Z_0 \setminus (Z_1 \cup \dots \cup Z_m)$, where the Z_i are like in lemma 12.2.0.7, with the property $|Z| = |Z_0| \setminus (|Z_1| \cup \dots \cup |Z_m|)$ (see fig. 70). So

$$\begin{aligned} p|Z| - n|Z| &= (p|Z_0| - (p|Z_1| + \dots + p|Z_m|)) - \\ &\quad -(n|Z_0| - (n|Z_1| + \dots + n|Z_m|)) \\ &= (p|Z_0| - n|Z_0|) - \\ &\quad -((p|Z_1| - n|Z_1|) + \dots + (p|Z_m| - n|Z_m|)) \end{aligned}$$

The lemma follows since each $p|Z_i| - n|Z_i|$ is divisible by 4 (by lemma 12.2.0.7). □

12.2.0.9 Lemma

Let Z be any zone intersecting two edges l and l' of \mathbf{T} with an inner-node $S = (s_1, s_2)$. Then $p|Z| - n|Z| \equiv 0$ or $1 \pmod 4$.

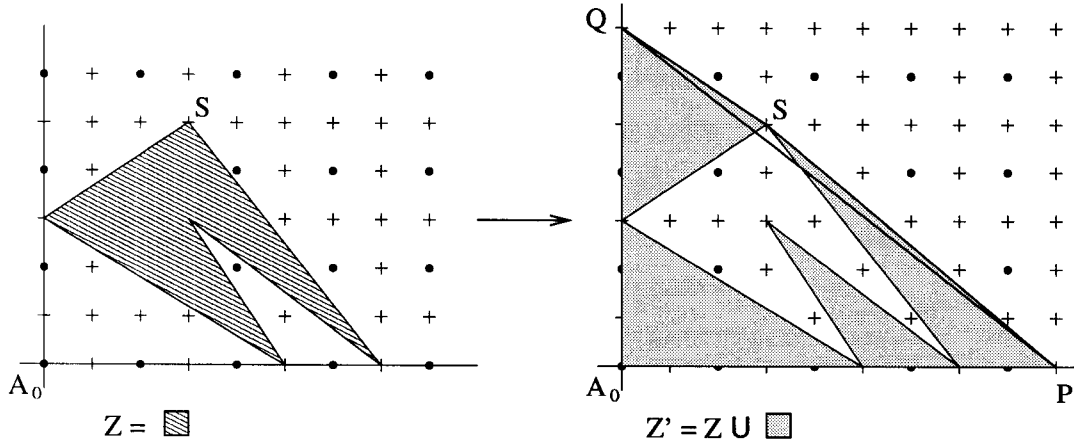


Figure 71: The zone Z seen as a difference and union of simpler zones. The zone Z'' is the triangular zone with vertices P, Q and A_0 .

proof. We assume without loss of generality that $l = l_1$ and $l' = l_2$. By adding or subtracting zones like in lemma 12.2.0.6 and 12.2.0.8 we transform Z into a zone Z' with vertices $S, P = (p, 0), Q = (0, q)$ and $A_0 = (0, 0)$ such that the area of the triangle SPQ has smallest absolute value (see fig. 71). So we get that $p|Z| - n|Z| \equiv p|Z'| - n|Z'| \pmod 4$. Moreover the zone Z'' with vertices P, Q , and A_0 is a triangular zone like in 12.2.0.6,

so $p|Z''| - n|Z''| \equiv 0 \pmod{4}$. Therefore we must look carefully what are the points of SPQ which belong or not to $|Z'|$ and to $|Z''|$. For instance S doesn't belong to $|Z'|$ but can belong to $|Z''|$.

Let $A/2$ be the area of the triangle SPQ (so A is an integer).

$$A = \begin{vmatrix} p - s_1 & -s_1 \\ -s_2 & q - s_2 \end{vmatrix} = (p - s_1)(q - s_2) - s_1s_2$$

Let $u = p - s_1$ and $v = q - s_2$. Since S connects l_1 , and l_2 , both its coordinates should be odd ($s_1 = 2s'_1 + 1$, and $s_2 = 2s'_2 + 1$). Since p and q are also odd, u and v are even ($u = 2u'$ and $v = 2v'$), so we get that

$$\begin{aligned} uv &= s_1s_2 + A \\ 4u'v' &= 4s'_1s'_2 + 2(s'_1 + s'_2) + 1 + A \end{aligned}$$

That the absolute value of $A/2$ is minimal implies that

1. $A = 1$ if $s'_1 + s'_2 \equiv 1 \pmod{2}$.
 2. $A = -1$ if $s'_1 + s'_2 \equiv 0 \pmod{2}$.
- In case 1 above (see fig. 72 (a)), let $2s'' + 1 = s'_1 + s'_2$. So we get that $u'v' = s'_1s'_2 + s'' + 1$, and we can take for instance

$$\begin{aligned} u' &= 1 \\ v' &= s'_1s'_2 + s'' + 1 \end{aligned}$$

In this case S doesn't belongs to $|Z'|$ but does belong to $|Z''|$. Therefore

$$\begin{aligned} p|Z''| &= p|Z'| \quad \text{and} \quad n|Z''| = n|Z'| + 1 \quad \text{so:} \\ p|Z| - n|Z| &\equiv p|Z''| - n|Z''| + 1 \equiv 1 \pmod{4} \end{aligned}$$

- In case 2 above (see fig. 72 (b)), let $2s'' = s'_1 + s'_2$. So we get that $u'v' = s'_1s'_2 + s''$ and we can take for instance

$$\begin{aligned} u' &= 1 \\ v' &= s'_1s'_2 + s'' \end{aligned}$$

In this case S belongs neither to $|Z'|$ nor to $|Z''|$. Therefore

$$\begin{aligned} p|Z''| &= p|Z'| \quad \text{and} \quad n|Z''| = n|Z'| \quad \text{so:} \\ p|Z| - n|Z| &\equiv p|Z''| - n|Z''| \equiv 0 \pmod{4} \end{aligned}$$

□

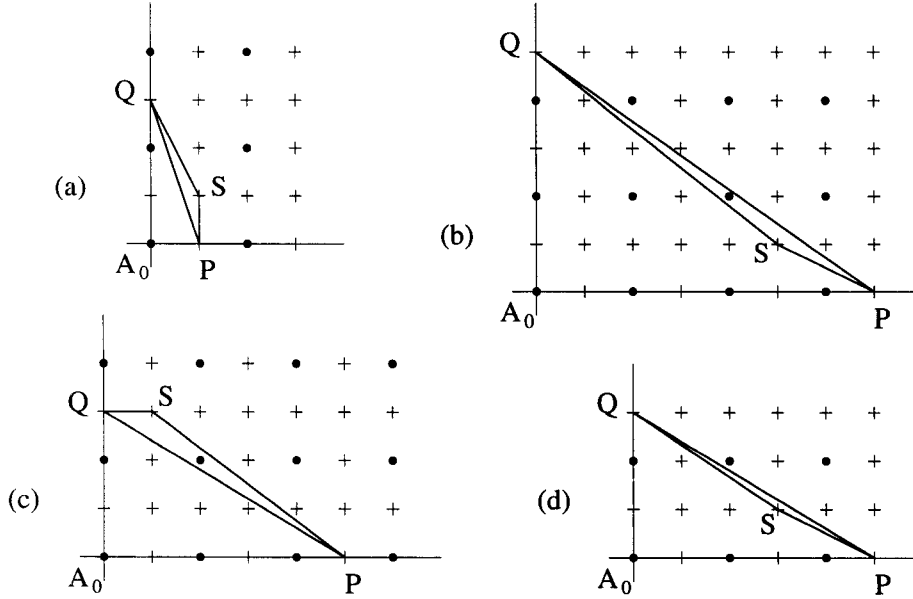


Figure 72: The two cases arising in the count of $p|Z| - n|Z| \pmod 4$.

12.3 Integral points in zones

Let Δ be an even-node-free odd-cycle-free zone decomposition of $\mathbf{T}(2k)$, let Y be a separating union of zones of Δ , and let $K = K(\Delta)$. We recall from the beginning of the section 12 that $p_c|Y|$ (resp. $n_c|Y|$) denote the number of points of even (of odd) parity in the union $\bigcup |Z|$ for all the zone Z of Δ in Y in which the distribution of sign is of type (c, a, b) for some $a, b \in \{0, 1\}$.

12.3.0.10 Lemma

Let Z be a zone intersecting only one edge l of \mathbf{T} . Then $p|Z| - n|Z| \leq 0$.

proof. Let S be the top node of Z , and let S_1, \dots, S_m be the other vertices of Z . Since the angle in Z at S is less than π , and the angles in Z at the S_i 's are all the angles greater than π in Z , we get from lemma 12.1.0.5 that $p(\text{int } Z) - n(\text{int } Z) \leq m + 1$.

Since $|Z| \cap \partial Z = \cup S_i$ and since the parity of each S_i is odd, we get that $p = p(\text{int } Z)$ and $n = n(\text{int } Z) + m$, so $p|Z| - n|Z| \leq 1$, but according to lemma 12.2.0.8, $p|Z| - n|Z| \equiv 0 \pmod 4$, so we have $p|Z| - n|Z| \leq 0$. \square

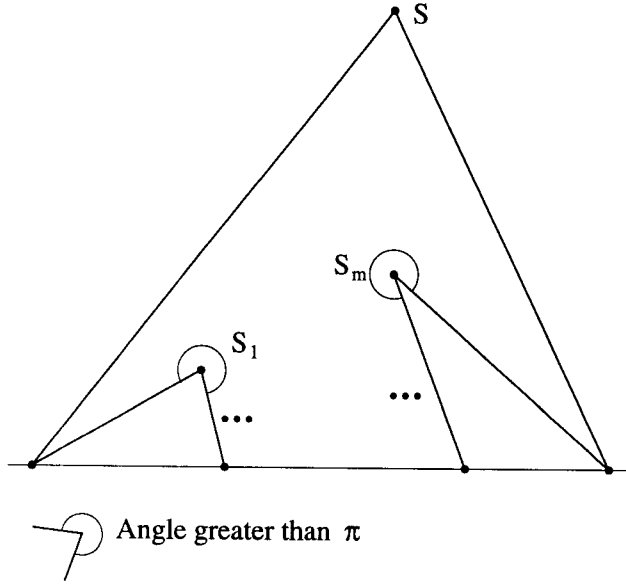


Figure 73: What vertices to consider to calculate a bound for $p|Z| - n|Z|$.

12.3.0.11 Proposition

Let Δ be an even-node-free odd-cycle-free zone decomposition of $\mathbf{T}(2k)$, and let $K = K(\Delta)$. Assume that the sign distribution defining K is of type $(1, 0, 0)$ in the special zone. Let Y be a separating union of zones of Δ .

1. Then $p_0|Y| - n_0|Y| \leq 0$.
2. If Y intersects only two edges of \mathbf{T} , then $p_1|Y| - n_1|Y| \leq 0$.
3. If Y intersects the three edges of \mathbf{T} , then $p_1|Y| - n_1|Y| \leq 4$.

proof. Let l and l' be two edges of \mathbf{T} intersected by Y , and let Z_1, \dots, Z_m be the zones of Δ in Y intersecting both l and l' (m may be equal to 1), indexed such that for $i = 1, \dots, m - 1$, the intersection $Z_i \cap Z_{i+1}$ is equal to the top-node S_i of Z_i and such that Z_m has no top-node. So Z_m is either the special zone if Y intersects the three edges of \mathbf{T} , either a zone with a separating edge e such that the completed zone Z_m^e contains all the other Z_i .

Let P_i (resp. N_i) be the number of points of even (of odd) parity in $\bigcup_{j=1}^i |Z_j|$. So $P_i = \sum_{j=1}^i p|Z_j|$ and $N_i = \sum_{j=1}^i n|Z_j|$.

1. Let R_1, \dots, R_k be all the inner-nodes of a zone Z_i , which are connected only to l or only to l' . The angles in Z_i at the R_j 's are greater than π ,

and the angles in Z_i at S_{i-1} (if $i \geq 2$) and at S_{i+1} (if $i \leq m-1$) may be also greater than π . So we get from lemma 12.1.0.5 that $p(\text{int } Z_i) - n(\text{int } Z_i) \leq k+3$. But since S_i (if $i \geq 1$) and all the R_j 's belong to $|Z_i|$, we get finally that

$$p|Z_i| - n|Z_i| \leq 2$$

2. According to lemma 12.2.0.9, $p|Z_i^{S_i}| - n|Z_i^{S_i}| \equiv 0$ or $1 \pmod{4}$ for any $0 \leq i \leq m-1$. Since $Z_i^{S_i} \setminus (\bigcup_{j=1}^i Z_j)$ is a union of zones like in lemma 12.2.0.8 and lemma 12.2.0.6, we get that

$$P_i - N_i \equiv 0 \text{ or } 1 \pmod{4}$$

3. If Y intersects only l and l' among the three edges of \mathbf{T} then we get from lemma 12.2.0.6 that $p|Z_m^e| - n|Z_m^e| \equiv 0 \pmod{4}$. Hence, for the same reason than in parag. 2, we get that

$$P_m - N_m \equiv 0 \pmod{4}$$

4. Assume that for some $1 \leq i \leq m-2$ one has $P_i - N_i \leq 1$, then from parag. 1 above we get that $p|Z_{i+1}| - n|Z_{i+1}| \leq 2$, so $P_{i+1} - N_{i+1} \leq 3$, but from parag. 2, $P_{i+1} - N_{i+1} \equiv 0$ or $1 \pmod{4}$, so finally $P_{i+1} - N_{i+1} \leq 1$. Since $P_1 = p|Z_1|$ and $N_1 = n|Z_1|$, the same arguments (from parag. 1 and 2) show that $P_1 - N_1 \leq 1$. Therefore we get by induction that

$$P_{m-1} - N_{m-1} \leq 1$$

5. If Y intersects only l and l' among the three edges of \mathbf{T} , we get again from parag. 4 and 1 that $P_m - N_m \leq 3$, but now parag. 3 shows that $P_m - N_m \equiv 0 \pmod{4}$, so finally

$$P_m - N_m \leq 0$$

6. From observation 11.1.0.7 and 11.1.0.9, it is clear that while we go from Z_i to Z_{i+1} around S_i , the Harnack types of the distributions in the zones with top node S_i alternate. Since they alternate an even number of time, the distributions in Z_i and in Z_{i+1} are of same type. Therefore the distribution is of same type (say (c, a, b)) in the union $\bigcup_{j=0}^m Z_j$. If Y intersects the three edges of \mathbf{T} , we have $c = 1$ because the distribution of signs is of type $(1, 0, 0)$ in the special zone Z_m .
7. Any zone Z of Δ in $Y \setminus (\bigcup_{j=0}^m Z_j)$ is like in lemma 12.3.0.10, so $p|Z| - n|Z| \leq 0$. Therefore we get from parag. 6 that

$$p_{c+1}|Y| - n_{c+1}|Y| \leq 0$$

8. If Y intersects only l and l' among the three edges of \mathbf{T} , we get from parag. 5, parag. 6 and parag.7, that

$$p_c|Y| - n_c|Y| \leq 0$$

This, together with parag. 7, proves part 1 and part 2 of the proposition.

Assume now that Y intersects the three edges l , l' and l'' of \mathbf{T} . Let $P = P_{m-1}$ and $N = N_{m-1}$. So we have from paragraph 4 that $P - N \leq 1$. It is clear that by taking l' and l'' (resp. l'' and l) instead of l and l' we get also some number P' and N' (resp. P'' and N'') satisfying the same inequality. So $p_1|Y| = P + P' + P'' + p|Z_m| + \sum p|Z|$, where the last summation is on the zones of Δ which intersect each only one edge of \mathbf{T} , and in which the Harnack distribution of signs is of type $(1, a, b)$ for some $a, b \in \{0, 1\}$. Similarly we get that $n_1|Y| = N + N' + N'' + \sum n|Z|$ where the last summation is on the same zones than for $p_1|Y|$. Therefore

$$\begin{aligned} p_1|Y| - n_1|Y| &\leq (P - N) + (P' - N') + (P'' - N'') + \\ &\quad + p|Z_m| - n|Z_m| + \sum (p|Z| - n|Z|) \\ &\leq 3 + (p|Z_m| - n|Z_m|) + \left(\sum (p|Z| - n|Z|) \right) \end{aligned}$$

- Since the angles in Z_m at all the inner nodes may be greater than π , and since all the inner nodes belong to $|Z_m|$, we get from lemma 12.1.0.5 that $p|Z_m| - n|Z_m| \leq 1$.

- From the same argument than in parag. 7 we get that $\sum(p|Z|-n|Z|) \leq 0$.

Therefore we get that $p_1|Y|-n_1|Y| \leq 4$. This proves part 3 of the proposition. \square

12.4 Proof of the Main Theorem

12.4.0.12 Theorem

The number of even ovals of a maximal T -curve of even degree $2k$ is no more than $\frac{3k(k-1)}{2} + 1$, and the number of its odd ovals is no more than $\frac{3k(k-1)}{2} + 4$.

proof. Let $K = K(\Delta)$ be a maximal T -curve of degree $2k$. As we noticed at the beginning of section 11 we assume without loss of generality that the odd-cycle-free zone decomposition Δ is even-node-free. We assume also that the distribution of signs in the special zone is of Harnack type $(1, 0, 0)$. Let P (resp. N) be the number of even (of odd) ovals of K .

1. From corollary 11.4.2.2 we get that

$$P = 1 + \sum(p_0|Y| + n_1|Y|) \quad \text{and} \quad N = \sum(p_1|Y| + n_0|Y|)$$

the summations being over all the separating unions Y of zones of Δ .

2. Proposition 12.3.0.11 states that for each separating union Y of zones of Δ , and each $c = 1$ or 0 , one has $p_c|Y| - n_c|Y| \leq 0$ except for the only one separating union of zone Y_{spe} intersecting l_1, l_2 , and l_3 when $c = 1$ for which one has $p_1|Y_{spe}| - n_1|Y_{spe}| \leq 4$. So we get that

$$p_1|Y_{spe}| + n_0|Y_{spe}| \leq n_1|Y_{spe}| + n_0|Y_{spe}| + 4$$

and that for $(Y, c) \neq (Y_{spe}, 1)$ we get that

$$p_c|Y| + n_{c+1}|Y| \leq n_c|Y| + n_{c+1}|Y|$$

3. The number of points of odd parity in the interior of \mathbf{T} is equal to $\frac{3k(k-1)}{2}$. From parag. 1 and parag. 2 we get now that $P \leq 1 + \sum(n_0|Y| +$

$n_1|Y|$). Since the summation is over all the separating zones Y of Δ it is equal to the number of odd points in \mathbf{T} . Therefore we get that

$$P \leq \frac{3k(k-1)}{2} + 1$$

Similarly, from parag. 1 and parag. 2 we get also that $N \leq 4 + \sum(n_1|Y| + n_0|Y|)$ therefore

$$N \leq \frac{3k(k-1)}{2} + 4$$

□

12.5 Further Remarks

Let $K = K(\Delta)$ be a maximal T-curve of even degree $2k$, and assume that Δ is an even-node-free odd-cycle-free zone decomposition of \mathbf{T} . Let Z_{spe} be the special zone of Δ , let Y_{spe} be the separating union of zones of Δ containing Z_{spe} , and let P (resp. N) be the numbers of even (odd) ovals of K .

12.5.0.13 Proposition

If $N > \frac{3k(k-1)}{2} + 1$ then $N = \frac{3k(k-1)}{2} + 4$.

proof. Let $p|\mathbf{T}|$ (resp. $n|\mathbf{T}|$) be the number of points of even (odd) parity in the interior of \mathbf{T} .

1. Since $p|\mathbf{T}| - n|\mathbf{T}| = 1 - k^2$ and $k^2 \equiv 1$ or $0 \pmod{4}$, we get that $p|\mathbf{T}| - n|\mathbf{T}| \equiv 1$ or $0 \pmod{4}$.
2. From section 12.4 we get that the cases $N = \frac{3k(k-1)}{2} + i$, $i = 2, 3$ or 4 imply that $p|Y_{spe}| - n|Y_{spe}| = i$.
3. Since $\mathbf{T} \setminus Y_{spe}$ is a union of zones like in lemmas 12.2.0.7 and 12.2.0.6, we get that $p|Y_{spe}| - n|Y_{spe}| \equiv p|\mathbf{T}| - n|\mathbf{T}| \pmod{4}$, so from parag. 1 we get that $p|Y_{spe}| - n|Y_{spe}| \equiv 0$ or $1 \pmod{4}$, which implies that i must be different than 2 or 3.

□

For every circular permutation $\{i, j, k\}$ of $\{1, 2, 3\}$ let V_i be the union of the zones Z of Δ in Y_{spe} which intersect l_j and l_k and let $p|V_i|$ (resp. $n|V_i|$) be the summation over all these zones of the numbers $p|Z|$ (resp. $n|Z|$).

From section 12.4 we get that $N = \frac{3k(k-1)}{2} + 4$ implies that $p|V_i| - n|V_i| = 1$, for $i = 1, 2, 3$, and that $p|Z_{spe}| - n|Z_{spe}| = 1$. This is the case (a) illustrated on fig. 74. But such a configuration hasn't been found yet, and it is likely that it doesn't exist. According to prop. 12.5.0.13, this nonexistence is the only thing to prove to get rid of the inelegant $+3$ in theorem 12.4.0.12. Moreover it is likely too that a configuration such that only $p|Z_{spe}| - n|Z_{spe}|$ or such that only one of the $p|V_i| - n|V_i|$ equals one (see fig. 74 (b) and (c)), does not exist. This would imply that $N \leq \frac{3k(k-1)}{2}$ (like in the initial Ragsdale conjecture), so in particular the curves constructed by Viro with $N = \frac{3k(k-1)}{2} + 1$ (see 8.1) would not be realizable as T-curves.

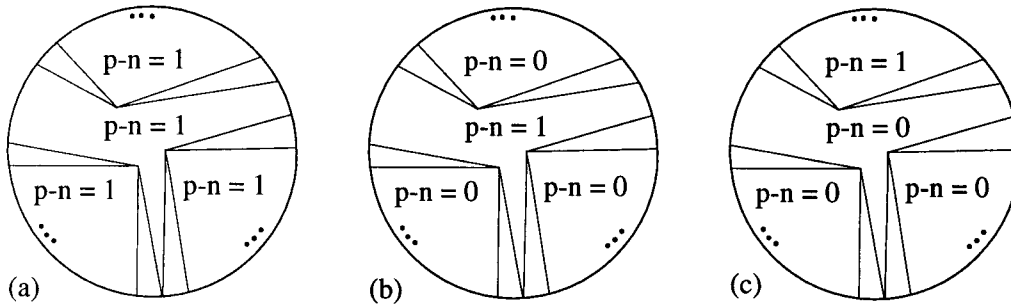


Figure 74: These three cases seem to be not possible.

References

- [1] ARNOLD, V. On the arrangement of the ovals of real plane curves, involutions of 4-dimensional smooth manifolds, and the arithmetic of integral quadratic forms. *Funct. Anal. Appl.* 5 (1971), 1–9.
- [2] HAAS, B. Les multilucarnes: Nouveaux contre-exemples à la conjecture de Ragsdale. *C. R. Acad. Sci. Paris* 320, Ser. I (1995), 1507–1512.
- [3] HARNACK, A. Über Vieltheiligkeit der Ebenen algebraischen Kurven. *Math. Ann.* 10 (1876), 189–199.
- [4] ITENBERG, I. Contre-exemples à la conjecture de Ragsdale. *C. R. Acad. Sci. Paris* 317, Ser. I (1993), 277–282.
- [5] ITENBERG, I. Counter-examples to Ragsdale conjecture and T-curves. In *Real Algebraic Geometry and Topology* (1995), S. Akbulut, Ed., vol. 182, A.M.S., pp. 55–72.
- [6] ITENBERG, I. Viro’s method and T-curves. In *Algorithms in Algebraic Geometry and Applications* (1996), L. Gonzales-Vega, Ed., vol. 143, Birkhäuser, pp. 177–192.
- [7] O.VIRO. Curves of degree 7, curves of degree 8, and the Ragsdale conjecture. *Soviet Math. Dokl.* 22 (1980), 566–569.
- [8] PETROWSKI, I. On the topology of plane algebraic curves. *Ann. of Math.* 39 (1938), 187–209.
- [9] RAGSDALE, V. On the arrangement of the real branches of plane algebraic curves. *Amer. J. Math.* 28 (1906), 377–404.
- [10] ROKHLIN, V. Complex topological characteristics of real algebraic curves. *Russian Math. Surveys* 33, 5 (1978), 85–98.
- [11] VIRO, O. Real algebraic plane curves: Constructions with controlled topology. *Leningrad Math. J.* 5 (1990), 1059–1134.

Index

- algebraic curve, 76
- ambient surface, 10
- arc, 28
- arc:surround, 37, 40, 41, 53, 55, 82, 84–86, 90, 93, 94, 99–103, 107
- atlas, 23

- boundary-node, 81
- broken edge, 8

- carrier polygon, 11
- chart of $S(\Pi)$, 20
 - canonical system of, 20
- completed zone, 70, 83
- congruence of curves, 4
- consecutive boundary-nodes, 81
- cycle of zones, 66, 76
 - edge of a, 66, 76

- dividing curve, 42

- edge
 - of a cycle of zones, 66, 76
 - of a polygon, 7
 - of a triangulation, 7
 - separating, 81

- gluing of lattice T-curves, 45
- gluing transformation, 21

- Harnack distribution of signs
 - definition, 37
 - type, 37
- Harnack T-curves, 37

- incidence graph
 - of a triangulation
 - of Π , 30
 - of $S(\Pi)$, 30
 - of a zone decomposition, 66
- injective pair, 5
- inner-node, 81
- integral
 - length, 28
 - points of a zone, 106
 - polygon, 7
 - polygonal line, 7
 - segment, 6
 - even, 89
 - total parity of an, 60

- lattice T-curve, 2
 - carrier polygon, 11
 - maximal, 2
- lattice T-curves
 - definition, 11
 - gluing of, 45
 - introduction to, 3–13
 - on a toric surface, 11
 - on $\mathbb{R}P^2$, 3
- length, 28

- maximal curve, 77
 - lattice T-curve, 2
 - T-curves, 36

- neighbor, 28
- neighborly inside, outside, 83
- node, 81
 - boundary, 81
 - inner, 81
 - top, 105

- non-dividing curve, 42
- nontrivial component, 28
- obtuse vertex, 110
- oval, 28
 - empty, 28
 - even, odd, 77
 - inside, outside, 28
 - outermost, 28
 - sign of an, 29, 92
- parity, 7
 - even, odd, 8
 - of a broken edge, 8
 - of a vertex of a polygon, 7
 - of an edge of a polygon, 8
 - of an integral segment, 7
- parity matrix, 20
- pie-diagram, 82
- polygon, 7
 - broken edge, 8
 - edge of a, 7
 - vertex of a, 7
- polygonal line, 7
 - integral, 7
- primitive
 - segment, 28
 - triangulation, 28
- quadrant
 - of a chart, 20
 - of $\mathbb{R}P^2$, 15
 - of $S(\Pi)$, 18
- r -connected sum, 51
- Ragsdale bound, 78
- sector, 82
- segment
 - integral, 6
 - even, 89
 - total parity of an, 60
 - primitive, 28
 - separating edge, 81
 - separating union of zones, 98
 - sign of an oval, 29, 92
 - special zone, 98
 - surround, 37, 40, 41, 53, 55, 82, 84–86, 90, 93, 94, 99–103, 107
- T-curve, 2
- T-filling, 32
- thick Y, 31
- top node, 105
- total parity of an integral segment, 60
- triangulation, 7
 - edge of a, 7
 - primitive, 28
 - vertex of a, 7
- twist, 31
- type I, *see* dividing curve
 - orientation, 44
- type II, *see* non-dividing curve
- vertex
 - obtuse, 110
 - of a polygon, 7
 - of a triangulation, 7
- zone, 12, 63
 - completed, 70, 83
 - special, 98
- zone decomposition, 63
 - even-node-free, 96
 - incidence graph of a, 66
 - minimal, 66
 - odd-cycle-free, 13, 67

zone decompositions

 intersection of two, 64

zones

 cycle of, 66, 76

 edge of a, 66, 76

 separating union of, 98

Lebenslauf

Am 1. Oktober 1964 wurde ich, Bertrand Haas, in Guer (Departement Morbihan, Frankreich) geboren. Meine Eltern sind Françoise Jacquesson und Bruno Haas; ich lebe jetzt in Toronto, Ontario, Canada.

- 1979 – 1983 Lycee Saint-Joseph, Epinal (Vosges, Frankreich).
1988 – 1991 DEUG de Sciences Exactes et Licence de Mathématiques pures à l'Université de Lille-Flandre-Artois, Lille (Nord, France)
- 1991 – 1993 Maitrise et DEA de Mathématiques pures à l'Université Louis Pasteur, Strasbourg (Bas-Rhin, France)
- 1993 – 1995 Assistentstelle in Mathematik an der Universität Bern.
- 1995 – 1997 Doktorandenstelle beim Schweizerischen Nationalfond in Mathematik an der Universität Basel.

Meine akademischen Lehrer der Mathematik:

Licence, Maitrise und DEA: Proff. J-F. Robinet, X. Fernique, D. Bénéquin, N. Shappacher, V. Avanissian, M. Audin.

Prof. V. Kharlamov von der Universität Louis Pasteur in Strasbourg, mit dem ich meine Dissertation begonnen habe.

Prof. P. Mani von der Universität Bern, von dem ich viel über kombinatorische Geometrie gelernt habe.

Prof. N. A'Campo von der Universität Basel, der während die zwei letzten Jahre meine Dissertation geleitet hat.